APTD 0669

PB 198 822

ESSO RESEARCH AND ENGINEERING COMPANY

A REGENERATIVE LIMESTONE PROCESS FOR FLUIDIZED BED COAL COMBUSTION AND DESULFURIZATION

BY

G. A. HAMMONS

A. SKOPP

PREPARED UNDER CONTRACT NO. CPA 70-19
FOR
PROCESS CONTROL ENGINEERING PROGRAM
AIR POLLUTION CONTROL OFFICE

FINAL REPORT

FEBRUARY 28, 1971

ESSO RESEARCH AND ENGINEERING COMPANY
GOVERNMENT RESEARCH DIVISION
LINDEN, NEW JERSEY

government research

Reproduced by
NATIONAL TECHNICAL
INFORMATION SERVICE
Springfield, Va. 22151

P. O. BOX 8 ■ LINDEN, NEW JERSEY 07036

PB 198 822

BIBLIOGRAPHIC DATA SHEET	1. Report No. APTD-0669	2	3. Recipient's Accession No.
4. Title and Subtitle A Regenerative Limestone Process for Fluidized Bed Coal Combustion and Desulfurization			5. Report Date February 28, 1971 6.
7. Author(s) G. A. Hammons, A. Skopp			8. Performing Organization Rept. No.
9. Performing Organization Name and Address ESSO Research and Engineering Company Government Research Division P. O. Box 8 Linden, New Jersey 07036			10. Project/Task/Work Unit No. 11. Contract/Grant No. CPA 70-19
12. Sponsoring Organization Name and Address Process Control Engineering Program Air Pollution Control Office Technical Center, Box 12055 Research Triangle Park, N. C. 27709			13. Type of Report & Period Covered Final 14.

15. Supplementary Notes

16. Abstracts

An experimental study was conducted on a fluidized bed coal combustion system using lime as a bed material. The lime reacts with SO_2 and O to form $CaSO_4$ under oxidizing conditions, thus reducing SO_2 emissions. The reductive regeneration of the sulfated lime back to CaO^2 and recycle of the regenerated lime back to the combustor was investigated as a method of reducing fresh limestone feed rates to the system. A three inch diameter combustor and a two inch diameter were utilized in this experimental program.

17. Key Words and Document Analysis. 17a. Descriptors

Fluidized bed processors
Coal
Combustion
Limestone
Regeneration (engineering)
Flue gases
Desulfurization
Sulfur dioxide
Economic comparison

17b. Identifiers/Open-Ended Terms

Regenerative limestone process

17c. COSATI Field/Group 13/B

18. Availability Statement	19. Security Class (This Report)	21. No. of Pages
Unlimited	UNCLASSIFIED	121
	20. Security Class (This Page) UNCLASSIFIED	22. Price 3.00 MF

FORM NTIS-35 (10-70)

USCOMM-DC 4032

BLANK PAGE

TABLE OF CONTENTS

		Page
1.	SUMMARY	1
2.	INTRODUCTION	6
3.	EXPERIMENTAL APPARATUS, MATERIALS AND PROCEDURES	9
	3.1 Experimental Combustion Apparatus	9
	3.1.1 Coal Feeding Equipment	9
	3.1.2 Fluid Bed Reactor	9
	3.1.3 Gas Cleanup and Analysis System	12
	3.2 Experimental Regeneration Apparatus	14
	3.3 Feed Materials	16
	3.3.1 Limestone	16
	3.3.2 Coal	17
	3.3.3 Inert Bed Material	17
	3.4 Range of Operating Variables	18
	3.5 Experimental Procedure	19
4.	REACTOR COMBUSTION EFFICIENCY	21
	4.1 Effect of Gas-Solid Contacting	23
	4.2 Effect of Bed Temperature	24
	4.3 Effect of Gas Velocity	26
	4.4 Effect of Excess Air	28
	4.5 Effect of Bed Height	29
	4.6 Effect of Lime Particle Size	31
5.	FLUE GAS DESULFURIZATION IN NON-CYCLIC OPERATIONS	32
	5.1 Esso FBC Operation and Typical Desulfurization Data	32
	5.2 Effect of Excess Air	36
	5.3 Effect of Limestone Particle Size	38
	5.4 Effect of Temperature	38
	5.5 Effect of Gas Velocity	39
	5.6 Effect of Settled Bed Height	42
	5.7 Kinetic Analysis of $CaO-SO_2-O_2$ Reaction System	43
	5.7.1 Location of SO_2 Release in the Bed	44
	5.7.2 Effect of Stone Particle Size on R(X)	45
	5.7.3 Effect of Settled Bed Height on R(X)	46

TABLE OF CONTENTS (CON'T)

		Page
6.	OTHER GASEOUS EMISSIONS	52
6.1	NO_x Emissions	52
6.1.1	Inert Bed Operations	53
6.1.2	Typical NO_x and SO_2 Emissions With Limestone Beds	54
6.1.3	Simulated Gas Studies	56
6.1.4	Other Variable Effects on NO_x Emissions	59
6.2	CO Emissions	62
6.2.1	Effect of Bed Temperature	62
6.2.2	Effect of Excess Air	62
7.	SORBENT REGENERATION	63
7.1	Experimental Procedure and Conditions in Sorbent Regeneration Studies	64
7.2	Process Conditions for Regeneration	65
7.3	SO_2 Concentration in Regenerator Off Gas	66
7.4	Cyclic Stone Reactivity	68
7.5	Cyclic Stone Attrition	71
8.	ECONOMIC COMPARISON OF REGENERATIVE AND SINGLE PASS (LIMESTONE) FBB SYSTEMS	74
8.1	Process Design Considerations	74
8.1.1	Regenerative Limestone System	74
8.1.2	Single Pass Limestone System	86
8.2	Economic Comparison	88
8.2.1	Basis for Cost Estimates	88
8.2.2	Important Factors in Comparing Single-Pass & Regenerative Systems	89
8.2.3	Operation of Acid Plant by the Power Plant	91
8.2.4	Operation of Acid Plant by Outside Contractor	95
8.2.5	Sulfuric Acid Return	95
APPENDIX 1		103
APPENDIX 2		104
APPENDIX 3		106
APPENDIX 4		107
APPENDIX 5		108
APPENDIX 6		109
APPENDIX 7		111
APPENDIX 8		113

LIST OF TABLES

Number		Page
1	Composition of Limestone Used In Esso FBC Program	16
2	Composition of Coal Used in Esso FBC Program	17
3	Range of Operating Variables Examined in Esso FBC	19
4	Effect of Bed Temperature on Stone Capacity	39
5	NO_x-SO_2 Interaction in a Fluidized Bed of Limestone ..	57
6	NO_x Emissions From Esso FBC Are Independent of Excess Air Level	60
7	NO_x Emissions Increase with Bed Temperature	61
8	Conditions for Stone Regeneration Studies	64
9	Fly Ash Accumulated in Bed When Using 460 μ Stone	70
10	Operating Conditions in Regenerative FBB System	76
11	Factors for Estimating Operating Costs	89
12	Factors of Importance in Economic Comparison Of Regenerative and Non-Regenerative FBB Systems	90
13	Credits or Debits Allowed in Economic Comparisons	90
14	Incremental Investment for Regenerative FBB System Over Investment Required for Single Pass FBB System ...	92
15	Incremental Operating Costs for a Regenerative FBB System as Compared to a Single Pass System	93

LIST OF ILLUSTRATIONS

Number		Page
1	Esso Fluidized Bed Combustion Unit	10
2	Fluidized Bed Combustor	11
3	Flow Diagram for the Fluidized Bed Regeneration Unit .	15
4	Particle Size Distributions of Limestone And Coal Feeds to Esso FBC	18
5	Grid Used in Esso FBC	22
6	Increasing Bed Temperature Decreases The Carbon Loss in the Flyash	25
7	Carbon Loss in Fly Ash Increases With Increasing Gas Velocity	27
8	Combustion Efficiency Not Affected By Excess Air in 7 to 30 Percent Range	28
9	Carbon Loss Increases with Bed Height	30
10	Small Variation in Carbon Loss in Fly Ash With Bed Particle Size	31
11	Typical Desulfurization Data	34
12	Desulfurization Data in Form to Allow Comparison	34
13	Stone Capacity Dependent on Excess Air	37
14	Increasing Gas Velocity Changes Breakthrough Characteristics	40
15	Increasing Superficial Gas Velocity Increases Stone Attrition	41
16	Stone Capacity Reflects Decreasing Contacting Efficiency with Bed Height	42
17	SO_2 Formation Occurs Primarily Near Reactor Inlet	44
18	Effect of Stone Particle Size on Kinetic Constants ...	45
19	Kinetic Constants from Esso Data	46

LIST OF ILLUSTRATIONS (CON'T)

Number		Page
20	Kinetic Results at Ho/D = 1.3	48
21	Kinetic Results at Ho/D = 2.0	49
22	Kinetic Results at Ho/D = 4.0	50
23	Desulfurization with 460 μ Stone at Ho/D = 2.0	51
24	Inert Bed Material Produces Lower NO_x Emissions	54
25	Typical NO_x Emissions with Limestone Bed	55
26	CO Emission Decrease with Increasing Bed Temperature .	62
27	Proposed Fluidized Bed Combustion - Sorbent Regeneration System	63
28	Typical SO_2 Concentration from Stone Regeneration	66
29	Regeneration Reaction Attains Equilibrium	67
30	Sorbent Cyclic Capacity	68
31	Cyclic Sorbent Attrition Low After First Cycle	72
32	Particle Decrepitation in Regenerative System	73
33	Comparison of Regenerative and Single Pass Limestone FBB Systems for a 600 MW Power Plant	75
34	Average Cyclic Stone Utilization at 90% SO_2 Removal ..	77
35	Ca/S Ratios Required for 90% SO_2 Removal	78
36	Bed Height Required for 90% SO_2 Removal	79
37	Material Balance on FBC - FBR System	83
38	Gas Purification System	85
39	Material and Energy Balance for Single Pass Limestone 600 MW FBB System	87
40	Effect of Sulfuric Acid Return	94
41	Experimental Breakthrough Data	111

BLANK PAGE

1. SUMMARY

An experimental study was conducted on a fluidized bed coal combustion system using lime as a bed material. The lime reacts with SO_2 and O_2 to form $CaSO_4$ under oxidizing conditions, thus reducing SO_2 emissions. The reductive regeneration of the sulfated lime back to CaO and recycle of the regenerated lime back to the combustor was investigated as a method of reducing fresh limestone feed rates to the system.

Initial experiments were directed towards defining the operational characteristics of the three inch diameter coal combustor used. The maximum combustion efficiency observed in these experiments was 97 percent at a bed temperature of 1800°F, a superficial gas velocity of three feet per second and an excess air level of 10 percent. The combustion efficiency of the three inch diameter fluidized bed combustor (FBC) was found to decrease as bed temperature was decreased, to increase as superficial gas velocity was decreased, to be independent of the excess air level over the range of seven to thirty percent and to decrease with increasing bed height . The unusual bed height effect was apparently a result of severe slugging conditions in the deeper beds. Lower excess air levels than seven percent caused a reduction in the combustion efficiency. The combustion efficiency of the FBC was not changed when the average particle diameter of the bed material, lime, was increased from 460 μ to 930 μ.

In order to define desirable operating conditions for the regeneration studies, numerous experiments were conducted in the FBC with batch charged quantities of freshly calcined lime. The CaO utilization, $CaSO_4/(CaO + CaSO_4)$, of the lime at 80 percent SO_2 removal was used to compare the reactivity of the stone under different operating conditions of the unit. The CaO utilization at 80 percent SO_2 removal was 19 percent for a 930 μ average particle diameter stone (N-1359, 97 weight per cent CaO) at a bed temperature of 1600°F, superficial gas velocity of 3 feet per second, settled bed height of six inches and excess air level of 10 percent. The reactivity of the lime decreased with increasing excess air, was relatively independent of superficial gas velocity over the range of 2 to 4 feet per second, and decreased with increasing bed height. The effect of bed height on lime reactivity apparently again reflects decreasing gas-solid contacting efficiency, because of slugging, as bed height was increased. The lime reactivity was independent of bed temperature over the range of 1600 to 1800°F. Decreasing the average lime particle size from 930 μ to 460 μ increased the CaO utilization at 80 percent SO_2 removal from 19 to 32 percent, at the conditions previously mentioned for the 930 μ stone.

A first order kinetic model for the $CaO-SO_2-O_2$ reaction system was used to correlate the results of this study. The model was based on on the assumptions of complete mixing of the solids, plug flow of the gas and release of all the SO_2 from the combusting coal at the reactor inlet. The results of this analysis were in close agreement with results obtained when using a simulated flue gas in a similar experimental system, indicating

that a large fraction of the SO_2 was indeed released at the reactor inlet. The Esso desulfurization data at a given (settled bed height)/(reactor diameter) and (settled bed height)/(superficial gas velocity) were found to be in agreement with data generated under similar conditions at Argonne National Laboratories on a similar reaction system.

The NO_x emissions from the Esso FBC in a typical batch lime operation decreased as a run progressed. A typical decrease was from 1100 ppm (dry) to 700 ppm, at a bed temperature of 1600°F and excess air level of 10 percent. The results of a series of experimental operations passing a simulated gas with varying concentrations of NO and SO_2 through different bed materials, including alundum, $CaSO_4$ and partially sulfated lime, indicated that the most probable reason for the NO_x reduction was a heterogeneous reaction between NO and SO_2 over a partially sulfated lime bed.

The NO_x emissions were not changed by varying excess air from 3 to 30 percent at 1600°F bed temperature. Increasing bed temperature from 1600 to 1800°F increased the NO_x emissions by approximately 30 percent.

In order to investigate the potential for the reductive regeneration of the partially sulfated lime ($CaSO_4$ + CaO) back to CaO, a series of experiments was conducted in the FBC and a two inch diameter fluid bed regenerator. The units were operated intermittently, with manual transfer of solids between the reactors. The bed temperatures in the combustor and regenerator were 1600°F and 2000°F, respectively. The superficial gas velocities in the combustor and regenerator were 3 and 2 feet per second, respectively. In cyclic operations with a 930 μ average particle diameter stone, an increase in the CaO utilization at 80 percent

SO_2 removal was observed after the first regeneration followed by a gradual decrease in capacity after subsequent regenerations. However, in cyclic operations with the 460 μ stone, a rapid decrease in capacity was observed following the first cycle. The different cyclic deactivation behaviors of the stone particle sizes appear to be related to the different amounts of coal fly ash retained in the lime beds during cyclic operation; considerably more fly ash was retained in the bed in the operations with the smaller (460 μ) stone. Apparently some component of the coal fly ash has a deactivating effect on the lime.

The reaction occurring in the high temperature (2000°F) regenerator

$$CaSO_4 + CO \longrightarrow CaO + SO_2 + CO_2$$

proceeded to thermodynamic equilibrium and produced an exit gas with approximately 7.8 percent SO_2. A gas with this SO_2 concentration is well suited as a feed to a sulfuric acid plant.

An economic comparison was made of two 600 MW fluidized bed boiler (FBB) systems. One of the FBB systems used the regenerative limestone process described in this paper; the other FBB was based on single pass usage of limestone. The combustor settled bed height required in the regenerative system for 90 percent SO_2 removal was calculated to be 2.8 feet at a superficial gas velocity of 10 feet per second. A fresh calcium/sulfur molar feed ratio of 0.55 was required, based on the experimental deactivation data for the 930 μ stone. The regenerator settled bed height, determined by scaling up from the equilibrium experimental system, was 2.5 feet. In the single pass system, the combustor settled bed height was also set at 2.8 feet and a calcium/sulfur molar ratio of 4.0 was assumed to be required for 90 percent SO_2 removal. The regenerative system required an incremental investment of 2.35 million dollars as compared to the single pass system. This incremental investment included the cost of constructing

a 583 short ton/day sulfuric acid plant to recover the SO_2 from the regenerator off-gas. However, the credit from the sale of sulfuric acid at $10 per short ton combined with various other credits (less limestone receiving, handling, disposal, etc.) caused the operating cost of the regenerative system to be 1.40 dollars per ton of coal desulfurized less than the operating cost of the single pass system. If an outside contractor constructed and operated the sulfuric acid plant in the regenerative system and allowed the power plant a "transfer credit" of $4.40 per short ton of sulfuric acid, the operating credit to the regenerative system, as compared to a single pass system, was reduced to 1.10 dollars per ton of coal desulfurized.

2. INTRODUCTION

The need for controlling air pollution from fossil fuel power plants is widely recognized. Emissions of SO_2 from such plants are the highest of any of the common class of air pollutants, including NO_x, CO and hydrocarbons. Efforts to control SO_2 emissions from conventional fossil fuel power plants have been hampered by the large volumes of gas which must be treated and the relatively dilute concentration of SO_2 in the flue gas (2000-3000 ppm).

One technique under consideration for control of SO_2 emissions involves contacting the flue gases with limestones or dolomites. Limestones and dolomites react with SO_2 to form solid $CaSO_4$ under oxidizing conditions. The chemical reaction system involved is the following:

$$CaCO_3 \longrightarrow CaO + CO_2 \qquad (2\text{-}1)$$

$$CaO + SO_2 + 1/2O_2 \longrightarrow CaSO_4 \qquad (2\text{-}2)$$

The use of limestone for capturing SO_2 is exceptionally well suited to a new combustion technique, fluidized bed combustion. In a fluid bed combustor (FBC), a fossil fuel (coal or fuel oil) is combusted in a bed of material maintained in a state of fluidization by the combustion gases. The high solids mixing rates and the high gas-solid heat transfer rates serve to maintain the bed temperature at a uniform level. The use of limestone or other suitable sorbents in such a system permits removal of SO_2 essentially simultaneously with the combustion process.

Although fluidized bed combustion appears to have considerable potential as an air pollution abatement method, the commercial application of this concept may depend on its economic potential (as compared to

conventional boilers) independent of its pollution abatement characteristics. Some of the factors which could make fluidized bed boilers more economically attractive than conventional boilers are as follows:

- The ability to combust lower quality fuels in a fluidized bed.
- The placing of steam tubes directly in the bed results in reduced tubing requirements because of the higher heat fluxes attainable in the bed.
- The maintenance of uniform low bed temperatures (1500-1800°F) may reduce tube corrosion and fouling.
- The higher volumetric heat release rates possible in a fluidized bed combustor may permit smaller unit sizes.

The Air Pollution Control Office, APCO, is sponsoring research on fluidized bed combustion because of its potential for pollution control. As part of APCO's program, Esso Research and Engineering Company is examining a system in which finely ground coal is fed to a bed of larger limestone particles. The calcined stone reacts with the SO_2 in the flue gas, reducing emissions of this air pollutant. The ash from the coal is entrained from the system leaving a bed composed primarily of partially sulfated stone. The natural separation of the coal ash and the bed material makes the regeneration of the stone (i.e., conversion of $CaSO_4$ into CaO) and cyclic use of the stone more feasible. The system proposed by Esso would involve transferring the sulfated stone from the combustor to a regeneration reactor in which the stone would be converted back to CaO by reaction with a reducing gas. The regenerated stone (CaO) would then be returned to the combustor in a cyclic system, reducing the fresh limestone requirements and, simultaneously, the amount of used limestone disposal burden. The gaseous effluent from such a regenerator has a high SO_2 concentration and can be used to produce a sulfuric acid or sulfur by-product.

A three inch diameter combustor and a two inch diameter regenerator were utilized in the Esso experimental program.

3. EXPERIMENTAL APPARATUS, MATERIALS AND PROCEDURES

3.1 Experimental Combustion Apparatus

A schematic diagram of the Esso fluid bed combustion unit is shown in Figure 1. The three primary components of this unit were as follows: (1) coal feeding system, (2) a fluid bed reactor, and (3) a gas cleanup and analysis system.

3.1.1 Coal Feeding Equipment

Coal was stored in a small hopper and gravity-fed to a vibrating low rate solids Vibro-Feeder. The output of the feeder was connected by pneumatic tubing to a 1/4 inch stainless steel tube, extending through the reactor grid approximately 1/8 inch into the bed. A small baffle was located directly above the coal inlet to promote dispersion. The feed rate of the coal was controlled by adjusting the vibration intensity of the feeder.

3.1.2 Fluid Bed Reactor

A schematic diagram of the fluid bed reactor utilized as the coal combustor in this study is shown in Figure 2. This reactor consisted of an air preheat section, a reactor section and a disengaging section. The entire reactor was constructed of Incoloy 800.

The air preheat section was a three inch diameter, eight inch high section, packed with 1/4 inch ceramic cylinders. It was attached directly to the reactor section. Beaded electrical heaters supplied the necessary heat to preheat the air to 600°F. The air preheat temperature was automatically controlled at the desired level.

Figure 1

ESSO FLUIDIZED BED COMBUSTION UNIT

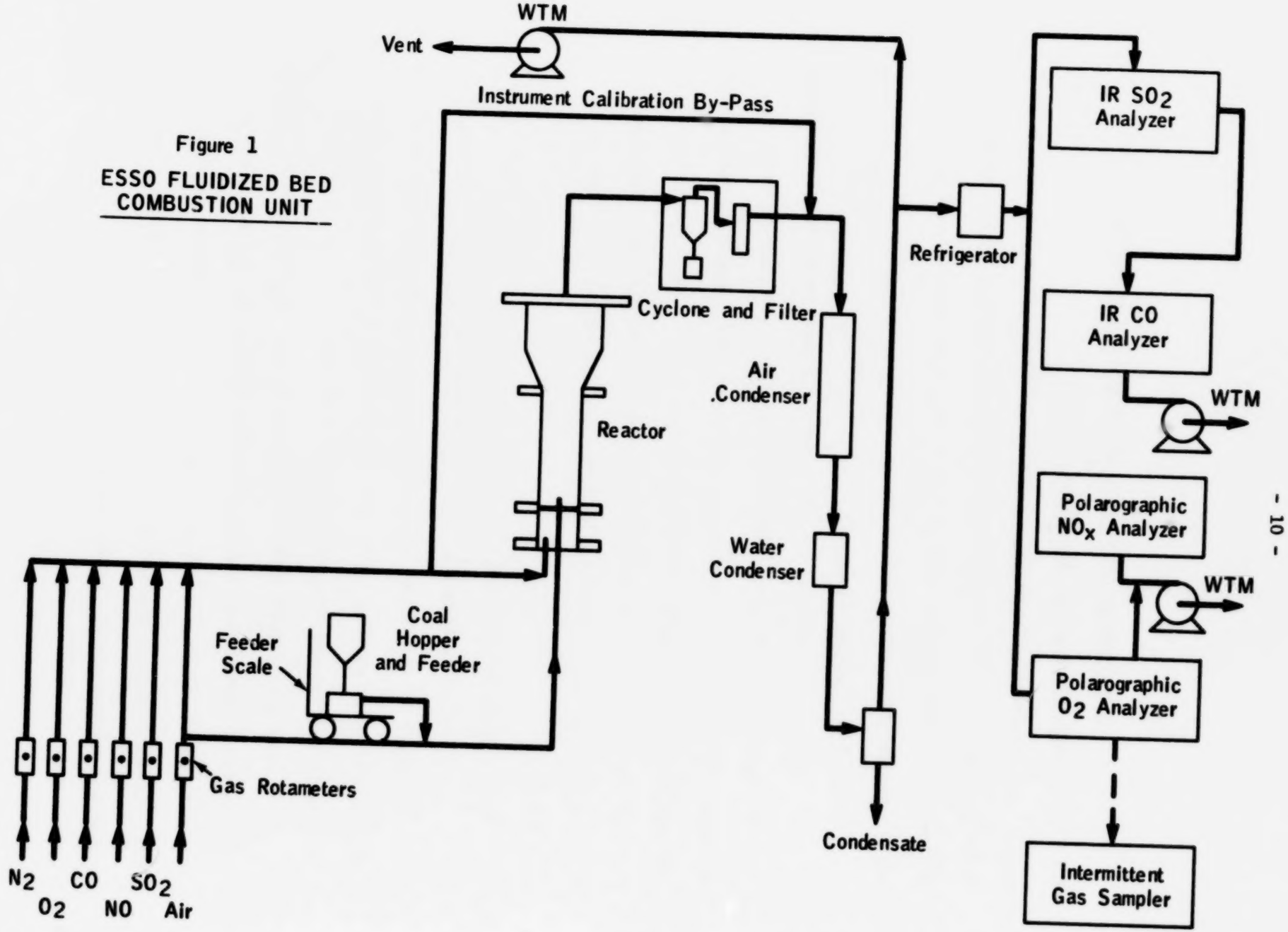

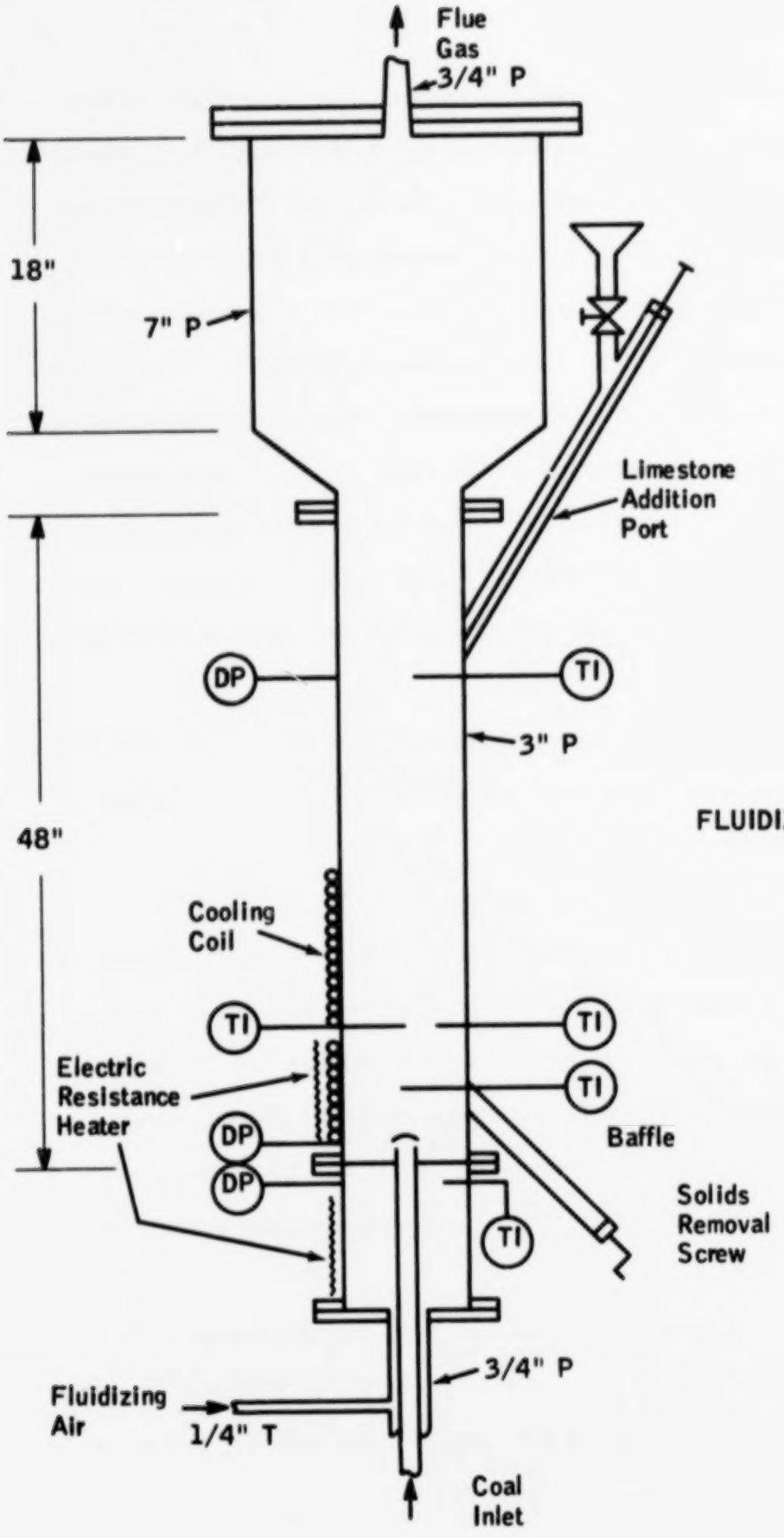

Figure 2

FLUIDIZED BED COMBUSTOR

The reactor was a three inch diameter, four feet high Incoloy tube. Air distribution was accomplished by six bubble caps, with eight 5/64 inch outlet holes in each bubble cap. The bed was preheated by use of beaded, resistance wire heaters. Bed temperature was controlled by use of an external cooling water coil. The water flow rate to the cooling coil was manually adjusted to yield the desired temperature. The bed was insulated to limit heat loss to the atmosphere. Average bed temperature was determined by five thermocouples in the bed. Pressure drop across the bed was continuously determined by use of a water manometer. Withdrawal of bed solids was accomplished by use of a screw conveyor; fresh limestone was batch charged to the unit by use of the inlet port located three feet above the distributor plate.

The disengaging section was a seven inch diameter, 18 inch high section, in which gas velocities were reduced to allow some entrained particles to be returned to the bed.

3.1.3 Gas Cleanup and Analysis System

The gas cleanup and analysis system is also shown in Figure 1. The gas exited the reactor through a 3/4 inch uninsulated pipe. The temperature of the gas dropped to approximatley 300°F before entering a glass cyclone and a fritted stainless steel filter. The gas leaving the filter was essentially free of entrained particulates. The cyclone and filter were enclosed in an electrical oven to prevent any moisture condensation.

The particulate-free flue gas was then passed through an air-cooled condenser and a water-cooled condenser to remove most of the water vapor. Approximately 80 percent of the flue gas was then metered by a

large wet test meter and vented; the remaining flue gas (~0.5 CFM) was diverted through a refrigerator which lowered the dew point of the gas to 35°F before it was sent to the gas analysis equipment. The gas analysis equipment included four continuous analyzers: two infrared analyzers for SO_2 and CO, and two polarographic instruments for O_2 and NO_x.

The IR instruments were both Beckman Model IR 315 analyzers. CO_2 and H_2O are interference gases for both instruments and appropriate corrections to the meter readings were made for these interference gases.

The polarographic NO_x instrument was manufactured by Dynasciences Corporation, a subsidiary of Whittaker Corporation, Chatsworth, California. It was a dual range instrument, with ranges of 0-1000 ppm and 0-5000 ppm NO_x. The manufacturer stated that the instrument gave a full response to the NO in the sample gas and approximately an 80 percent response to the NO_2. In our calibration tests, the instrument was found to respond linearly to NO in dry N_2. The response to NO_2 varied from 80 to 100 percent for different sensors. SO_2 was an interference gas for this instrument, but the manufacturer supplied a solid sorbent (malcosorb) or a liquid sorbent that removed all the SO_2 from the sample gas. The NO_x instrument did not exhibit significant interference to CO_2, O_2 or CO. Frequent calibration of the NO_x instrument (every one to two hours) was necessary.

The O_2 analyzer was a Beckman Model 715 polarographic instrument. This instrument had two ranges (0-5 percent and 0-25 percent), was easily calibrated with air, and showed no significant interference to any of the other components in the flue gas at the existing concentrations.

In addition to these continuous analyzers, gas samples were periodically collected in 200 cc glass sample bulbs and analyzed for CO_2 and O_2 by use of an Orsat analysis kit.

A laboratory combustor was constructed to analyze for carbon in the fly ash samples. This combustor was a 3/4 inch diameter vycor tube enclosed in an electrical furnace. The carbon content of a given sample was determined by combusting a two gram sample at 1600°F for 30 minutes. The total CO_2 emitted was determined by absorption in ascarite.

3.2 Experimental Regeneration Apparatus

The experimental fluidized bed unit utilized to contact the partially sulfated lime with a simulated reducing gas is shown in Figure 3. The primary reaction which occurred in this regenerator is given by equation (3-1).

$$CaSO_4 + CO \longrightarrow CaO + CO_2 + SO_2 \qquad (3\text{-}1)$$

The reactor was a two inch ID alumina-ceramic tube. An inlet section of packed alumina cylinders, 1/8" x 1/8", served as a dispersing grid. The gasketed reactor tube ends were placed outside of a small Lindberg furnace, which kept the rubber gaskets at a low temperature so that they would perform through numerous cycles. The outlet from the fluid bed fed into an oxygen combustion chamber where any H_2S, COS or S that was formed could be combusted, and then into a cyclone, filter and water condenser.

As in the combustion experiments, the sulfur dioxide was measured by use of an infrared Beckman analyzer (IR 315A). The range of this instrument was 0 to 15 volume percent SO_2.

Figure 3
FLOW DIAGRAM FOR THE FLUIDIZED BED REGENERATION UNIT

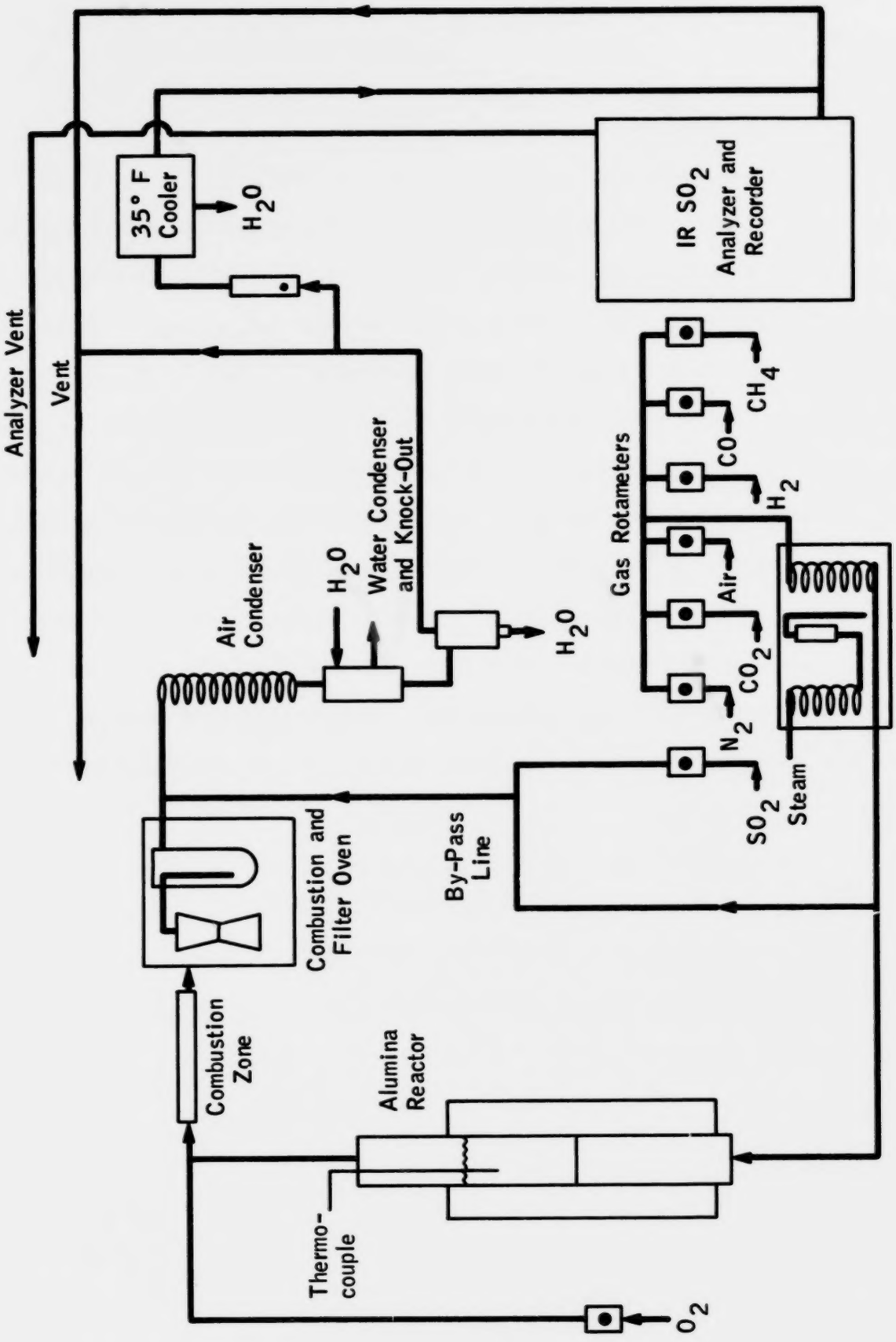

3.3 Feed Materials

3.3.1 Limestone

The limestone that was used in this study was obtained from the Grove Lime Company, Stephen City, Virginia. The chemical analysis of this stone is shown in Table 1. This material was ground, screened and batch calcined as required in the experimental program. The exact calcining procedure and conditions are given in Appendix 1. This calcining procedure was found to be simple and effective during previous studies under NAPCA Contract PH-86-67-130 and no attempt was made to further optimize this procedure. Precalcined stone was believed to be more representative of bed material in a regenerative process, since the feed rate of fresh stone to the combustor is expected to be small as compared to the feed rate of stone recycled from the regenerator. The particle size analyses for the two batches of calcined stone used in this program are shown in Figure 4.

Table 1

Composition of Limestone
Used In Esso FBC Program

Limestone - Grove BCR-1359

Component	Wt. Percent
CaO	97
MgO	1.16
SiO_2	1.07
Al_2O_3	0.29

3.3.2 Coal

The coal used was a high-volatile (A) bituminous coal from Northern West Virginia. It was obtained from the Humphrey Preparation Plant, Christopher Coal Company, a division of Consolidation Coal Company, Inc. The Bureau of Mines at Morgantown, West Virginia, obtained the coal from the preparation plant and subsequently shipped it to Esso. The chemical analysis of this coal is given in Table 2. The particle size analysis of the coal is given in Figure 4.

Table 2

Composition of Coal
Used in Esso FBC Program

Coal - Pittsburgh Bituminous (A)

Proximate Analysis		Ultimate Analysis	
Component	Wt. Percent	Component	Wt. Percent
Moisture	1.2	Ash	9.0
Volatile Matter	6.5	H	5.3
Fixed Carbon	53.3	C	74.1
Ash	9.0	N	1.3
		S	3.0
		O (by diff.)	7.3

3.3.3 Inert Bed Material

Abrasive-grade Alundum (20 mesh) was used as a bed material in selected runs. This material has been used by other investigators and is believed to have no effect on the SO_2 or NO_x emissions.

Figure 4

PARTICLE SIZE DISTRIBUTIONS OF LIMESTONE AND COAL FEEDS TO ESSO FBC

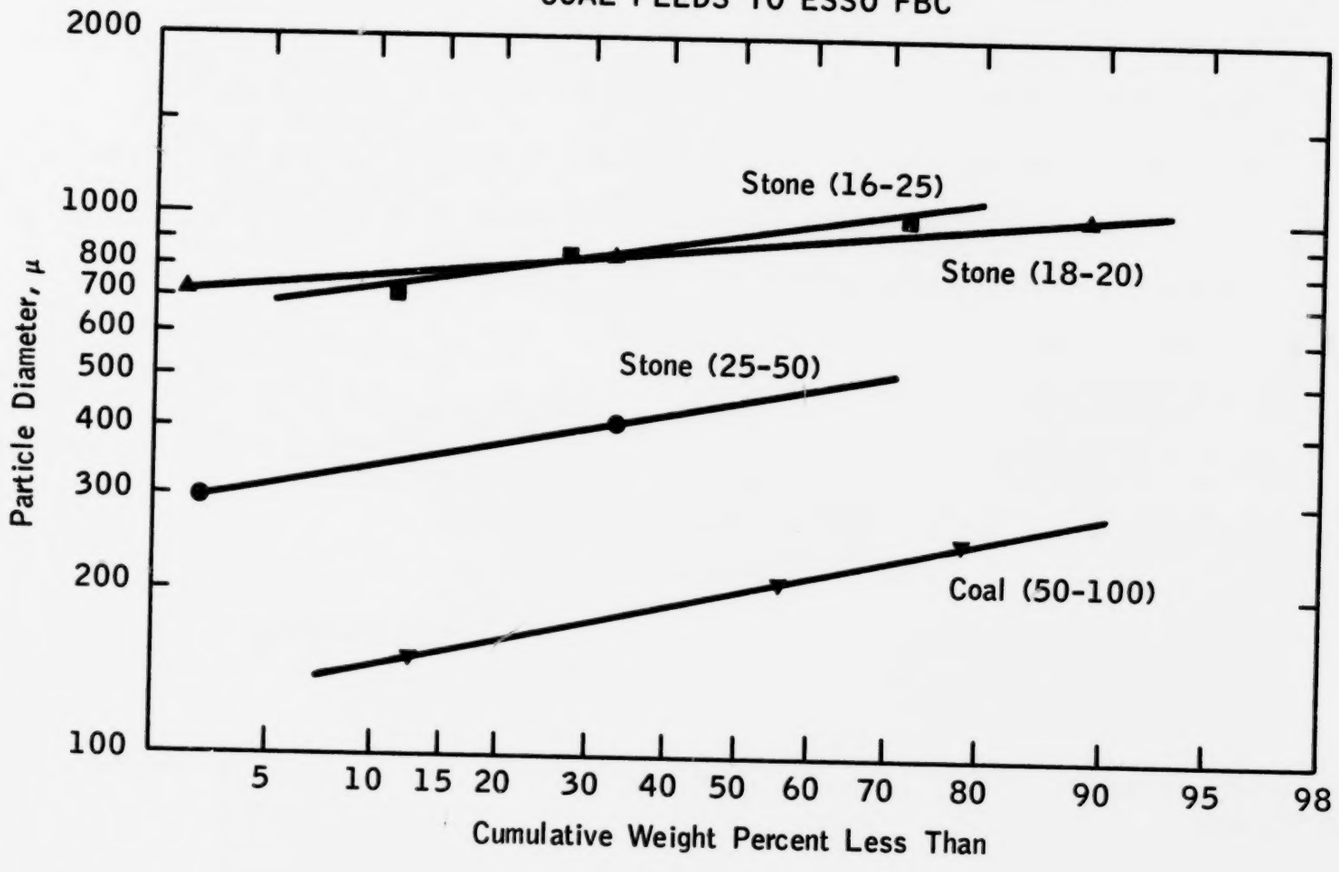

3.4 Range of Operating Variables

The range of operating variables examined in the Esso FBC program is shown in Table 3.

Table 3

Range of Operating Variables
Examined in Esso FBC

Operating Variable	Range
Bed Temperature	1500-1800°F
Settled Bed Height	4-16 inches
Superficial Gas Velocity	2-4 fps
Excess Air	3-50 percent
Average Stone Particle Diameter	460-930 μ
Average Coal Particle Diameter	200 μ

A summary of the operating conditions for each run and the results obtained is given in Appendix 2.

3.5 Experimental Procedure

The startup of the Esso FBC was accomplished by batch addition of the desired amount of calcined limestone to the unit and preheating the bed to approximately 1200°F. Upon reaching this temperature, coal feed to the unit was initiated. When the desired operating temperature of the unit was approached, the coal feed rate was adjusted to the desired operating rate and cooling water was introduced to the cooling coil for control of the bed temperature. A steady combustion condition was assumed to be attained when both the bed temperature and O_2 level in the flue gas stabilized.

Samples of the cyclone solids and bed solids were taken intermittently as the run progressed. At the termination of a run, samples of the bed and cyclone solids were also obtained. These solid samples were analyzed for carbon, sulfate, and sulfur, as desired.

In the regeneration studies, limestone particles were first sulfated by reaction with SO_2 in the combustor. A typical combustion run was of 5 to 5 1/2 hours duration. At the end of this period, the coal feed to the combustor was stopped and the bed temperature allowed to drop to room temperature. The bed was fluidized with N_2 during this period. The sulfated bed material was then withdrawn from the combustor and transferred to the regenerator. The regenerator was electrically heated to the desired operating temperature with a N_2 fluidizing gas. Upon reaching the operating temperature, the desired blend of reducing gases was introduced to the reactor. When the regeneration was complete, as evidenced by no SO_2 in the off gas, the reducing gases were replaced by N_2 and the bed allowed to cool. The regenerated bed material was then quickly transferred from the regenerator to a sealed vessel to minimize atmospheric exposure. The stone was now ready for another combustion-regneration cycle.

4. REACTOR COMBUSTION EFFICIENCY

High combustion efficiencies are required in modern power plants in order to minimize fuel costs and emission of air pollutants such as CO and hydrocarbons. Combustion efficiencies of 99 percent and greater are not uncommon for new pulverized coal power plants. Any new combustion technique, such as fluidized bed combustion, will also have to attain high combustion efficiencies in order to be economically competitive with conventional combustion techniques.

The efficiency of a combustion process can be defined as follows:

$$E = 1 - h_o/h_i \qquad (4\text{-}1)$$

where h_o = heating value of unburned fuel components, BTU (includes unburned carbon, CO, hydrocarbons, etc.)

h_i = heating value of fuel fed to system, BTU

E = combustion efficiency, dimensionless

In the experimental system examined in this study, the carbon loss in the fly ash ranged from 3 to 10 percent of the input carbon. Relative to this loss, the contribution of the gaseous losses (CO and hydrocarbons) to h_o was small. Hence, the carbon loss in the fly ash as a percent of the carbon fed was used in this study to approximate the reactor combustion efficiency as follows:

$$E' = 100 - L \qquad (4\text{-}2)$$

where E' - combustion efficiency, percent

L = carbon loss in fly ash as a percent of the carbon fed.

4.1 Effect of Gas-Solid Contacting

Tests conducted in a cold model of the Esso FBC (three inch diameter) indicated that slugging occurred over the entire range of gas velocities examined in the high temperature unit (see Table III). Slugging is defined as a type of fluidization in which the diameter of the gas bubbles becomes equal in size to the diameter of the containing vessel. In the operations with relatively low bed heights (four and six inches), the gas slugs did not attain the height that was attained in deeper bed. The gas distributor used in this study, shown in Figure 5, probably led to the formation of small bubbles near the grid and these small bubbles did not completely coalesce in the shallow beds.

Figure 5

GRID USED IN ESSO FBC

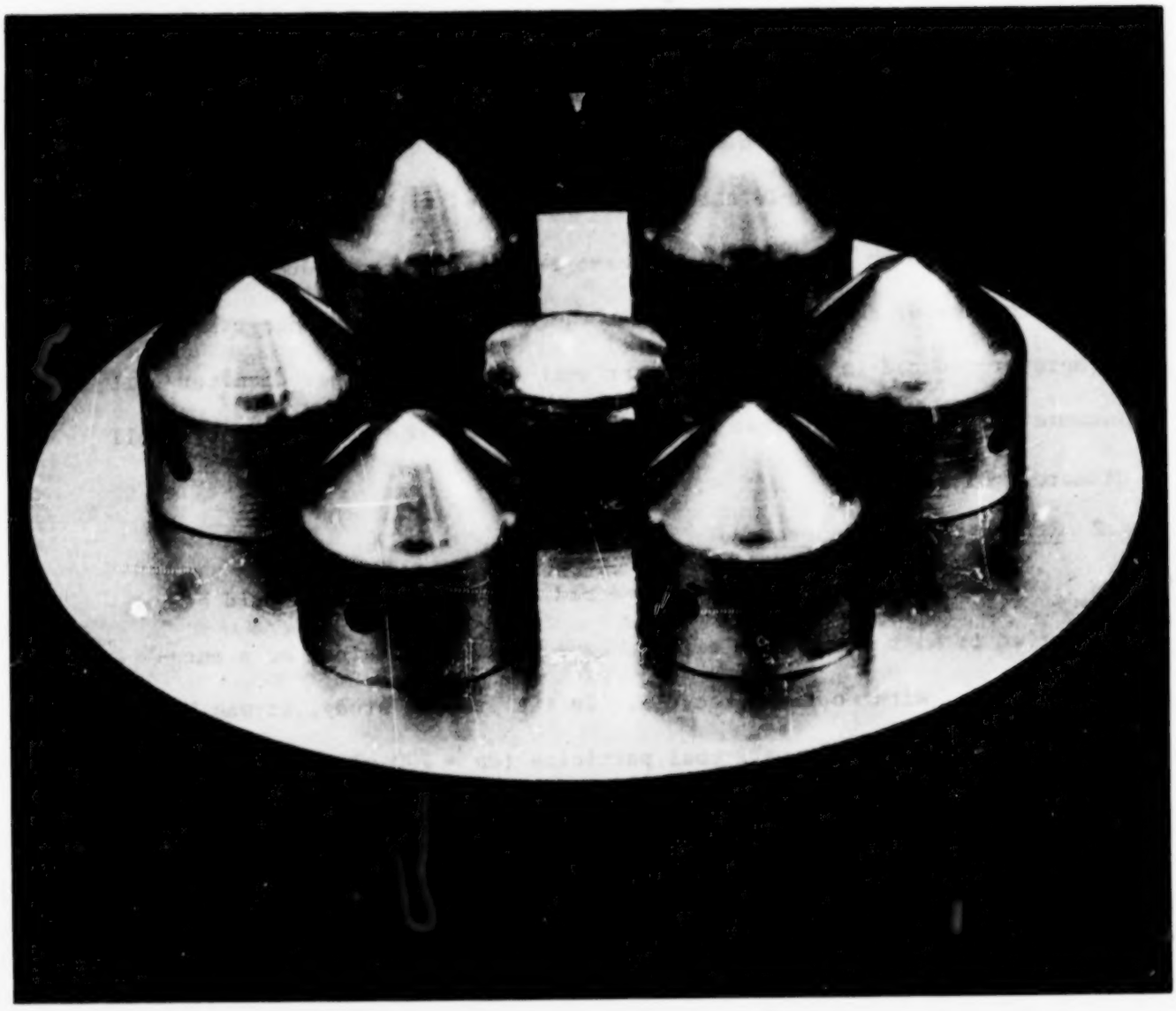

The effect of slugging upon the combustion efficiency of the Esso FBC is believed to be a reduction in the coal particle residence time in the bed as compared to a non-slugging unit. In a nonslugging unit, the residence time of the small coal particles in the bed would be many times the gas transit time due primarily to particle-particle collisions. However, if a coal particle entered a slug phase, it would be quickly transferred through the slug to the next emulsion phase, reducing the overall residence time of the coal particle in the bed. This residence time effect is more pronounced in a small diameter unit than in a larger diameter unit because of the reduced verticle solid mixing rates characteristic of small diameter units (1).

4.2 Effect of Bed Temperature

The operation of a fluidized bed combustion system would be simplified if high combustion efficiencies could be obtained on a once-through basis, with no fines recycle. In the present study, it was believed that the combination of small coal particles ($\bar{d}p$ = 200 μ) and high temperatures might enable us to attain combustion efficiencies in the 99 percent range.

The reactor combustion efficiency of the Esso FBC was examined over a temperature range of 1500 to 1800°F. The results obtained for a constant set of operating conditions are shown in Figure 6. The efficiency increased from 91 percent at 1500°F to 97 percent at 1800°F.

Figure 6

INCREASING BED TEMPERATURE DECREASES THE CARBON LOSS IN THE FLYASH

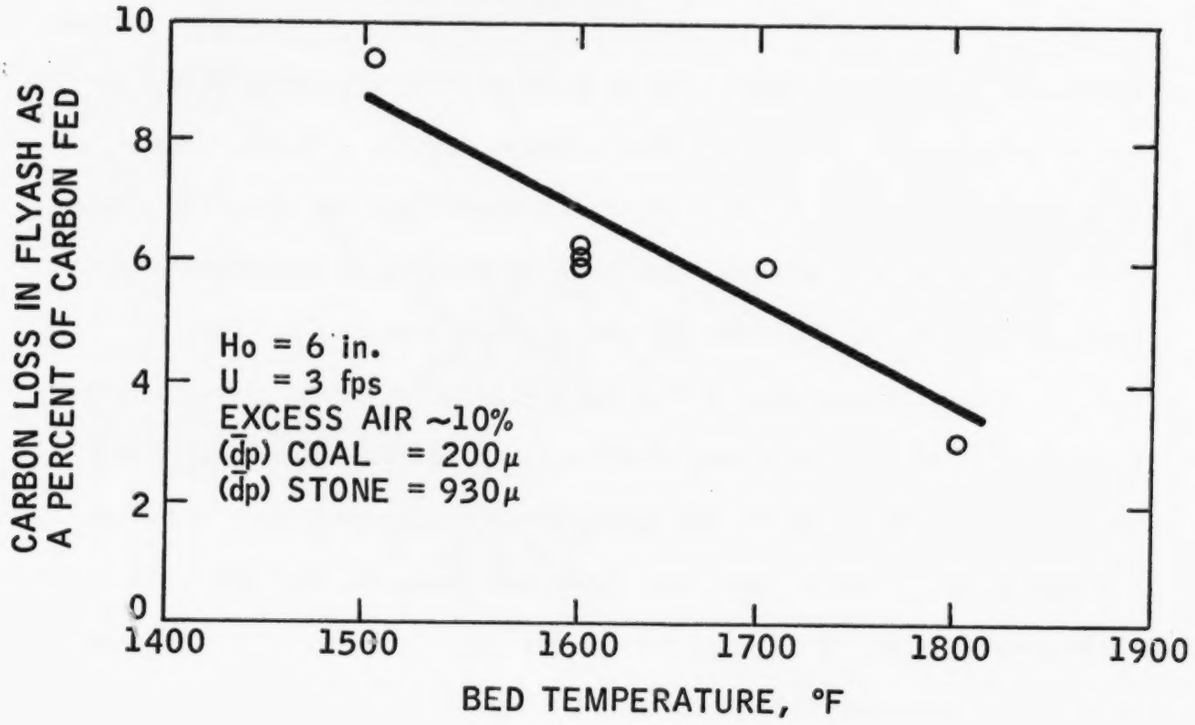

As previously discussed, a commercial vessel operating at a combustion efficiency of 97 percent and less would probably not be economically competitive with conventional combustion techniques. Hence, if the results of the present study are taken as a rough estimate of the combustion efficiency to be expected in a commercial unit, some method would have to be employed to reduce the carbon loss in the fly ash. Two methods have been advanced for reducing the loss of solid combustible in a fluidized bed combustor. One method involves recycling the carbon-bearing fly ash back to the combustor. An experimental study by Williams, et. al. (2) using a coal with a weight median average particle diameter of 320 μ showed that carbon losses of less than 0.5 percent were attained in a six inch diameter fluidized bed combustor operating at 1470°F

with fines recycle. This low carbon loss was sustained over an excess air of 5 to 30 percent. The coal used by Williams had a much higher concentration of fines (23 percent less than 66 μ) than the coal being used in the present Esso study (0.3 percent less than 74 μ). Hence, it would be anticipated that recycle of the fines from the Esso FBC (which should have a larger particle size than those used by Williams) should reduce the carbon loss in the fly ash to less than one percent.

Pope, Evans, and Robbins is examining a second system which involves the use of a separate fluidized bed (carbon burnup cell) for completion of combustion of the carbon-bearing fly ash (3). Although no experimental studies have been conducted using the fly ash from finely ground coal, it is anticipated that this concept also could be successfully applied to the proposed Esso system.

4.3 Effect of Gas Velocity

The reactor combustion efficiency was examined as a function of superficial gas velocity over the range of 2 to 4 fps. As shown in Figure 7, the efficiency increased with decreasing gas velocity. This result reflects a longer coal particle residence time within the bed at the lower velocities. The effect of gas velocity is probably more pronounced when using finely ground coal, as in the present study, than in other studies using crushed coal, because of the greater coal residence time dependence upon superficial gas velocity when using finely ground coal.

Figure 7

CARBON LOSS IN FLY ASH INCREASES WITH INCREASING GAS VELOCITY

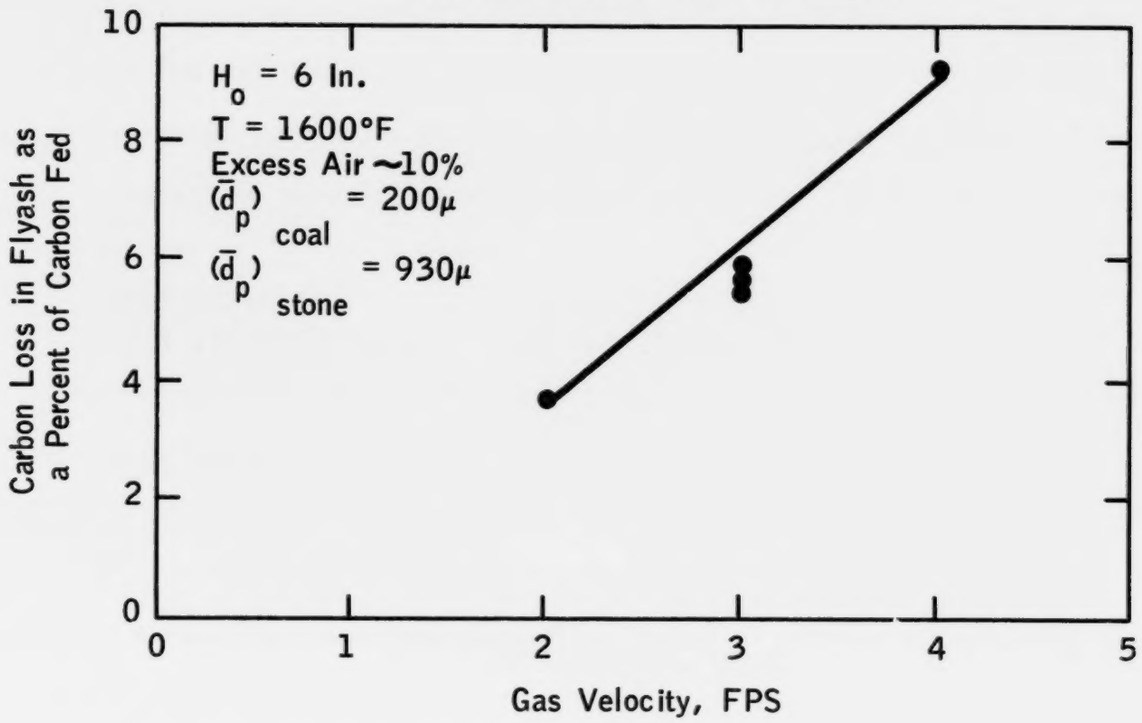

Increasing the superficial gas velocity in a fluidized bed combustor (at a constant temperature and excess air) reduces the plane area requirements of the combustor. It may be economically desirable in terms of initial investment to operate at higher gas velocities (8-10 fps) than have been examined in this study. However, the results of this study indicate that the combustion efficiency, on a once-through basis, will be adversely affected by an increase in superficial gas velocity. As discussed in Section 4.1, recycle of the fly ash back to the combustor or the use of a carbon burnup cell could increase the overall combustion efficiency of the unit and, hence, make the carbon loss on a once-through basis insignificant. However, the utility of these two concepts must be tested with the fly ash from a given unit before a specific conclusion can be drawn.

4.4 Effect of Excess Air

The effect of excess air on reactor combustion efficiency is illustrated in Figure 8. Both carbon loss in the fly ash and CO content of the flue gas are shown. Little effect of excess air was observed in the 7 to 30 percent range, but decreasing the excess air below approximately seven percent did significantly decrease the combustion efficiency.

Figure 8

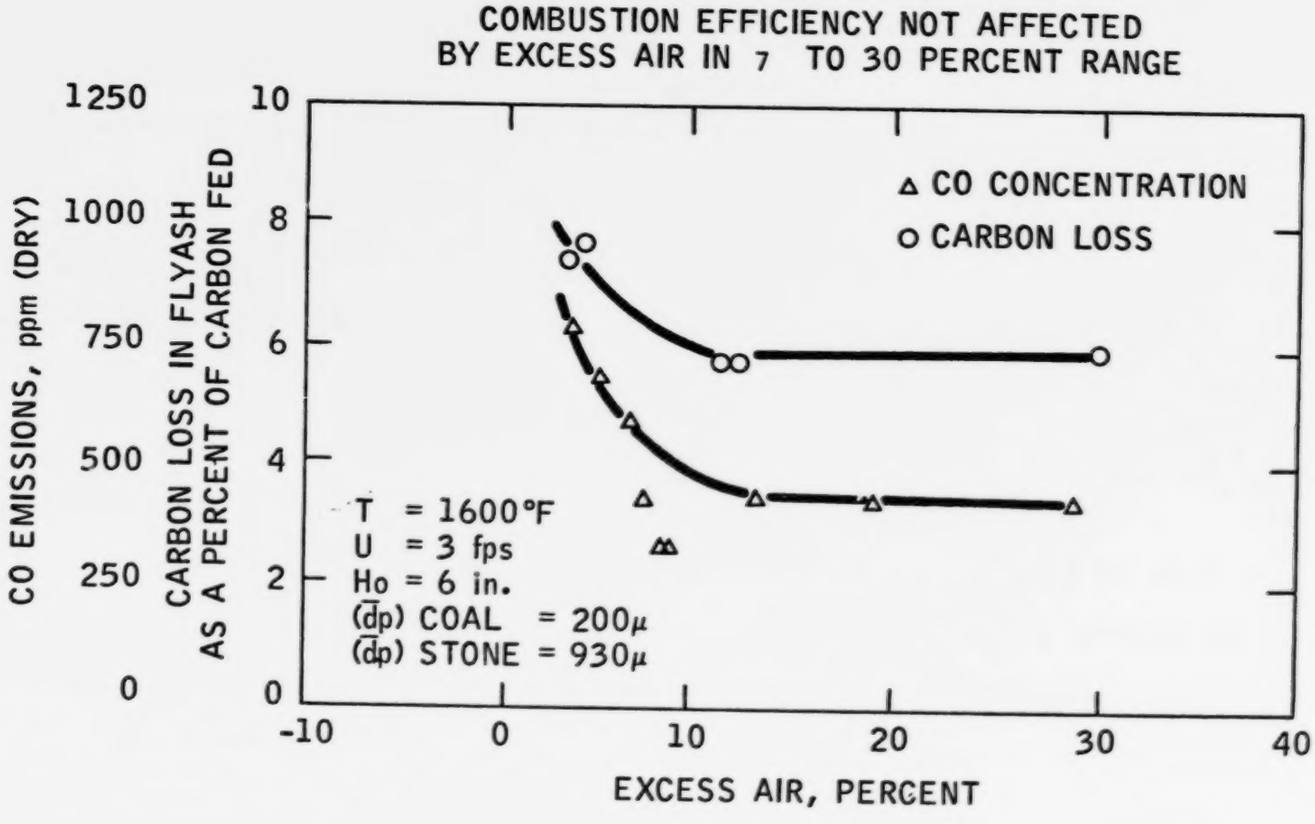

At lower excess air levels, localized reducing conditions can occur. In these reducing regions, carbon combustion rate decreases, due to a deficiency of oxygen, and the reaction

$$C + CO_2 \longrightarrow 2\ CO \qquad (4\text{-}3)$$

is promoted, resulting in higher CO concentrations. The gas-solid contacting pattern in a given unit will probably dictate the excess air level at which localized reducing conditions become severe enough to affect the overall combustion efficiency. In the small Esso combustor, this limiting excess air level appeared to be approximately seven percent; in a larger unit with better gas-solid contacting efficiency, it is anticipated that the limiting excess air level would be lower.

4.5 Effect of Bed Height

The data shown in Figure 9 illustrate that increasing the settled bed height in the Esso FBC increased the carbon loss in the fly ash. This result shows that the additional bed height did not yield an increase in the amount of reaction occurring. Instead an actual decrease in the overall system performance was observed. This decreasing performance is believed to be a consequence of poorer gas-solid contacting efficiency obtained as bed height was increased. This same type of system performance, although not frequently encountered, has been observed by Esso engineers in other fluidized bed systems.

Figure 9

CARBON LOSS INCREASES WITH BED HEIGHT

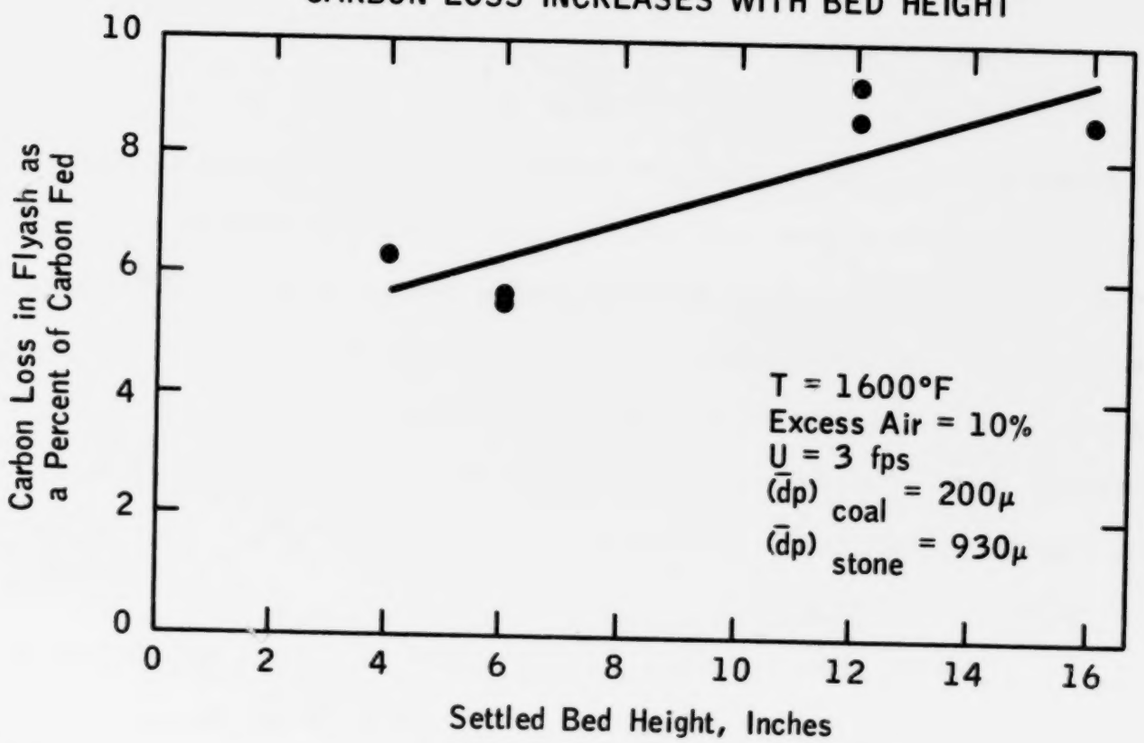

Another contributing factor to the higher carbon losses in the operations with deep beds was the reduced disengaging height. When using a 16 inch settled bed height, for example, the maximum expanded bed height was approximately 32 inches (at 3 fps). Slugs of solids were thrown as high as 48 inches, thus filling the entire three inch diameter reactor. In this case, the only disengaging space was the seven inch diameter, eighteen inch high expanded section. Hence, coal particle elutriation was greater in this case than in operations with less deep beds.

4.6 Effect of Lime Particle Size

The percentage carbon loss in the fly ash was not changed by varying the average stone particle diameter from 930 μ to 460 μ, as illustrated in Figure 10. However, a run with a relatively narrow stone particle size distribution ($\bar{d}p$ = 880 μ) did result in a greater carbon loss, apparently reflecting the commonly observed phenomenon that fluidized beds with narrow particle size distributions do not fluidize as smoothly as beds with broader distributions.

Figure 10

SMALL VARIATION IN CARBON LOSS IN FLYASH WITH BED PARTICLE SIZE

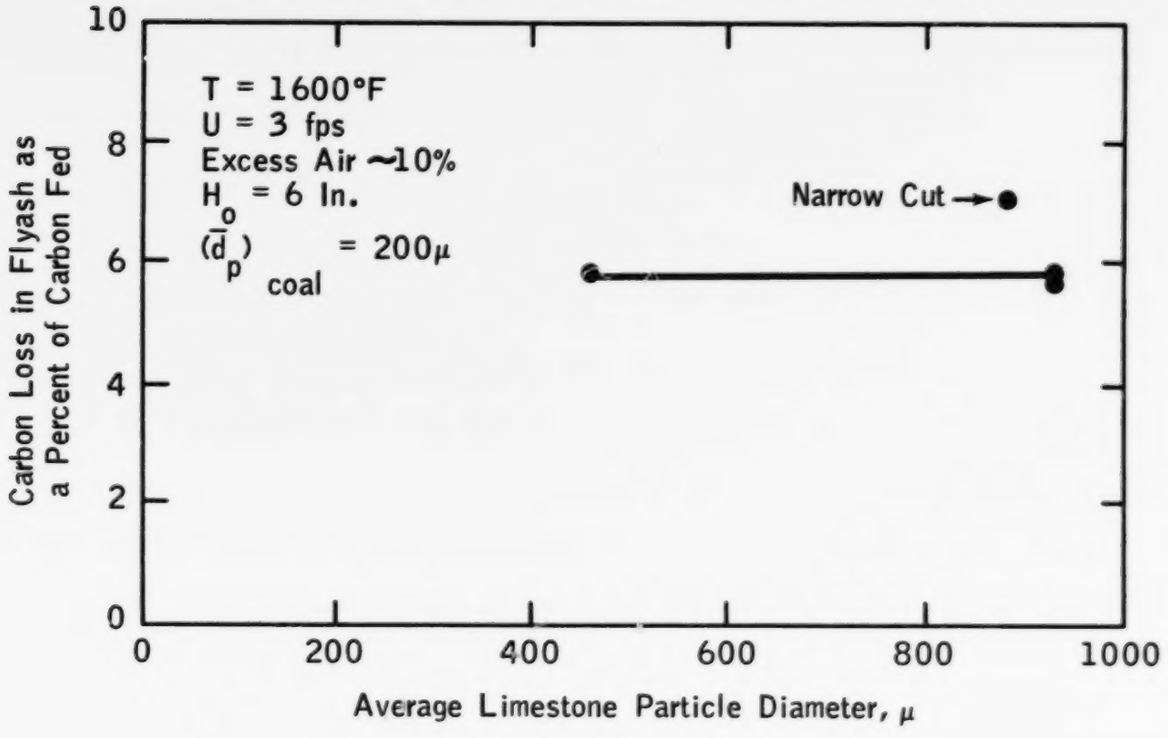

5. FLUE GAS DESULFURIZATION IN NON-CYCLIC OPERATIONS

In the proposed Esso system, finely ground coal is combusted in a bed of larger limestone particles. The fly ash from the coal is entrained from the system, leaving a bed composed primarily of limestone. The sulfated limestone is transferred from the combustor to a fluid bed regenerator in which the fluidizing gas is a reducing gas. In the regenerator, $CaSO_4$ is converted back to CaO which is returned to the combustor for further use.

High desulfurization efficiencies must be obtained under practical operating conditions of a fluidized bed combustor in order to make this system feasible as an SO_2 pollution abatement method. Also, the capacity of a given limestone, in terms of the fraction of the CaO which will react with SO_2 in yielding a given reduction of SO_2 emissions, must be reasonably high. In the following sections, the experimental desulfurization and stone capacity results obtained in the Esso FBC program while using fresh stone (non-cyclic operations) are reported.

5.1 Esso FBC Operation and Typical Desulfurization Data

The Esso FBC was batch-charged with calcined limestone at the beginning of a run and no limestone was added thereafter. Coal was continuously fed to the unit. The high reactivity* of the stone at the beginning of a run resulted in essentially complete initial flue gas desulfurization. As the run progressed and the stone became sulfated, the reactivity of the stone decreased. This decreasing stone reactivity is generally attributed

---

* Ability to react with SO_2

to the buildup of a shell of $CaSO_4$ on the particles which inhibits the diffusion of the SO_2 into the inner core of CaO. As stone reactivity decreased, a point was reached where the total capacity of the stone in the bed was no longer sufficient to retain all of the SO_2 formed, and SO_2 was emitted in the flue gas. A typical example of the SO_2 gaseous emissions is shown in Figure 11. The upper line shown is the SO_2 emission level which would be expected in the absence of control, assuming sulfur and carbon are combusted to an equal extent. The data were generally replotted in the form shown in Figure 12. In this form, the stone capacity for a given SO_2 removal efficiency can be compared for different unit operating conditions.

For this study, the curve shown in Figure 12 was characterized by specifying the CaO utilization at 20 percent SO_2 breakthrough. This method of data reduction is based on the assumption that only CaO reacts with SO_2 in the temperature range examined; as shown in a previous Esso study (4), MgO does not react to a significant extent. The CaO utilizations at 0, 10 and 20 percent SO_2 emission are tabulated in Appendix 2 for all experimental operations.

Figure 11

TYPICAL DESULFURIZATION DATA

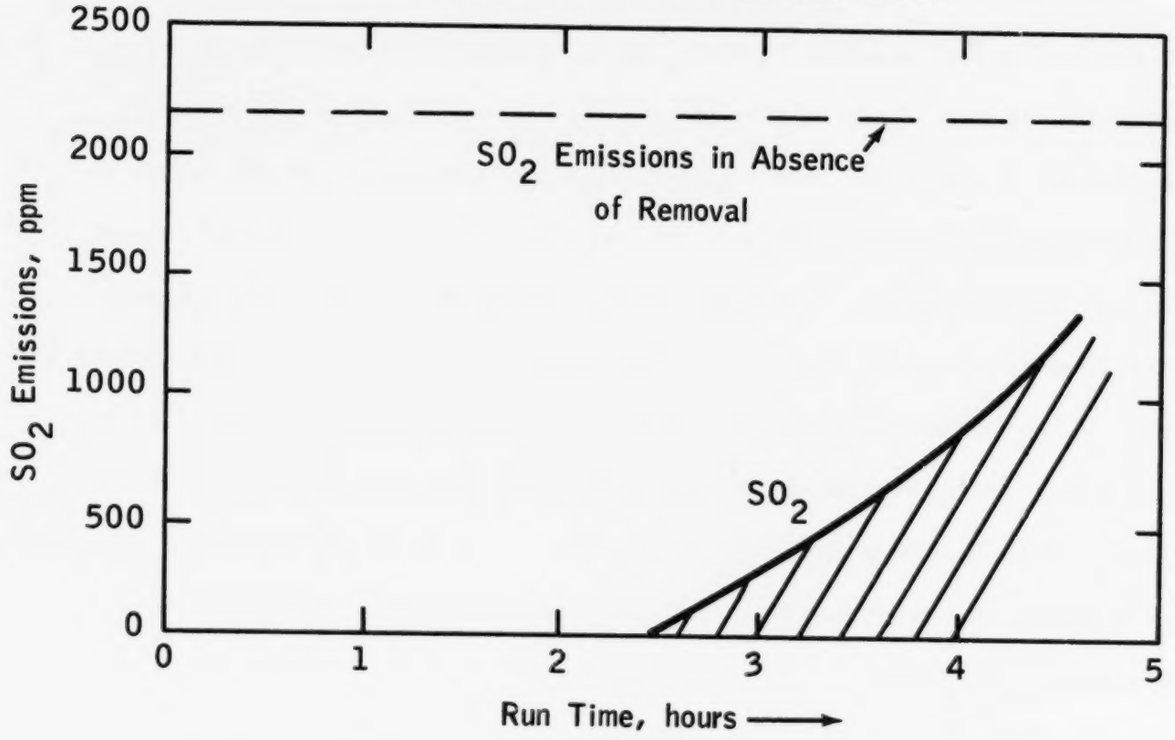

Figure 12

DESULFURIZATION DATA IN FORM TO ALLOW COMPARISON

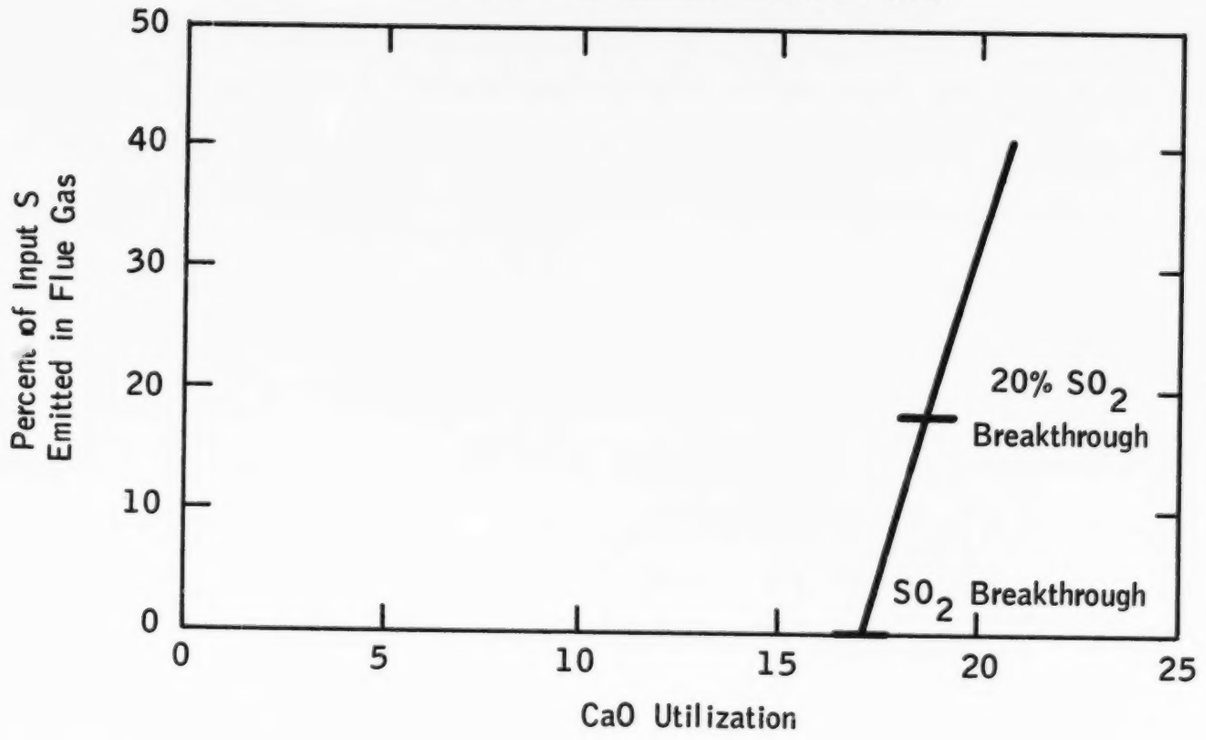

The normal method of determining the CaO utilization of the stone was as follows: (1) the total sulfur input was determined by monitoring the input coal rate and knowing the sulfur content of the coal, (2) the sulfur out in the gas was determined by graphically integrating the chart shown in Figure 11 (the shaded area represents the SO_2 emissions), (3) the percent of input sulfur emitted in the fly ash was assumed to be the same as the percent of input carbon emitted in the fly ash (which was experimentally verified), and (4) all input sulfur not emitted in the fly ash or flue gas was assumed to be retained by the bed as $CaSO_4$. An independent check on this method of calculating the CaO utilization was made by analytically determining the sulfur content of the discharged bed material from selected runs. Details of this comparison are given in Appendix 3 .

5.2 Effect of Excess Air

Decreasing the excess air increased the stone capacity in the Esso FBC, as illustrated in Figure 13. A likely explanation for this result is suggested by studies by Coutant, et al (5) indicating that $CaSO_3$ is a reaction intermediate in the formation of $CaSO_4$. The following reaction sequence is suggested by this work:

$$CaO + SO_2 \longrightarrow CaSO_3 \qquad (5\text{-}1)$$

$$CaSO_3 \longrightarrow CaO + SO_2 \qquad (5\text{-}2)$$

$$CaSO_3 + 1/2O_2 \longrightarrow CaSO_4 \qquad (5\text{-}3)$$

In the absence of an O_2 molecule, the $CaSO_3$ can decompose by reaction (5-2) to liberate SO_2. If this decomposition occurs in a pore, the SO_2 can then react with an adjacent active site (CaO) located deeper in the pore. Hence, this reaction-decomposition mechanism provides a "lubricating" action for SO_2 to penetrate deeper into the sorbent pore thereby increasing the capacity of the stone. However, if a large excess of O_2 molecules exists, the $CaSO_3$ is quickly stabilized as $CaSO_4$ by reaction (5-3), the reaction-decomposition mechanism does not occur, and the capacity of the stone is reduced.

Figure 13

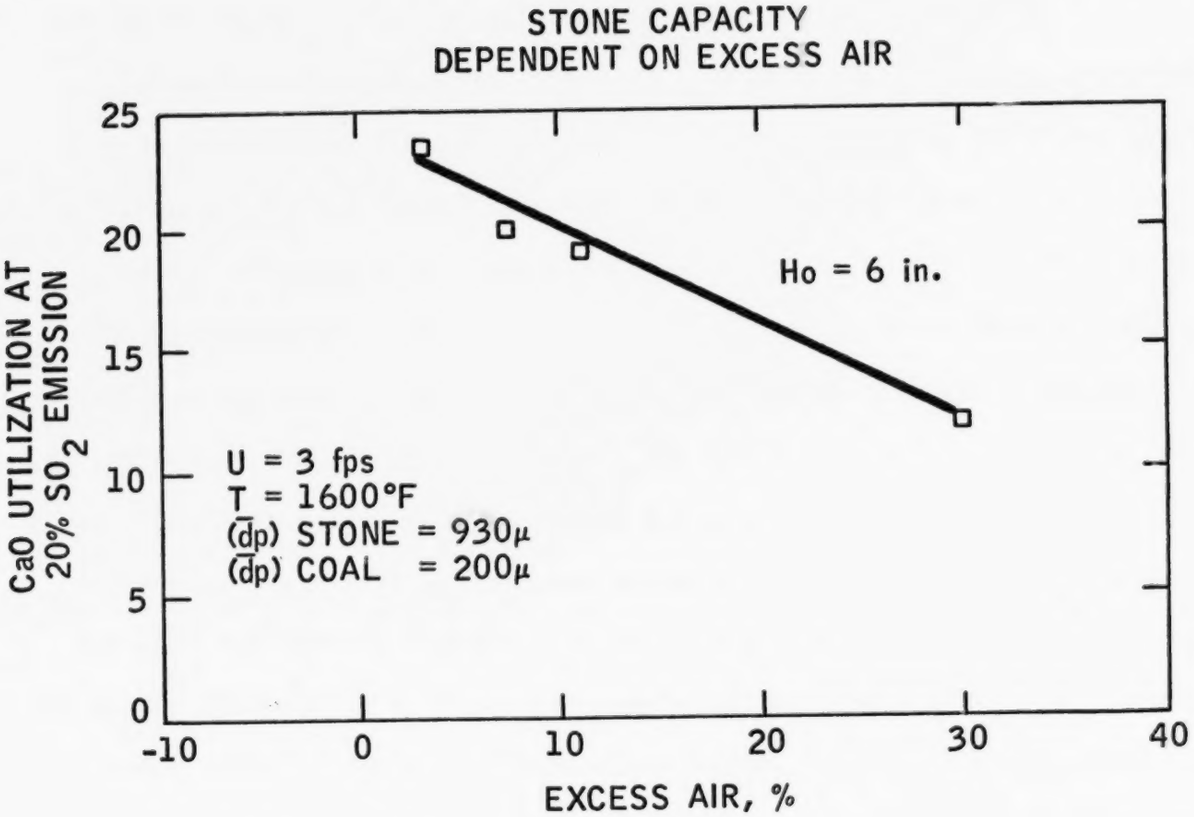

In a previous Esso study (4), we found that calcined limestone would react with SO_2 in the absence of oxygen (N_2 carrying gas) and that the SO_2 capacity of a given batch of stone was increased in the absence of oxygen. These results were obtained at 1600°F. Hence, although $CaSO_3$ is not thermodynamically stable at 1600°F, apparently the kinetics of the decomposition reaction are relatively slow so that a "semi-stable" species can exist. Another explanation might be that $CaSO_3$ is not formed but that SO_2 is physically adsorbed on the lime. Regardless of the reactions occurring, this result is in qualitative agreement with the observation that high excess air levels decrease the stone capacity.

5.3 Effect of Limestone Particle Size

Decreasing the average particle diameter of the stone increased the stone capacity significantly. Two particle sizes were utilized; a 460 μ and a 930 μ average particle diameter. The CaO utilization of the of the larger stone (930 μ) at 80 percent SO_2 removal was 19 percent; the corresponding utilization of the smaller stone was 32 percent. These results were obtained at the following unit operating conditions: bed temperature = 1600°F, settled bed height = 6 inches, excess air = 9 percent, superficial gas velocity = 3 fps and ($\bar{d}p$) coal = 200 μ. Hence, the indication is that decreasing the average stone particle size will significantly decrease the amount of limestone which must be fed to achieve a given SO_2 reduction. The higher the superficial gas velocity through the bed, the greater the particle size of the stone must be in order to avoid excessive entrainment; an economic trafeoff must be made between the lower stone feed rates obtainable with smaller lime particles and the smaller plane area requirements for the reactor at higher gas velocities.

5.4 Effect of Temperature

The effect of temperature upon the flue gas desulfurization is illustrated in Table 4. The indication is that temperature had little effect on the stone capacity over the temperature range of 1600 to 1800°F. Decreasing the bed temperature to 1500°F did apparently significantly decrease the stone capacity. However, it should be pointed out that the run at 1500°F showed considerable variation in the bed temperature and this may have adversely affected the desulfurization.

A comparison between the results in Table 4 is further complicated by the differing excess air levels. As shown in Section 5.2, decreasing the excess air increased the stone capacity.

Table 4

EFFECT OF BED TEMPERATURE ON STONE CAPACITY

Run No.	Bed T, °F	Excess Air, %	CaO Utilization At 20% SO_2 Emission
8	1500	12.6	10.5
3	1600	10.7	19
14	1600	11.6	16.5
25	1600	7.4	19.8
28	1700	7.4	22
27	1800	15.5	21.3

5.5 Effect of Gas Velocity

The stone capacity was approximately the same at superficial gas velocities of 2 fps and 3 fps, as illustrated in Figure 14. However, increasing the gas velocity to 4 fps resulted in a lower CaO utilization at the SO_2 breakthrough point and a more gradual breakthrough curve. The lower CaO utilization at SO_2 breakthrough is a result of the decreased gas-solid contact time at the higher velocity. The 3 fps utilization at breakthrough is lower than the 2 fps utilization, which reflects this same phenomenon.

An increased stone particle decrepitation occurred in the 4 fps run as compared to the 3 fps run, as shown in Figure 15. The result of this decrepitation was the creation of smaller stone particles; as shown in Section 5.3, reducing the stone diameter increased stone capacity. The particle decrepitation is believed to occur gradually throughout the run, resulting in a continual creation of smaller stone particles. The gradual breakthrough curve of the 4 fps is believed to reflect this particle decrepitation phenomenon.

Figure 14

INCREASING GAS VELOCITY CHANGES
BREAKTHROUGH CHARACTERISTICS

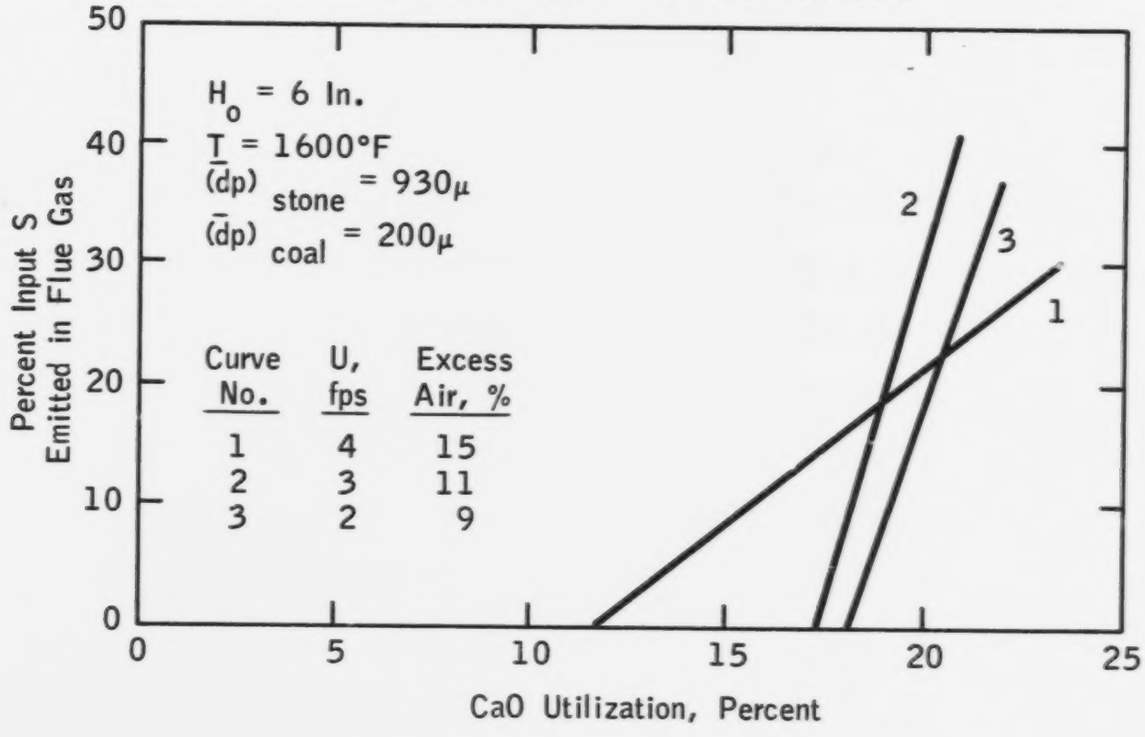

Figure 15

INCREASING SUPERFICIAL GAS VELOCITY
INCREASES STONE ATTRITION

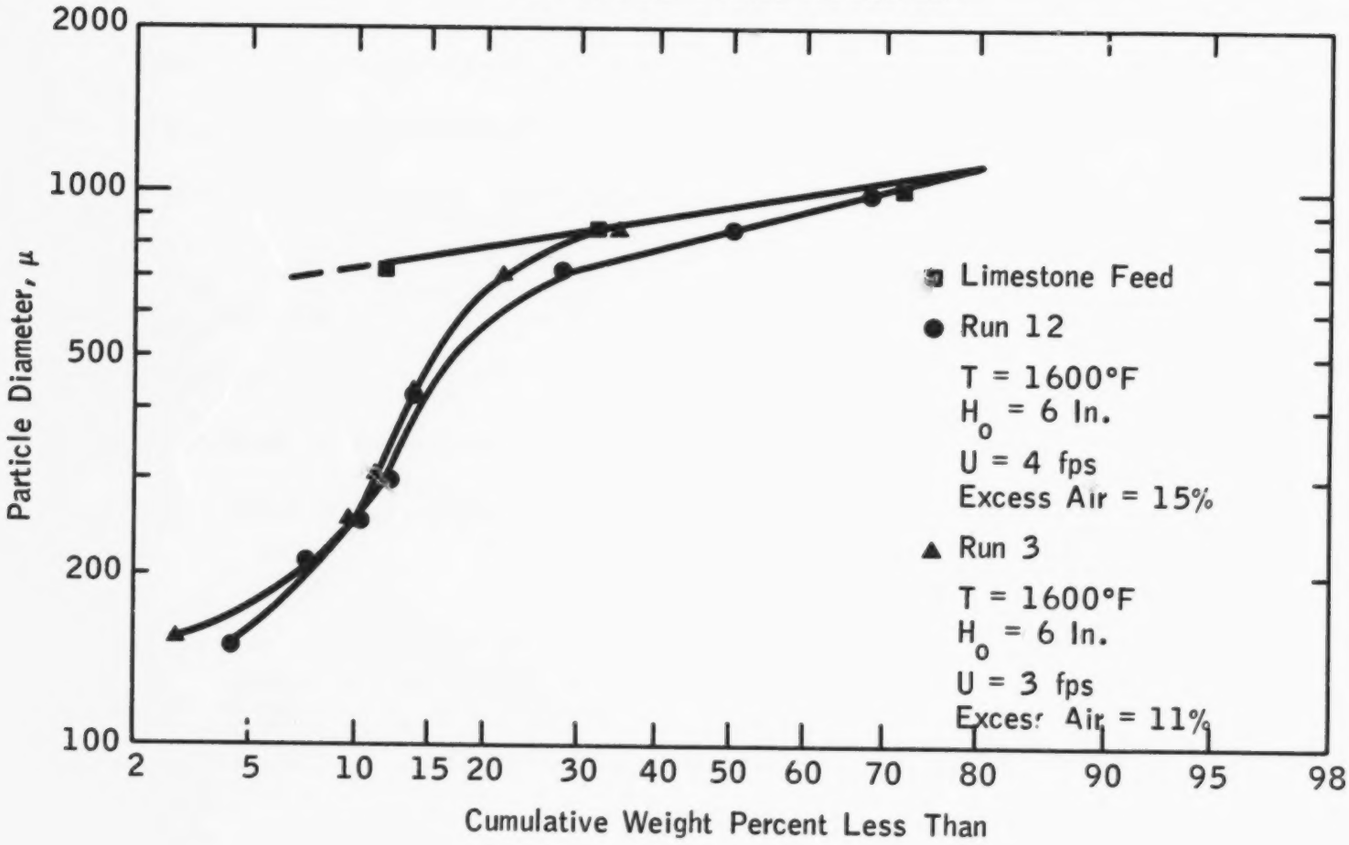

5.6 Effect of Settled Bed Height

Increasing the settled bed height of the Esso FBC decreased the CaO utilization at 20% SO_2 breakthrough, as shown in Figure 16. For a constant gas-solid contacting efficiency, it would be anticipated that increasing the settled bed height would allow the same SO_2 removal with sorbent less active than that in the shorter bed. The opposite effect was observed in the present study.

This negative effect of bed height was also observed when examining the combustion efficiency of the Esso FBC, as discussed in Section 4.5. The explanation for both of these effects appears to be that the gas-solid contacting efficiency of the Esso FBC decreased as bed height was increased.

Figure 16

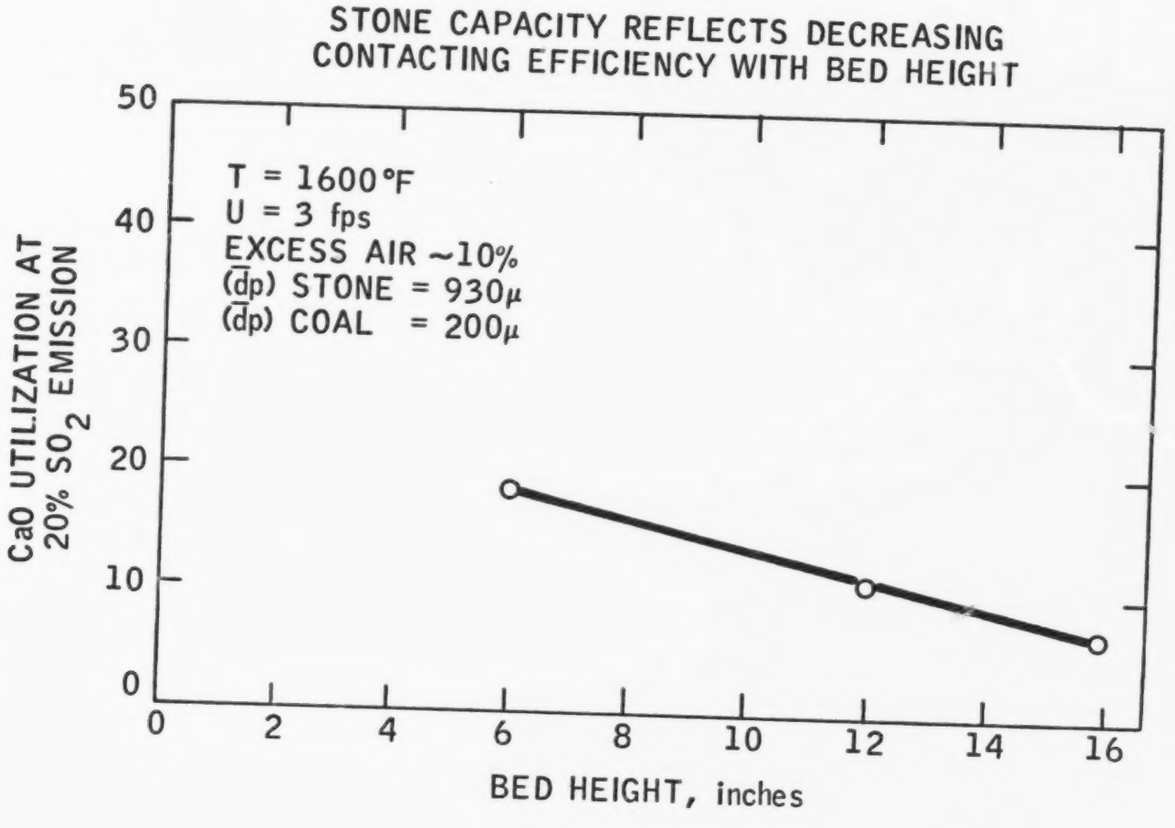

The Esso FBC operated in the slugging regime. At the lower settled bed heights examined (four and six inches) apparently the bubbles did not attain as a great a height as in the deeper beds (12 and 16 inches), and less bypassing of the solids occurred. In the deeper beds, a greater fraction of the gas passed through the bed in the bubble phase, which caused poorer desulfurization at a given stone reactivity (utilization).

5.7 Kinetic Analysis of $CaO-SO_2-O_2$ Reaction System

A first order kinetic model for the $CaO-SO_2-O_2$ reaction system was developed in a previous Esso study (4) under NAPCA contract PH 86-67-130. The model was based on the assumptions of complete mixing of the solids and plug flow of the combination gas. Details of the model development are given in Appendix 4. The integrated model resulted in the following rate equation:

$$\ln(C_H/C_o) = -R(X)\ (H_o/U) \qquad (5\text{-}4)$$

where H_o = settled bed height

U = superficial gas velocity

C_H = outlet SO_2 concentration

C_o = inlet SO_2 concentration

$R(X)$ = first order rate constant (function of sorbent utilization, X)

5.7.1 Location of SO_2 Release in the Bed

The experimental data obtained in the present fluidized bed combustion study were reduced to the kinetic rate constants described above. A comparison between the rate constants determined from the present research and those obtained from the previous Esso desulfurization study is shown in Figure 17. In the previous study, a simulated flue gas was fed to the reactor (three inch diameter) so that all of the SO_2 was available for reaction at the reactor inlet. In the present study, the location of SO_2 release was dependent upon where the coal was combusted in the bed.

Figure 17

SO_2 FORMATION OCCURS PRIMARILY NEAR REACTOR INLET

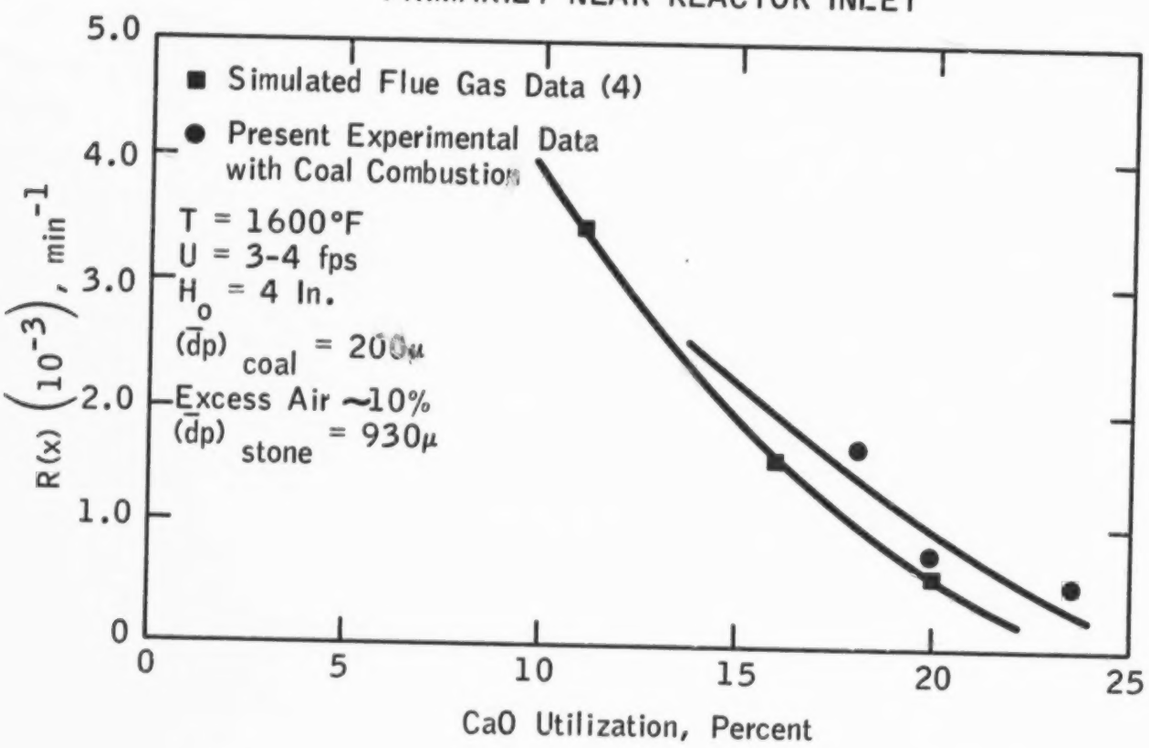

The close agreement between the results shown in Figure 17 indicates that a large fraction of the SO_2 from the burning coal was released near the reactor inlet.

5.7.2 Effect of Stone Particle Size on R (X)

Decreasing the average stone particle size caused a significant increase in R (X), as shown in Figure 18. The functional dependency for N-1359 at 20 percent CaO utilization was found to be

$$R \alpha \bar{d}p^{-1.3}$$

which is in agreement with results reported by Skopp (4) in simulated gas operations.

Figure 18

EFFECT OF STONE PARTICLE SIZE ON KINETIC CONSTANTS

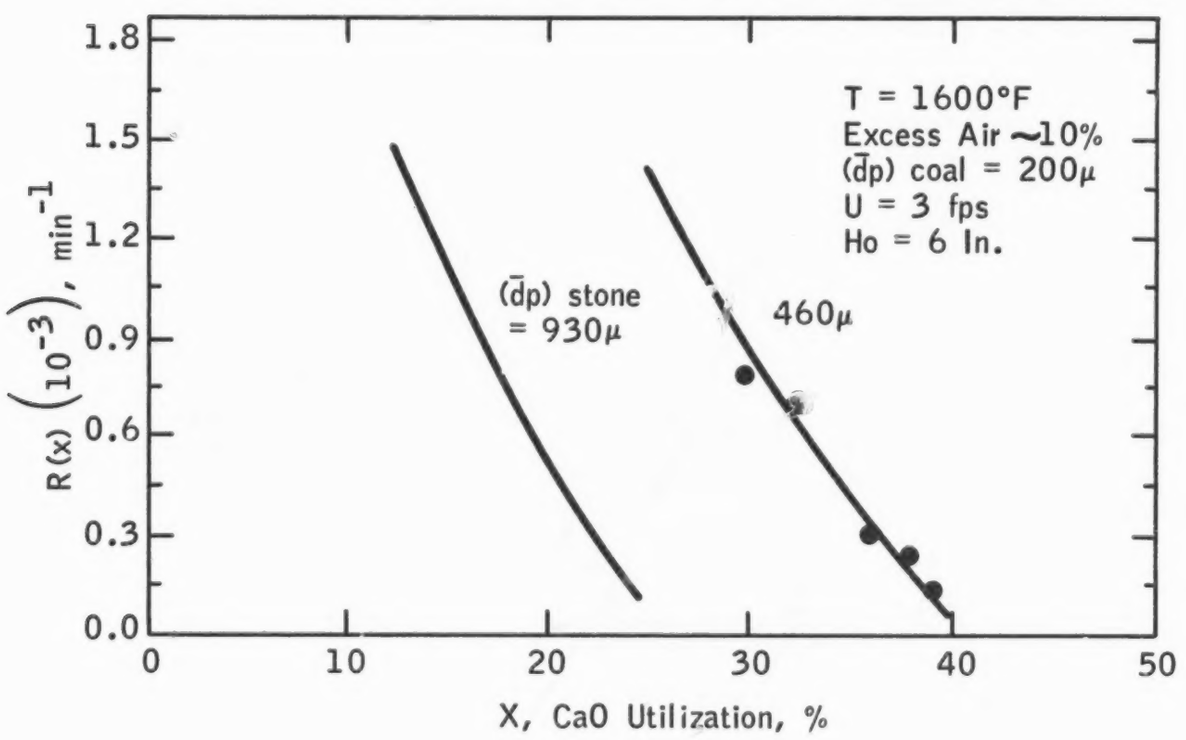

5.7.3 Effect of Settled Bed Height on R (X)

Increasing the settled bed height caused a reduction in R (X) as illustrated in Figure 19. The same system behavior was observed in the previous Esso flue gas desulfurization study (4) and is a reflection of the poorer gas solid contacting efficiency which resulted as bed height was increased, as discussed in Section (5.6). There was no apparent effect of superficial gas velocity, over the range of 2 to 4 fps, on R (X), as shown in the results with a six inch settled bed depth.

Figure 19

KINETIC CONSTANTS FROM ESSO DATA

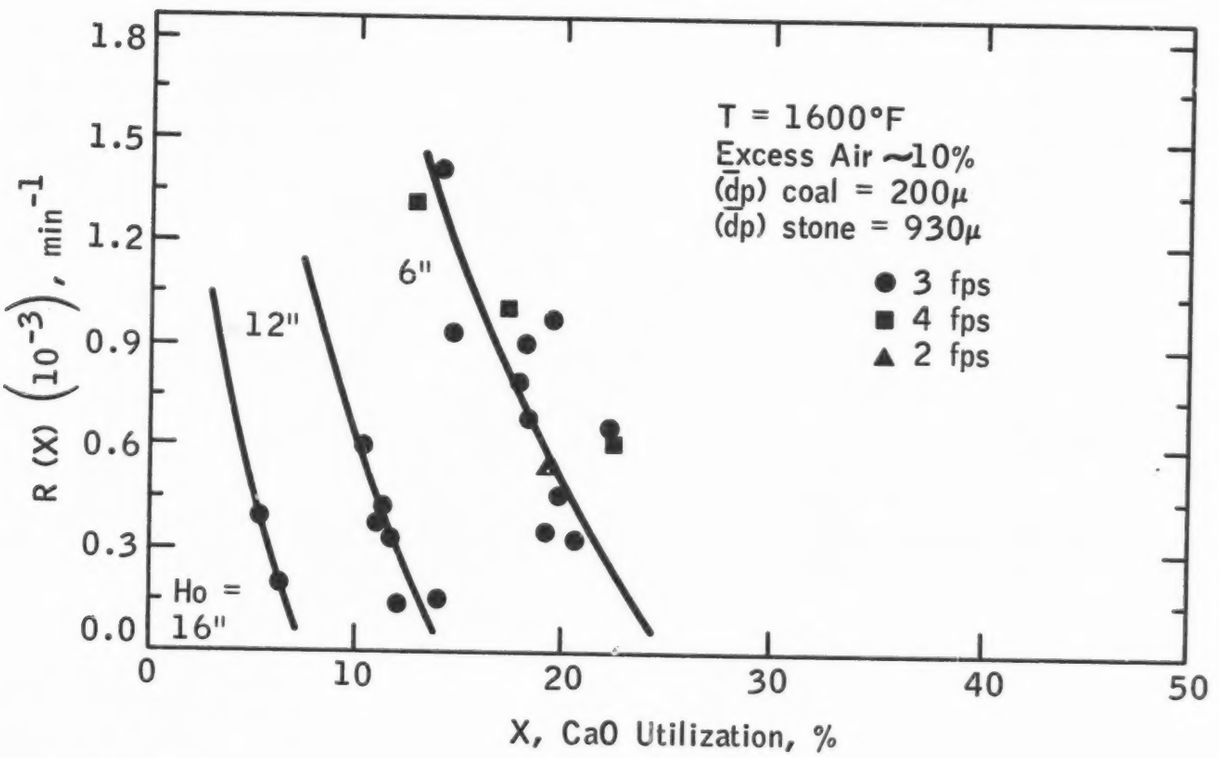

Skopp, et. al. (4) proposed the use of a contacting factor to extrapolate the R(X) values obtained in a previous Esso study to zero bed height. The kinetic constants obtained by use of this contacting factor were shown (6) to be in close agreement with differential rate constants obtained in a study by Borgwardt (7). Use of such differential rate constants does not give a true design bed height since there is no allowance for the imperfect gas solid contacting which occurs in an actual fluidized bed.

Recognizing that the quality of gas solid contacting was decreasing in the Esso FBC as bed height was increased, the objective was to identify the bed height at which the gas solid contacting efficiency in the experimental combustor approximated that in larger combustors. Since the (settled bed height)/(reactor diameter), Ho/D, has been used as a scaling parameter in other fluidized bed systems (8, 9), the data from the present study were reduced to constant Ho/D ratios, (or constant bed height). The R(X) values shown in Figure 19 were used to calculate the fraction SO_2 removal, $(1-C_H/C_o)$, by applying equation (5-4). The resulting fractional SO_2 removals are shown in Figures 20, 21, and 22 for Ho/D ratios of 1.3, 2.0 and 4.0, respectively. Figure 23 shows similar data for a 460 μ average stone particle diameter at an Ho/D = 2.0.

In order to determine at what Ho/D ratio the Esso FBC gave comparable SO_2 removal to that obtained in larger diameter reactors, experimental results reported by Argonne National Laboratories (10) obtained using the same stone (N-1359) in a larger diameter reactor were examined. The Argonne National Laboratories data were generated at the following conditions :

average stone particle size	=	615 u
bed temperature	=	1600°F
settled bed height	=	15 inches
expanded bed height	=	24 inches
superficial gas velocity	=	2.8 fps
reactor diameter	=	6 inches
Ho/D	=	2.5
Ho/U	=	0.45 sec.

The Argonne National Laboratories researchers reported that the experimentally determined Ca/S molar ratio required for 79 percent SO_2 removal was 2.3. From Figure 23,based on Esso experimental data at an Ho/D of 2.0,the CaO utilization X, at 79 percent SO_2 removal and Ho/U = 0.45 sec, is 38 percent and the corresponding Ca/S ratio is 79/38 = 2.1. This is in reasonable agreement with the Argonne's experimental value of 2.3; the lower Ca/S ratio probably reflects the smaller stone used in the Esso study. Hence, the indication is that good agreement can be obtained between the Argonne and Esso data by maintaining a constant Ho/D and Ho/U ratio.

Figure 20

KINETIC RESULTS AT Ho/D = 1.3

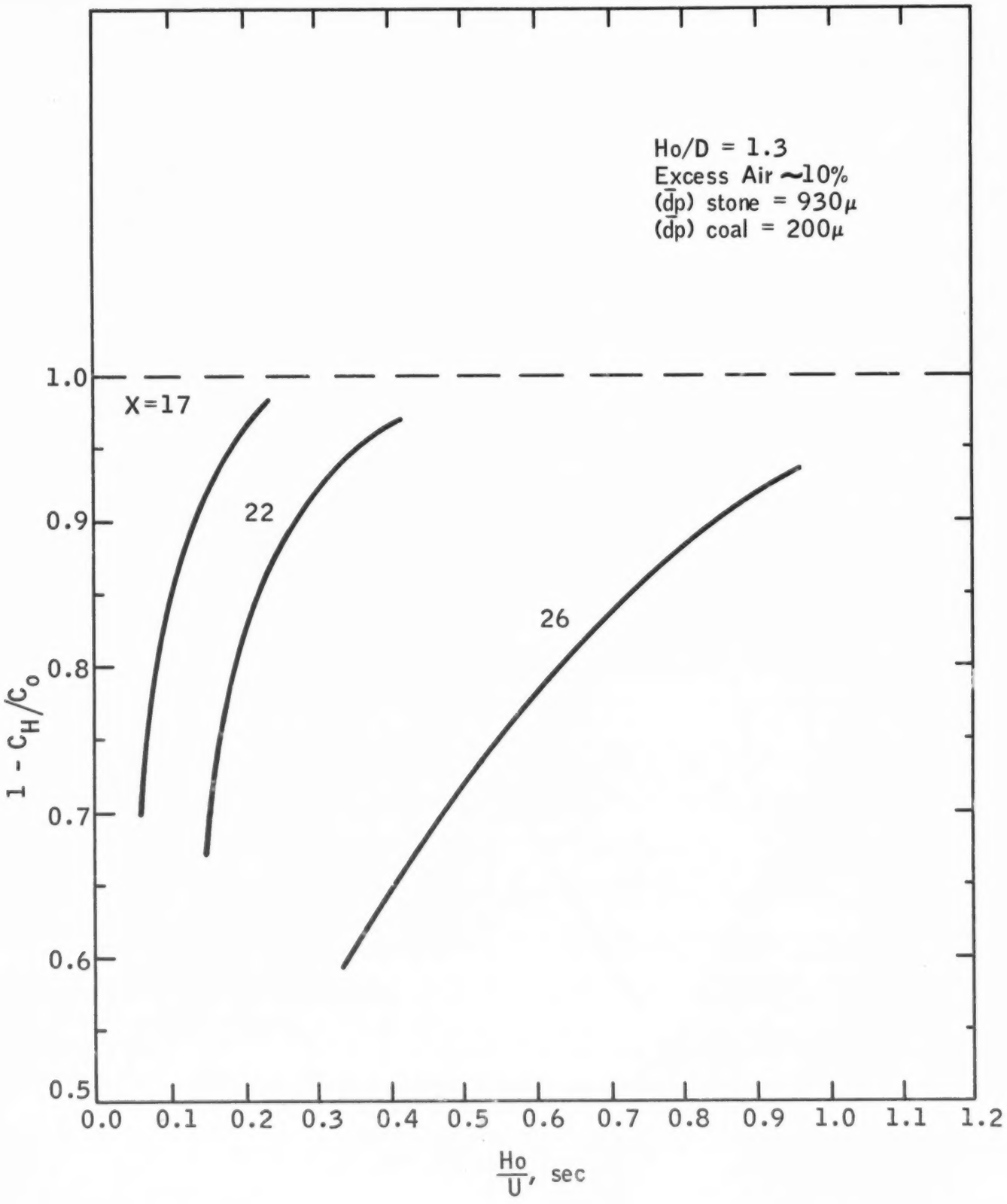

Figure 21

KINETIC RESULTS AT Ho/D = 2.0

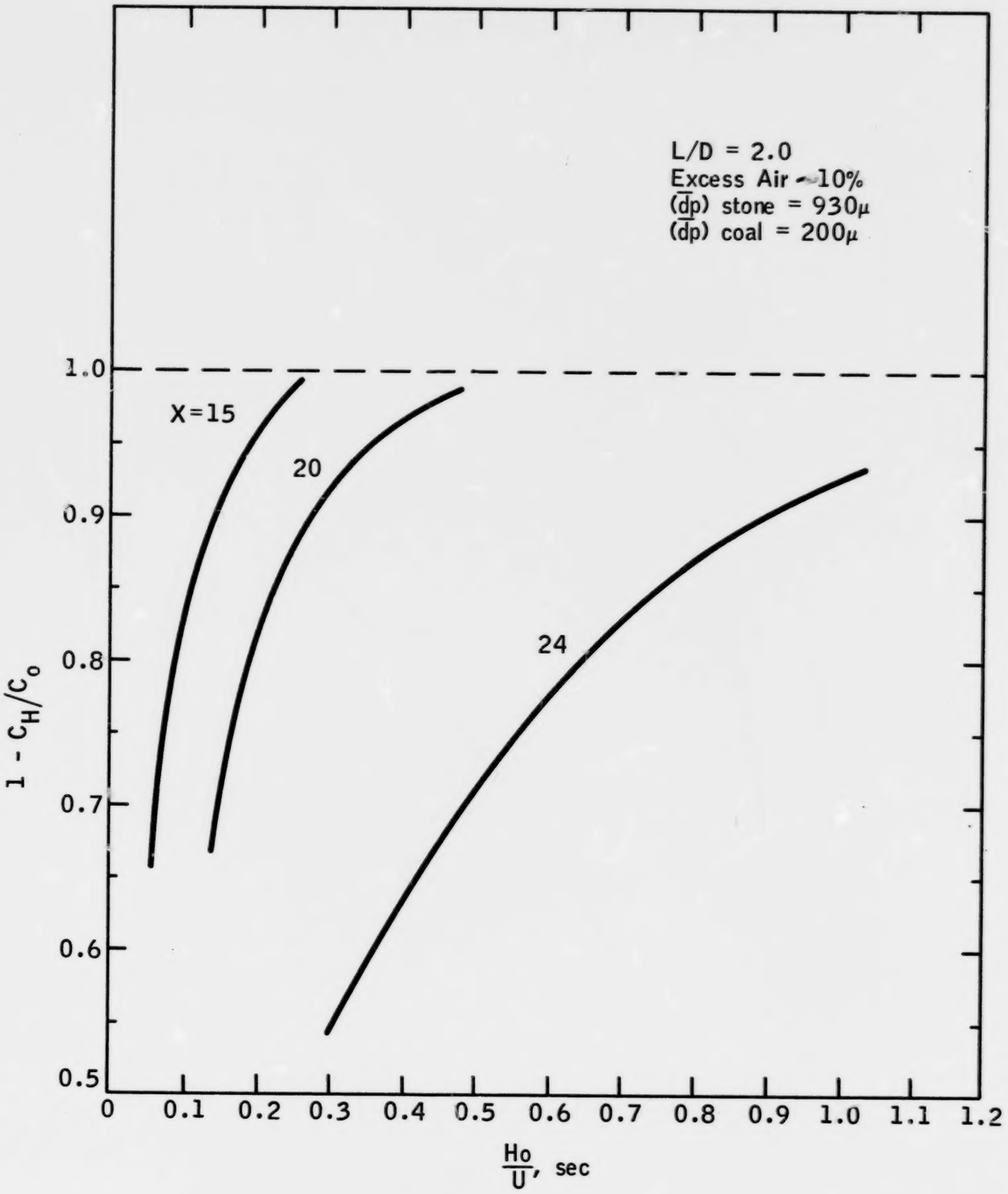

Figure 22

KINETIC RESULTS AT Ho/D = 4.0

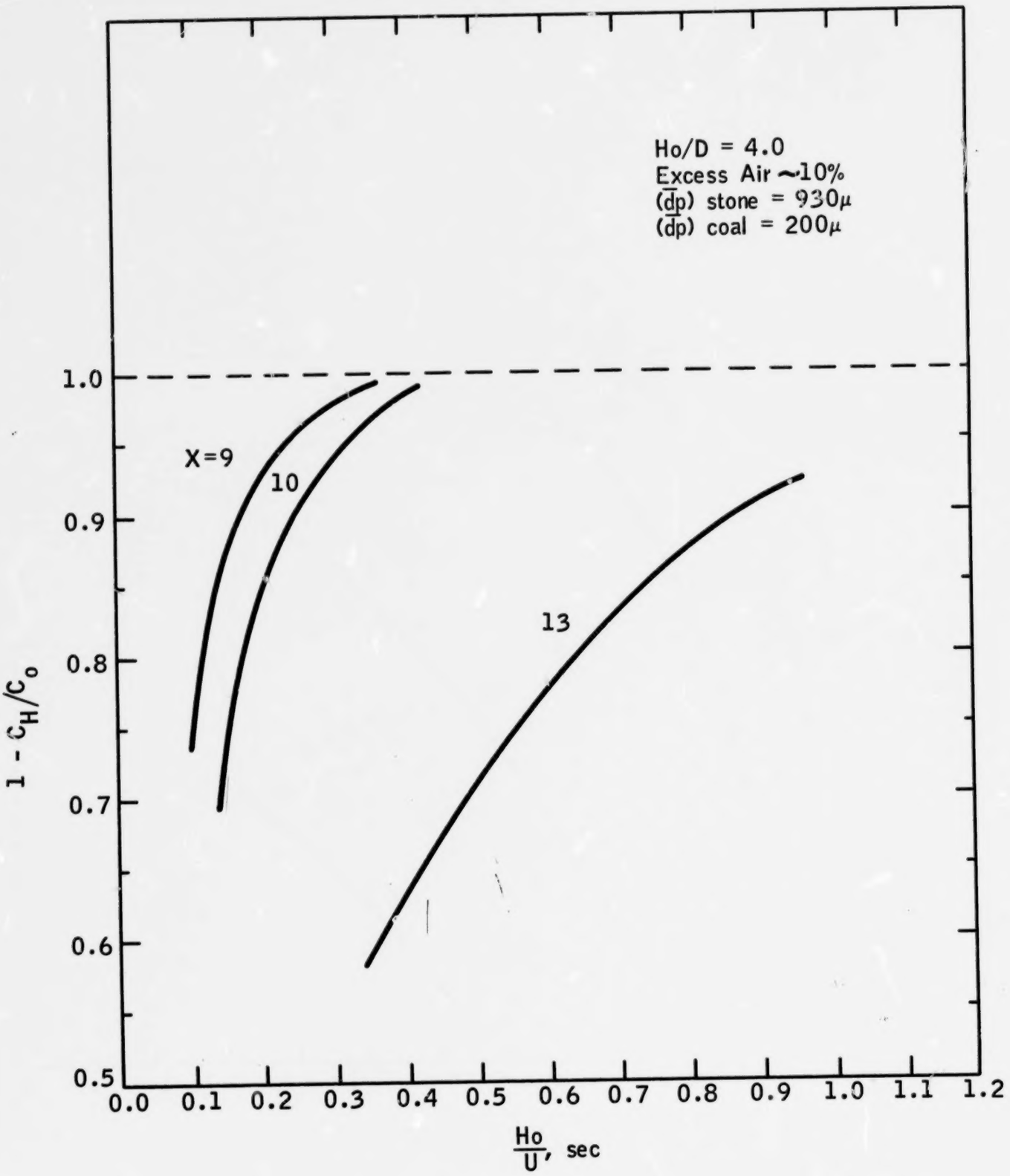

Figure 23

DESULFURIZATION WITH 460μ STONE AT Ho/D = 2.0

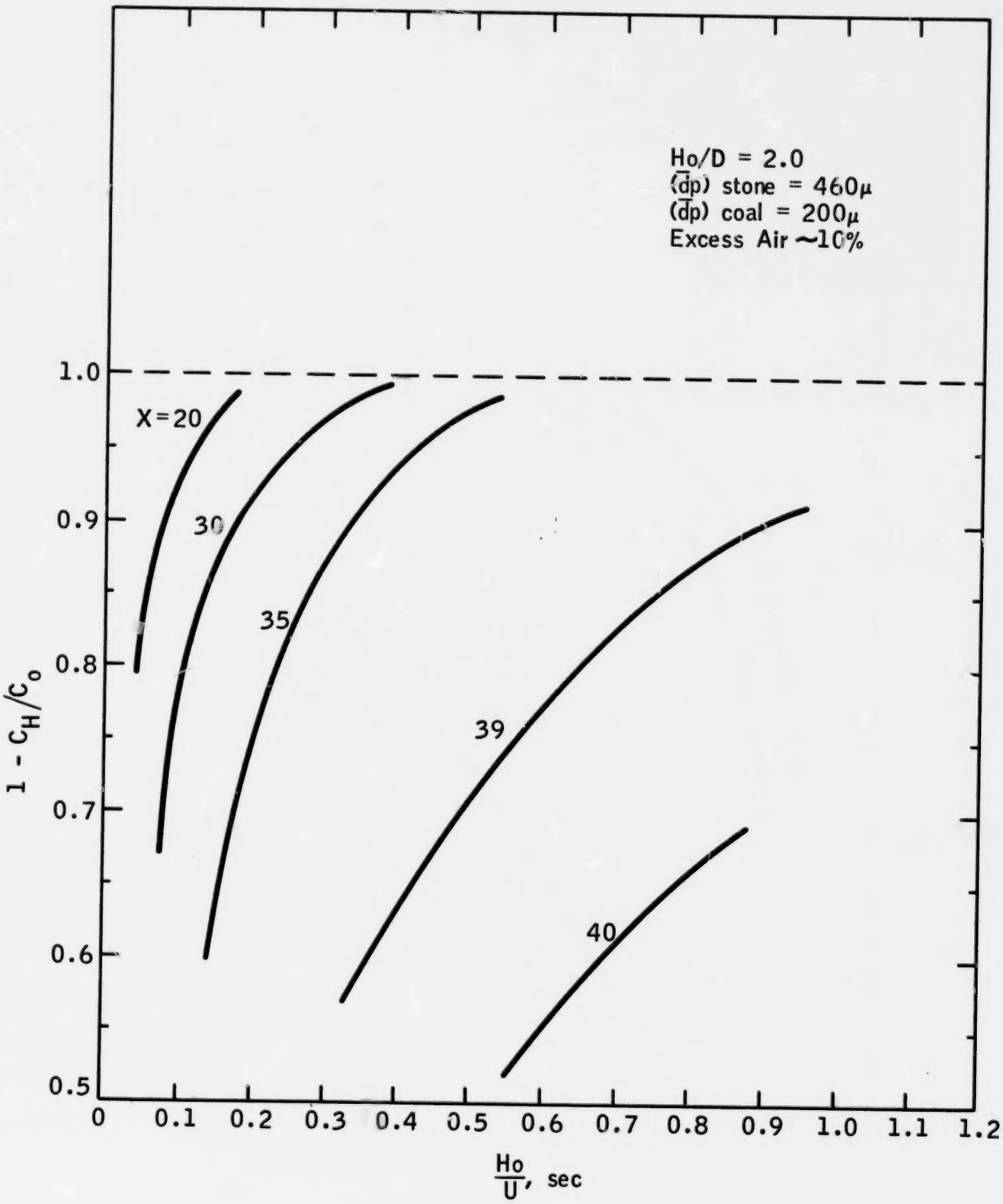

6. OTHER GASEOUS EMISSIONS

6.1 NO_x Emissions

The oxides of nitrogen, NO and NO_2, are known air pollutants. The participation of these gaseous compounds in the photochemical reactions leading to smog formation is well documented.

The principal NO_x compound found in the flue gas of conventional power plants is NO which is primarily formed by the high temperature oxidation of atmospheric nitrogen. The equilibrium for NO formation is a very sensitive function of flame temperature as shown by equation(6-1).

$$Keq = \frac{(NO)^2}{(N_2)(O_2)} = 21.9\ e^{-43,4000/RT} \qquad (6\text{-}1)$$

where Keq = equilibrium constant

$$R = 1.98\ \frac{cal}{g\text{-}mol\ °K}$$

T = absolute temperature, °K

(NO) (N_2) (O_2) - concentration of respective species in consistent units

The low bed temperatures (1600-1800°F) used in fluidized bed combustion were anticipated to result in low NO_x emissions; the predicted equilibrium value for 1600°F using Equation (6-1) is 74 ppm (10 percent excess air).

However, researchers at Argonne National Laboratories showed (11) that the NO_x emissions in a fluidized combustor were much higher than those predicted by Equation (6-1). Argonne later showed that these high NO_x emissions were caused by oxidation of the nitrogen in the fuel and were not limited by the equilibrium relationship for the oxidation of atmospheric nitrogen.

Several investigators (11,3) have reported that limestone or dolomite caused reduced NO_x emissions as compared to an inert bed. As a part of Esso's present fluidized bed combustion study, the NO_x emissions were continuously monitored by use of a Whittaker NO_x polarographic analyzer, the operation of which is described in Section 2.3. NO_x emissions for all runs are reported in Appendix 2. The emissions at the beginning of a run (initial) and emissions at the end of a run (final) are reported.

6.1.1 Inert Bed Operations

Two runs were made with alundum as an inert bed material in order to provide a base point to compare emissions obtained with limestone beds; the resulting SO_2 and NO_x emissions are shown in Figure 24. Although these operations were of relatively short duration, the NO_x emissions were constant over each run period.

Figure 24

INERT BED MATERIAL PRODUCES LOWER NO_x EMISSIONS

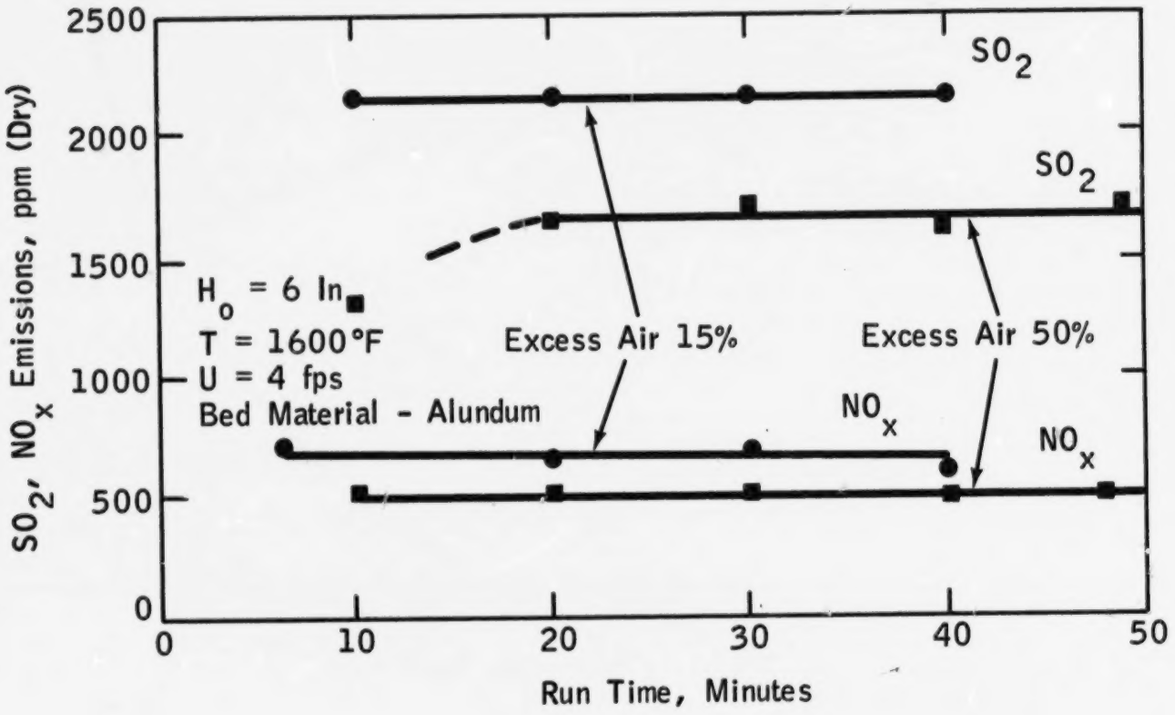

6.1.2 Typical NO_x and SO_2 Emissions With Limestone Beds

A typical record of the gaseous emissions obtained while using limestone as a bed material is shown in Figure 25. The NO_x emissions appeared to decrease as a run progressed and, simultaneously, as the SO_2 concentration in the bed and flue gas increased. A higher initial NO_x emission level was obtained when using a limestone bed than when using the inert bed.

The NO_x levels obtained in the Esso combustor were much higher than those predicted by equation (6-1). The decrease in the NO_x level as a run progressed in our reactor reflected the batch nature of the Esso combustor.

Figure 25

TYPICAL NO_x EMISSIONS WITH LIMESTONE BED

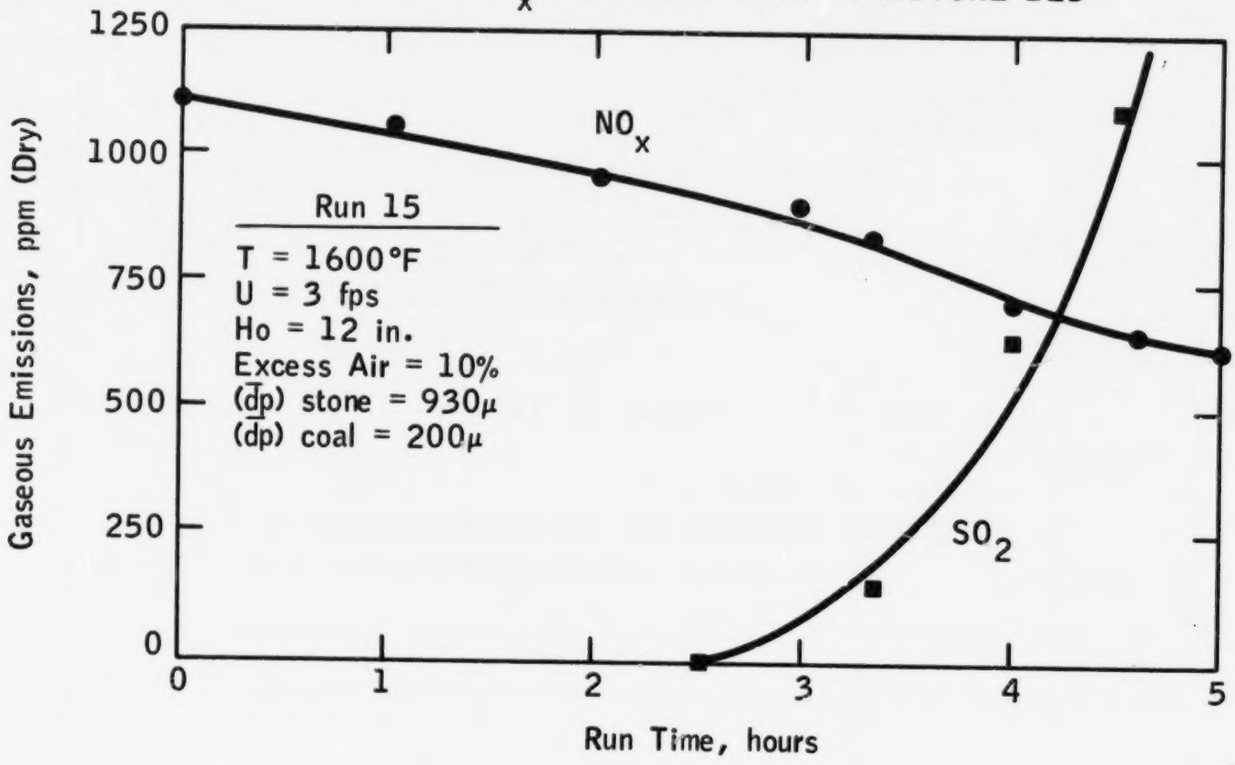

As a typical run progressed in the Esso FBC, the amount of $CaSO_4$ increased and, simultaneously, the average SO_2 concentration in the gas above the bed increased. The decrease in NO_x emissions could be related to one or both of these transient effects as follows:

1. The $CaSO_4$ may act as a decomposition catalyst to reduce NO to N_2 and O_2.
2. A chemical reaction may occur between SO_2 and NO. This reaction could occur either in the gas phase or between absorbed or reactant species on the surface of the bed material.

6.1.3 Simulated Gas Studies

In order to investigate these two possible mechanisms for the reaction of NO in fluidized beds, a series of experiments was conducted in the two inch diameter regeneration reactor. A simulated gas containing different concentrations of NO and SO_2 in a transport gas of air, N_2 or (5% O_2 in N_2) was used for these experiments. The experimental procedure was as follows:

1. The reactor was charged with the desired bed material and electrically heated to 1630°F. Initially, the reactor was fluidized with the transport gas.
2. NO was introduced into the hot reactor at the desired concentration, usually in the 800 to 900 ppm range.
3. After attaining a steady value of NO_x emissions, SO_2 was fed to the reactor at a desired inlet concentration.
4. NO_x and SO_2 emissions were continuously monitored.

A summary of the results obtained in this set of exploratory experiments is given in Table 5.

The following general observations result from these data:

1. SO_2 and NO did not react to an appreciable extent in the gas phase at 1630°F at a one second gas residence time.
2. NO_x emissions were reduced by introduction of SO_2 into a fluid bed of partially sulfated stone, with N_2 as a transport gas. The magnitude of the NO_x reduction was dependent upon the SO_2 concentration in the bed.
3. When N_2 was used as a transport gas through an inert bed (alundum or $CaSO_4$), NO_x emissions were not affected by injection of SO_2 into the bed.

TABLE 5

NO_x-SO_2 INTERACTION IN A
FLUIDIZED BED OF LIMESTONE

Reactor Temperature - 1600°F; Electrically Heated Reaction Zone - 2 Feet; Superficial Gas Velocity - 2 fps; Settled Bed Height - Approximately 6 In.

Bed Material	NO_x Conc., ppm Before SO_2 Intro.	NO_x Conc., ppm After SO_2 Intro.	SO_2 Conc., ppm Inlet	SO_2 Conc., ppm Outlet
Transport Gas - N_2				
1. Gas Phase	900	900	1290	1290
2. Partially-Sulfated	840	440	785*	300
Stone From Combustor	830	180	1510*	480
3. Alundum	820	820	1000	1000
4. $CaSO_4$ (Anhydride)	860	860	670	670
Transport Gas - Air				
1. Gas Phase	800	760	1290	1290
2. Partially-Sulfated Stone From Combustor	710	710	785*	0
3. Alundum	620	380	1090	1090
Transport Gas - 5% O_2 In N_2				
1. $CaSO_4$	790	670	670	670
2. $CaSO_4$	790	540	1760	1760

* Based on rotometer settings; remaining inlet concentrations assumed equal to outlet concentration.

4. When air or 5% (O_2 in N_2) was used as a transport gas through an inert bed (alundum or $CaSO_4$), NO_x emissions were reduced by injection of SO_2 into the reactor.

5. $CaSO_4$ gave similar results to alundum.

These observations lend support to the hypothesis that NO and SO_2 can react in partially sulfated beds of lime. Apparently an active site,

such as $CaSO_3$, is required for the reaction to proceed since no reaction was observed over an inert in the absence of oxygen. Thus, the first three observations reported on the previous two pages are consistent with the following reaction sequence:

$$CaO + SO_2 \longrightarrow CaSO_3 \qquad (6\text{-}2)$$

$$CaSO_3 + 2NO \longrightarrow CaSO_3 \cdot (NO)_2 \qquad (6\text{-}3)$$

$$CaSO_3 \cdot (NO)_2 \longrightarrow CaSO_4 + N_2O \qquad (6\text{-}4)$$

$$N_2O \longrightarrow N_2 + 1/2\ O_2 \qquad (6\text{-}5)$$

However, the fourth observation is not consistent with this mechanism, implying that some other mechanism for reducing NO_x emissions may be operative in an inert bed system in which a large excess of O_2 is present (air). This mechanism has not been clearly identified but could involve the formation of NO_2 in a high O_2 atmosphere.

The possibility of $CaSO_4$ being a decomposition catalyst for NO_x was not supported by these data. Using anhydride ($CaSO_4$) as a bed material, the NO_x levels in the effluent gas were approximately the same as the calculated inlet NO concentration, based on rotameter settings. Introduction of SO_2 into a $CaSO_4$ bed did not reduce the NO_x emissions in the absence of O_2. In the presence of O_2, the $CaSO_4$ bed behaved essentially the same as the inert alundum bed.

The operation of the Esso combustor was on a batch limestone basis. Essentially complete removal of the SO_2 from the flue gas was achieved at

the beginning of each run with fresh stone. However, as each of the runs progressed, the stone became less active and evantually all of the SO_2 was not captured by the stone. During this period, the NO_x level in the flue gas decreased. This NO_x reduction with increasing SO_2 emissions further supports the hypothesis that the concentration of $CaSO_3$ in the fluidized bed is an important factor in determining the amount of NO_x reduction, since the $CaSO_3$ concentration would be related to the SO_2 concentration in the bed. The $CaSO_3$, of course, is thermodynamically unstable at FBC conditions and is eventually oxidized to $CaSO_4$. Initially, the average SO_2 concentration in the flue gas above bed is low because of the high activity of the stone and consequently the concentration of the intermediate $CaSO_3$ is low. However, as the stone became less active, the average SO_2 concentration and therefore the amount of $CaSO_3$ increases, and with it the reduction of NO.

6.1.4 Other Variable Effects on NO_x Emissions

There was no apparent effect of excess air on NO_x emissions, as illustrated in Table 6. The NO_x emissions reported are those taken at the end of a given run. There is a fairly wide scatter in the data, possibly reflecting the varying SO_2 emissions at the end of each run. As discussed in Section 6.1.2, higher SO_2 concentrations above the bed reduced NO_x emissions.

It might be anticipated that excess air would have little effect on the level of NO_x emissions from a fluid bed combustor, since essentially all of the NO_x comes from the fuel nitrogen. The oxidation of the fuel nitrogen probably occurred to a great extent at the bed entrance, as did the oxidation of the fuel sulfur (see Section 5.7.1). The oxygen concentration at the bed entrance is not strongly affected by the excess air level.

Table 6

NO_x Emissions From Esso FBC Are Independent on Excess Air Level

Bed Temperature = 1600°F
Superficial Gas Velocity = 3 fps
$(\bar{d}p)$ coal = 200 μ
H_o = 6 In

Run Number	O_2, Percent (dry)	NO_x* ppm (dry)	NO_x, Corr. To 3% O_2, ppm (dry)
C14	4.5	700	764
C16	6.0	700	840
C22	4.0	650	688
C23	3.9	650	684
C24	2.8	750	742
C25	3.2	800	809
C26	2.5	820	798

* Recorded at the end of a run

Increasing the bed temperature in the Esso combustor from 1600 to 1800°F increased the initial NO_x emissions from 1100 to 1500 ppm, as illustrated in Table 7. Since the final NO_x emissions in Table 7 were not necessarily measured at the same SO_2 emission level, these values should be compared cautiously.

Since bed temperature had such an obvious effect on the NO_x emission level, it would appear that the surface temperature of the burning coal particle might also be an important variable. Fine grinding of coal might lead to more intense combustion and, hence, greater NO_x emissions. Only one coal particle size (200 μ) was examined in this study so no direct comparison can be made.

TABLE 7

NO_x EMISSIONS INCREASE WITH BED TEMPERATURE

Run No.	Bed Temperature, °F.	Excess Air, %	NO_x Emissions, ppm (dry) Initial - Final
14	1600	11.6	1100 - 700
16	1600	30.0	1100 - 700
18	1700	4.2	1300 - 750
28	1700	7.5	1350 - 750
27	1800	15.5	1500 - 900
29	1800	27.0	1500 - 850

6.2 CO Emissions

6.2.1 Effect of Bed Temperature

CO emissions decreased with increasing temperature, as shown in Figure 26. This coincides with the decrease in combustion efficiency indicated in Section 4.2.

Figure 26

CO EMISSIONS DECREASE WITH INCREASING BED TEMPERATURE

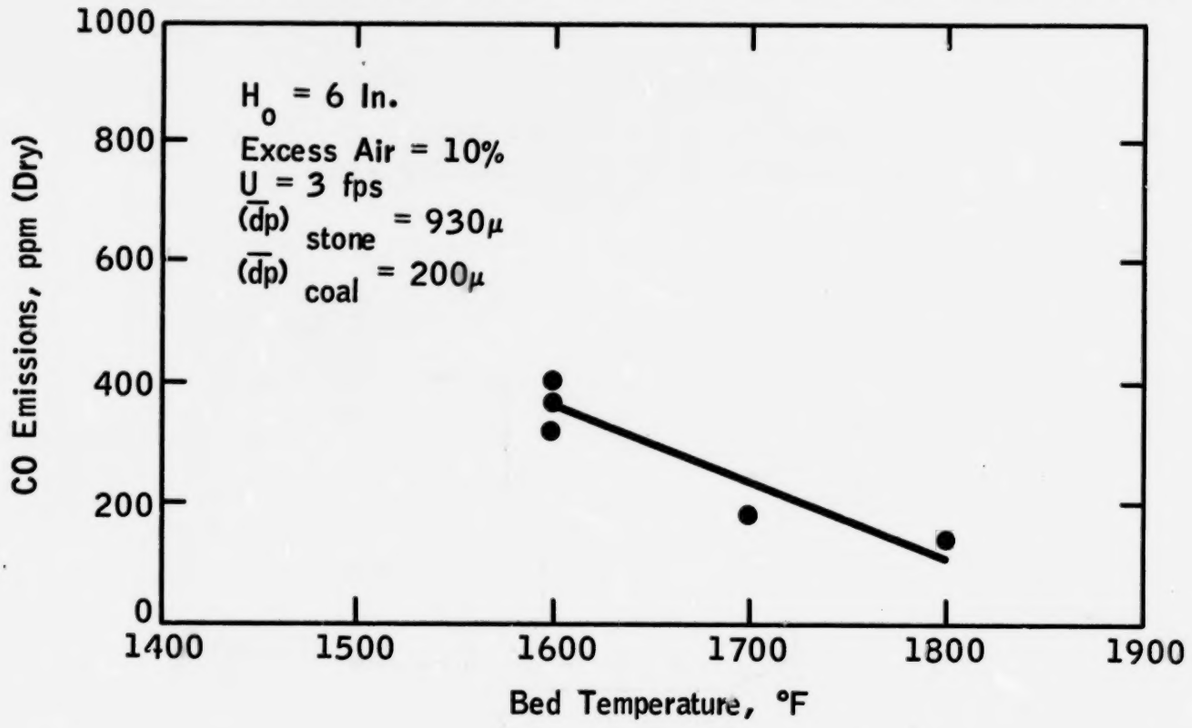

6.2.2 Effect of Excess Air

As discussed in Section 4.4, CO emissions were relatively constant at 400 ppm over the excess air range of 7 to 30 percent. Decreasing the excess air below 7 percent caused a substantial increase in the CO emissions.

7. SORBENT REGENERATION

Using limestone as a reactant to remove sulfur dioxide from flue gases has the disadvantage of increasing the quantity of solid waste material for disposal. In order to partially overcome this disadvantage, our study investigated a system in which the partially-sulfated stone is converted back to CaO by reaction with a reducing gas and then returned to the FBC. Thus the sorbent can be used numerous times before it must be discarded due to activity loss. A schematic diagram of a fluidized bed combustion system using this sorbent regeneration procedure is shown in Figure 27.

Figure 27

PROPOSED FLUIDIZED BED
COMBUSTION-SORBENT REGENERATION SYSTEM

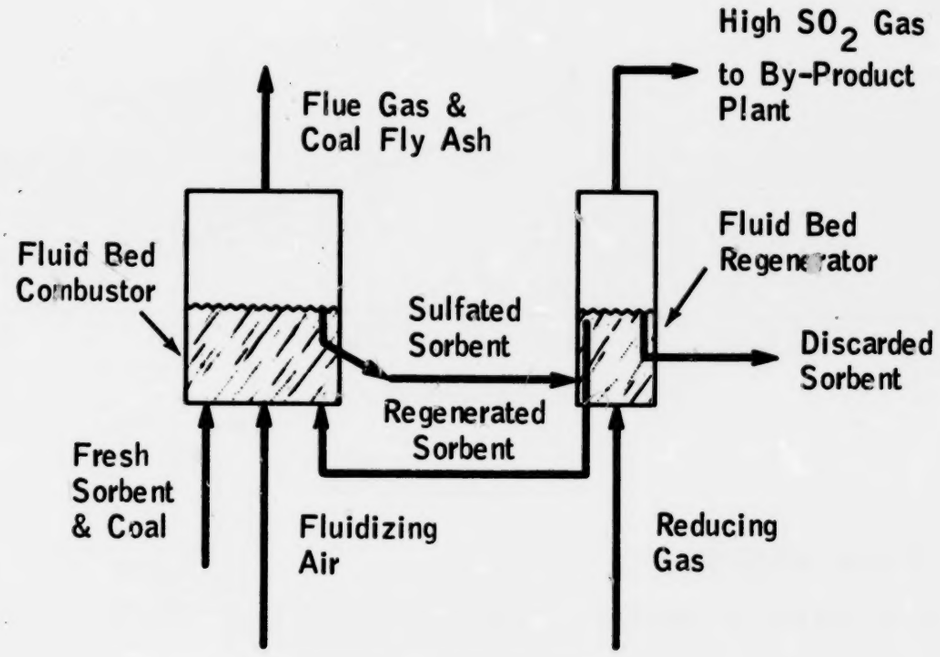

7.1 Experimental Procedure and Conditions in Sorbent Regeneration Studies

In order to investigate the potential for the reductive regeneration of the partially-sulfated stone ($CaSO_4$+CaO) back to CaO, a series of experiments was conducted in the two units, shown in Figures 1 and 3. The units were operated on an intermittent basis; a combustion (SO_2 absorption) run was completed, the combustor was cooled, the stone was removed and batched-transferred to the regenerator. The temperature of the regenerator was then raised to the operating temperature and reducing gas introduced into the regenerator. This procedure was repeated numerous times in order to accumulate cyclic stone capacity data.

The conditions selected for the combustor and regenerator for the cycle operations are given in Table 8. Two sorbent particle sizes were examined; 460 and 930 μ (see Figure 4). The selection of the operating conditions for the regenerator were based on results obtained in a previous Esso study (4). The combustor operating conditions were set by consideration of the results previously presented. The various factors considered in the selection of these operating conditions are discussed in the following sections.

TABLE 8

CONDITIONS FOR STONE REGENERATION STUDIES

Variable	Combustor	Regenerator
Bed Temperature, °F	1600	2000
Superficial Gas Velocity, fps	3	2
Excess Air, %	10	--
Settled Bed Height, Inches	6	6
$(\overline{dp})$ stone, μ	930, 460	930, 460
$(\overline{dp})$ coal, μ	200	--
CO_2/CO (regenerator feed)	--	2
CO, MOL % (regenerator feed)	--	10

7.2 Process Conditions for Regeneration

In a reducing environment, partially sulfated lime can react as follows:

$$CaSO_4 + \begin{pmatrix} CO \\ H_2 \end{pmatrix} \longrightarrow CaO + SO_2 + \begin{pmatrix} CO_2 \\ H_2O \end{pmatrix} \quad (8\text{-}1)$$

$$CaSO_4 + 4\begin{pmatrix} CO \\ H_2 \end{pmatrix} \longrightarrow CaS + 4\begin{pmatrix} CO_2 \\ H_2O \end{pmatrix} \quad (8\text{-}2)$$

$$3CaSO_4 + CaS \longrightarrow 4\,CaO + 4SO_2 \quad (8\text{-}3)$$

Since the objective of the regeneration was to produce CaO for reuse in the combustor, it was necessary to define process variables which would maximize the conversion of $CaSO_4$ to CaO and minimize the conversion to CaS. To define such conditions, a thermodynamic equilibrium analysis was made in a previous Esso study (4) of the relationships involved in the system represented by the above equations. An equilibrium program developed by the Rand Corporation (12) was utilized; some results of this analysis are shown in Appendix 5. The principal conclusions reached from this analysis are as follows:

- Temperatures in excess of 1900°F favor the formation of CaO.
- The ratio of $(CO_2+H_2O)/(CO+H_2)$ is important in determining the conversion to CaS. A 2/1 ratio results in low conversions to CaS.
- The equilibrium SO_2 concentration in the off gas is dependent upon the concentration of reducing components (CO, H_2, etc.) in the regenerator.

7.3 SO_2 Concentration in Regenerator Off Gas

One of the anticipated advantages of the proposed regenerative system is that the off gas from the regenerator would have a high SO_2 concentration and could be used to produce sulfuric acid or elemental sulfur. The revenues from the sale of this by-product should be a significant factor in the economic analysis of the system. In order to be an acceptable feed to a by-product producing system, the gas from the regenerator must have a relatively high and constant SO_2 concentration over a large number of cycles. A typical record of the SO_2 concentration in the regenerator off gas obtained in the experimental program is shown in Figure 28.

Figure 28

TYPICAL SO_2 CONCENTRATION FROM STONE REGENERATION

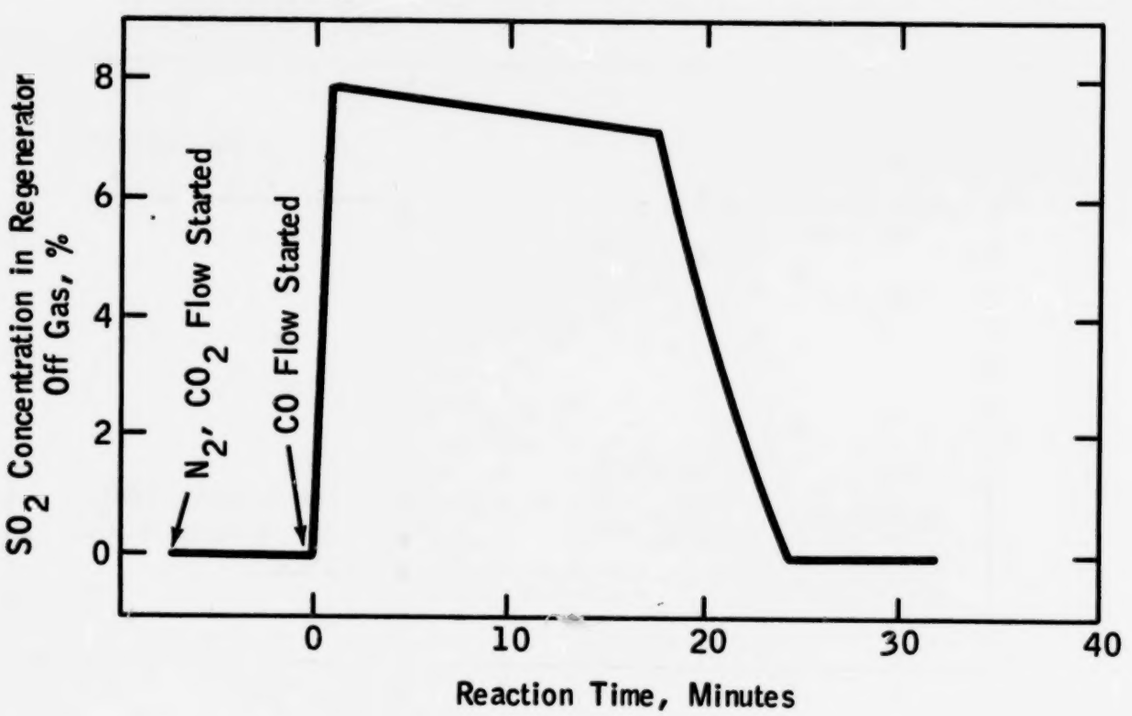

The SO_2 concentration was relatively constant over the entire regeneration cycle, showing a slight downward trend. The maximum SO_2 concentration from the regenerator, which approximated a steady state concentration, is shown in Figure 29 as a function of the number of cycles of combustion and regeneration. The solid line in Figure 29 represents the SO_2 concentration which would be attained at equilibrium (see Appendix 5). It is thus clear that the system examined attained thermodynamic equilibrium over the number of cycles examined.

Sulfur balances were made over all regeneration runs and are given in Appendix 6. The residual sulfur in the stone discharged from the regenerator which varied from 1.4 to 2.9 weight percent is also given.

Figure 29

REGENERATION REACTION ATTAINS EQUILIBRIUM

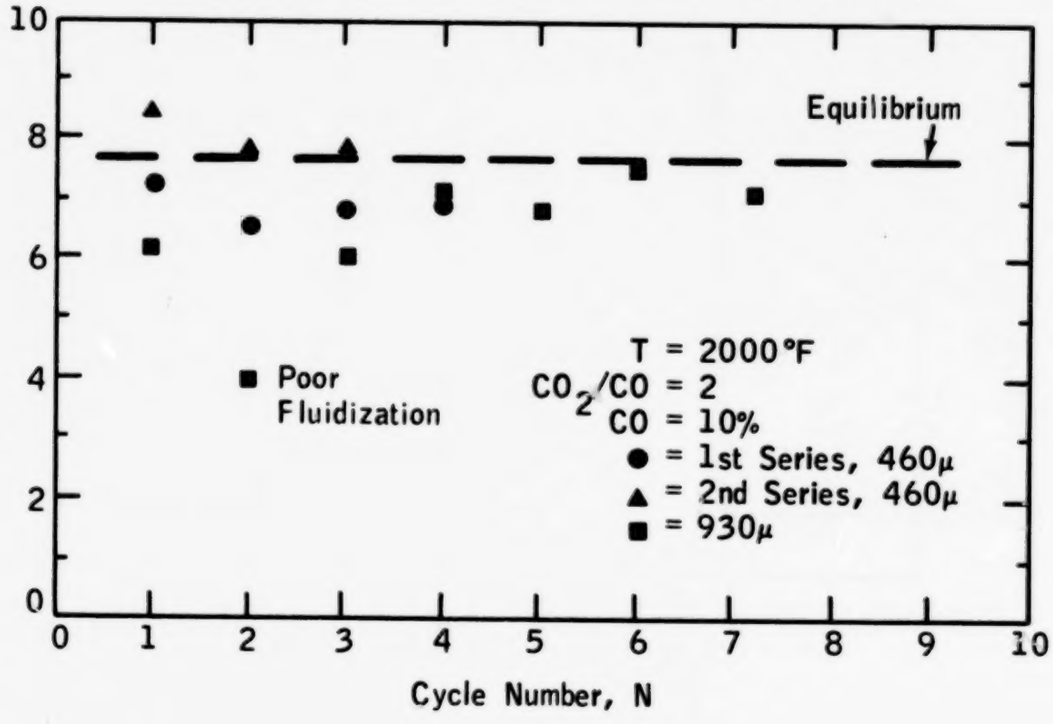

7.4 Cyclic Stone Reactivity

In order to effectively use a given sorbent in a regenerative system, the sorbent must maintain a relatively high capacity over numerous cycles of combustion (SO_2 absorption) and reductive regeneration (SO_2 desorption). Therefore, cyclic stone reactivity data were obtained using the procedure described in Section 7.1. These data are shown in Figure 30.

Figure 30

SORBENT CYCLIC CAPACITY

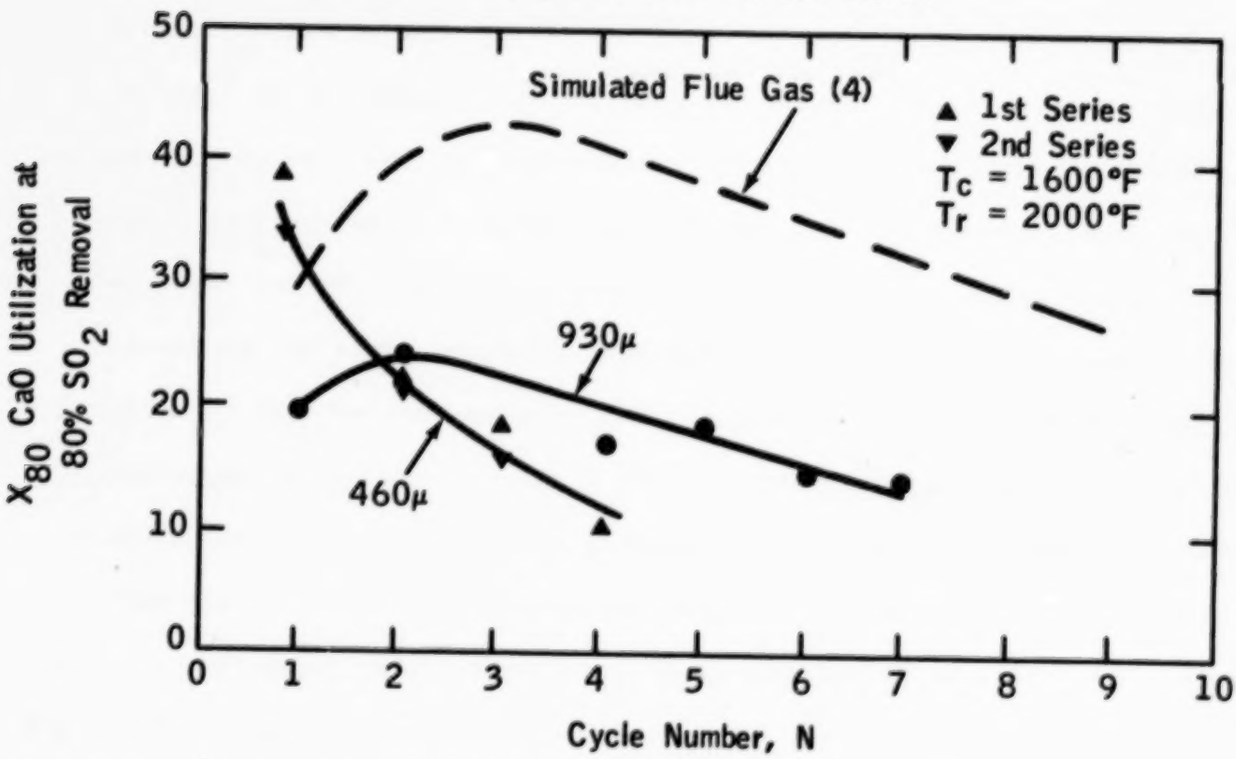

The CaO utilization ($CaSO_4/(CaO+CaSO_4)$) at 80 percent SO_2 absorption was chosen as a relative measure of the cyclic stone reactivity. Corresponding data at 90 percent SO_2 absorption showed a similar trend (see Appendix 2).

Two particle sizes were examined in our experimental program; a stone with an average particle diameter of 930 μ and another with an average particle diameter of 460 μ. The smaller stone had a higher SO_2 capacity initially but its capacity decreased more rapidly than the capacity of the 930 μ stone. Two series of cyclic experiments were initiated with the 460 μ stone to verify the more rapid cyclic deactivation obtained with this smaller stone.

Since a surface reaction is occurring in this system, the more rapid deactivation of the smaller stone (with the greater surface area per unit weight) led us to consider the possibility of something in the system "coating" or otherwise lowering the reactivity of the surface of the smaller stone. Some component of the coal fly ash appeared to be the most likely deactivating agent. It was found that more of the coal fly ash remained in the bed in the cyclic operations with the smaller stone. This is illustrated in Table 9, which shows the weight of bed material removed from the combustor at the end of each regeneration. If the regeneration went to completion in each cycle and no fly ash were retained in the bed, the weight of material removed from the regenerator would be expected to decrease slightly each cycle as a result of normal attrition and elutriation of fines from the bed. As shown in Table 9, with the 930 μ stone, there was a decrease in the weight over the first four cycles and a small increase thereafter. Calcium analyses on each of these materials indicated that there was essentially no coal fly ash retained in the bed for the first four cycles and small amounts during the last three.

TABLE 9

FLY ASH ACCUMULATED IN BED
WHEN USING 460 μ STONE

Initial Bed Weight (Cycle 1) in Each Series = 515 Grams

Run No. in Cyclic Series	Weight of Material Removed From Regenerator, Grams		
	460 μ, 1st Series	460 μ, 2nd Series	930 μ
1	476.5	470.5	490.5
2	538.5	497.5	449.0
3	626.7	625.0	416.0
4		655.5	413.0
5			419.5
6			446.5
7			481.5

However, in the two 460 μ-series, the weight of material discharged from the reactor decreased following the first regeneration but increased rapidly in the following cycles. This indicated that a considerable amount of the fly ash was being retained in the bed in these cycles. This result merely reflects the dependence of the elutriation rate on the particle size distribution of the bed; the closer the average particle size of the bed material to that of the coal fly ash, the lower the elutriation rate of the coal fly ash.

It appears, therefore, that the cyclic stone reactivity data obtained in small fluid bed combustion systems are very dependent upon the quantity of coal fly ash retained in these systems. The coal fly ash apparently has a deactivating effect upon the surface of the sorbent so that the more fly ash that is retained in the bed, the more rapid the deactivation of the sorbent. This hypothesis is supported by data taken in a previous Esso study (4) showing

that when using a simulated SO_2 containing flue gas (no fly ash present) the capacity of this same sorbent (N-1359) increased upon cycling and remained above the initial capacity for eight cycles. This leads to the conclusion that in order to obtain cyclic sorbent reactivity data representative of the reactivity in larger, continuous circulating systems, data must be taken in pilot units with continuous circulation of the sorbent between combustor and regenerator. Such pilot units must be designed to approximate the elutriation characteristics of commercial systems as closely as possible so as to obtain a representative amount of fly ash in the bed.

7.5 Cyclic Stone Attrition

In the regenerative process, which Esso has proposed, the fresh sorbent makeup rate is set by considering both stone attrition and stone deactivation; high attrition rates could significantly inceease this makeup rate. The stone used in this study (N-1359) was found in a previous Esso study (4) to have a relatively low attrition rate. The attrition data obtained in the previous study, shown in Figure 31, were obtained in an identical unit and under similar operation conditions to those used in this study and are therefore representative of the attrition rates obtained in this study.

Since the surface area/volume ratios of the experimental combustor and regenerator are much greater than would be the corresponding ratios of a commercial system, the wall-particle collisions should be greater in the experimental reactors. This should lead to higher attrition rates in the experimental units than in the commercial system. Thus, the data shown in Figure 31 should provide a high estimate of commercial attrition rates.

Figure 31

CYCLIC SORBENT ATTRITION
LOW AFTER FIRST CYCLE

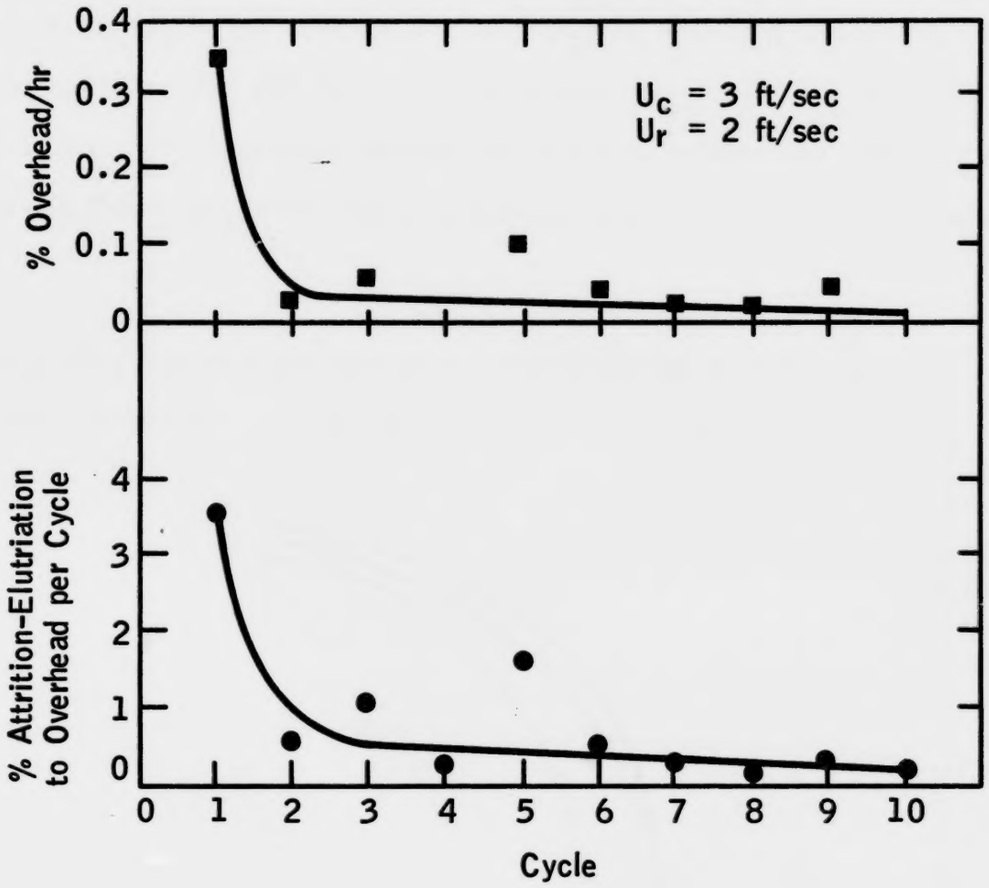

Sorbent attrition rates are dependent upon the gas velocity and these data were taken at relatively low velocities and would not be representative of attrition rates at higher velocities.

To obtain more detailed information on the physical behavior of the cycled sorbent, a complete particle size distribution of the bed material removed from the combustor was measured following each of the runs in the 930 μ cyclic series. The resulting distributions are shown in Figure 32. There was essentially no coal fly ash retained in the bed in these operations as shown by calcium analyses. These distributions verify that there is not excessive stone attrition with limestone N-1359.

Figure 32

PARTICLE DECREPITATION IN REGENERATIVE SYSTEM

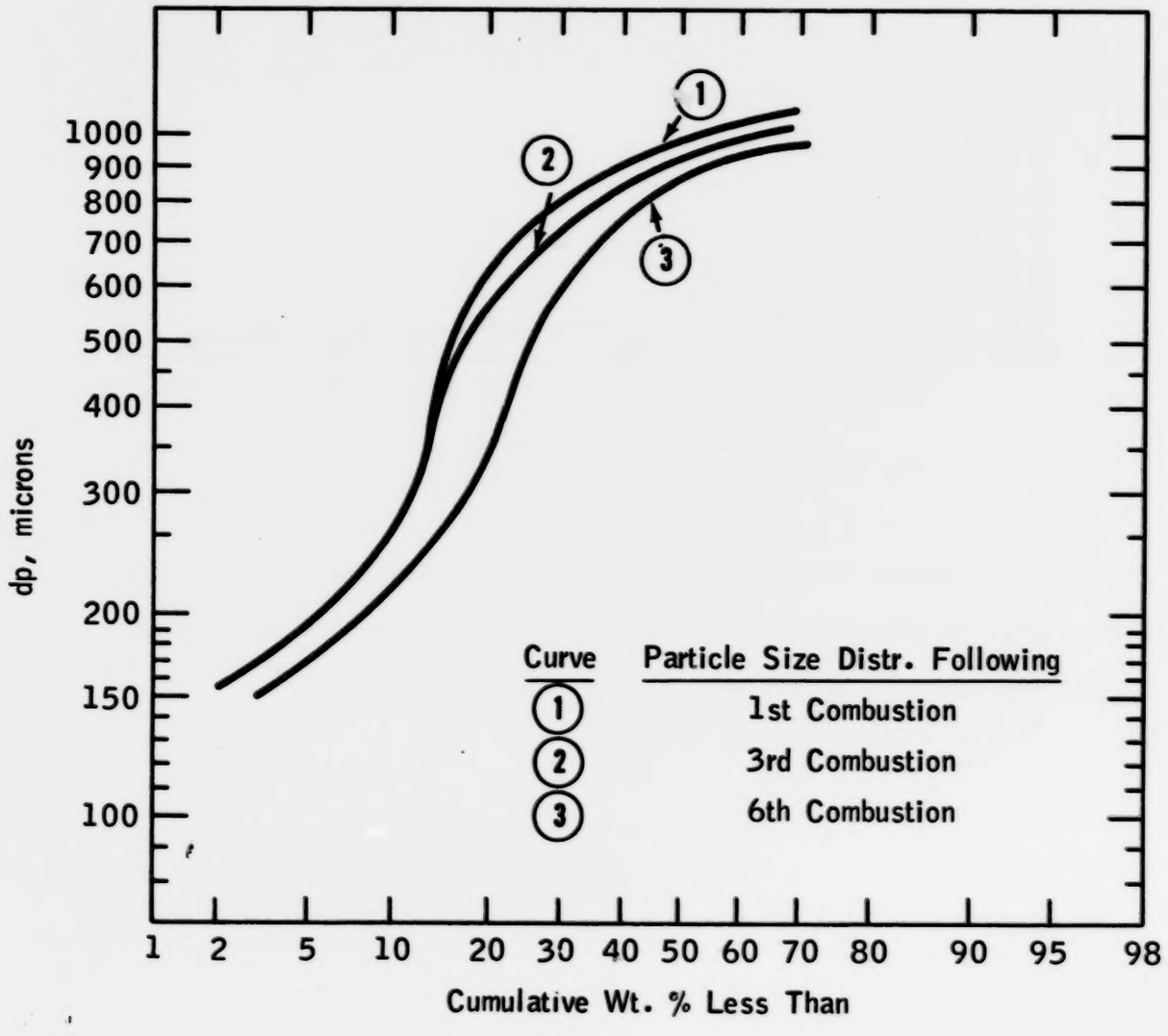

8. ECONOMIC COMPARISON OF REGENERATIVE AND SINGLE PASS (LIMESTONE) FBB SYSTEMS

An economic comparison was made of two 600 MW fluidized bed boiler (FBB) systems; one system based on the limestone regeneration concept described in this study and the other system based on single pass limestone usage. Schematic representations of these two systems are given in Figure 33. The economic analysis made considered only incremental cost differences between the two systems. While this type of analysis will indicate which system is preferable from an economic standpoint, it will not give an absolute capital investment or yearly operating cost for either system.

The process design factors considered for each system are described in the following sections. These design considerations were used to develop the economics for each FBB system.

8.1 Process Design Considerations

8.1.1 Regenerative Limestone System

- System Operating Conditions

The operating conditions shown in Table 10 were selected for the design basis of the regenerated limestone system.

Figure 33

COMPARISON OF REGENERATIVE AND SINGLE PASS LIMESTONE FBB SYSTEMS FOR A 600 MW POWER PLANT

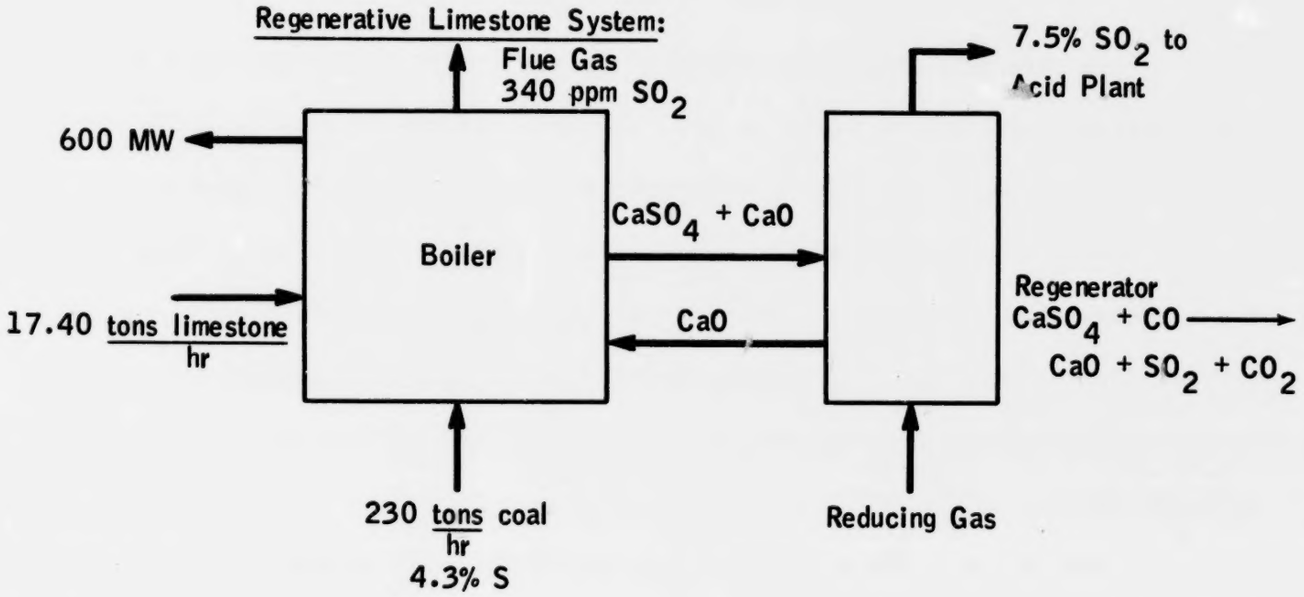

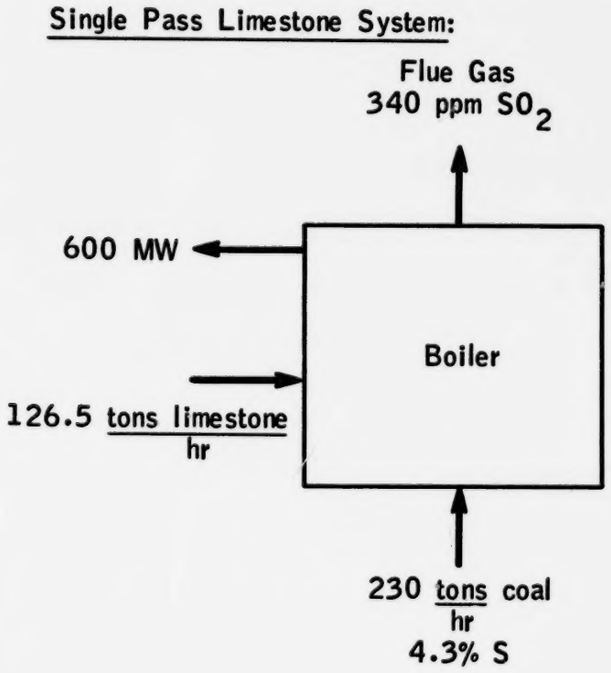

TABLE 10

OPERATING CONDITIONS IN REGENERATIVE FBB SYSTEM

Regenerator		Combustor	
T	= 2000°F	T	= 1600°F
U	= 10 fps	U	= 10 fps
$(CO_2 + H_2O)/(CO + H_2)$	= 2.37	Excess Air	= 10%
$(CO + H_2)$	= 10 mol %	Limestone	= N-1359
Limestone	= N-1359	$(\overline{dp})_{stone}$	= 1000 μ
$(\overline{dp})_{stone}$	= 1000 μ	SO_2 Removal	= 90%
Reducing Fuel	= Natural Gas	Coal	= 4.3% S

(See Appendix for coal analysis)

The particle size distribution of the coal feed to the combustor was not assigned, but the desulfurization data taken in our experimental program with a 200 μ coal feed were assumed to be applicable. A superficial gas velocity of 10 fps was selected as a compromise between a high velocity (~15 fps) FFB system and a low velocity (~3 fps) FFB system. The 1000 μ stone is large enough to prevent excessive entrainment at 10 fps (4).

- Limestone Feed Rates

The cyclic deactivation data for the 930 μ stone presented in Section 7.4, were used to determine the required fresh limestone feed rates and the total Ca/S feed ratio. A calculation procedure suggested by Curran (13) was used to evaluate the required fresh and circulating sorbent feed rates. This procedure uses equation (8-1) to calculate the average CaO utilization in the combustor for a given cyclic decline in stone capacity.

$$\bar{X} = \int_0^{\infty} \alpha e^{-\alpha n} X(n)\, dn \qquad (8\text{-}1)$$

where:

α = $\frac{\text{mols/hour fresh CaO fed to process}}{\text{mols/hour CaO circulated through process}}$

α = makeup rate

$X(n)$ = cyclic CaO utilization required for a given SO_2 removal

n = number of cycles

$\bar{X}$ = average CaO utilization in combustor

Using equation (8-1), the average CaO utilization in the combustor was calculated for 90 percent SO_2 removal. A plot similar to that in Figure 30, except for 90 percent SO_2 removal, was used to evaluate X(n). The average CaO utilization in the combustor is shown in Figure 34 as a function of α, the makeup rate.

Figure 34

AVERAGE CYCLIC STONE UTILIZATION AT 90% SO_2 REMOVAL

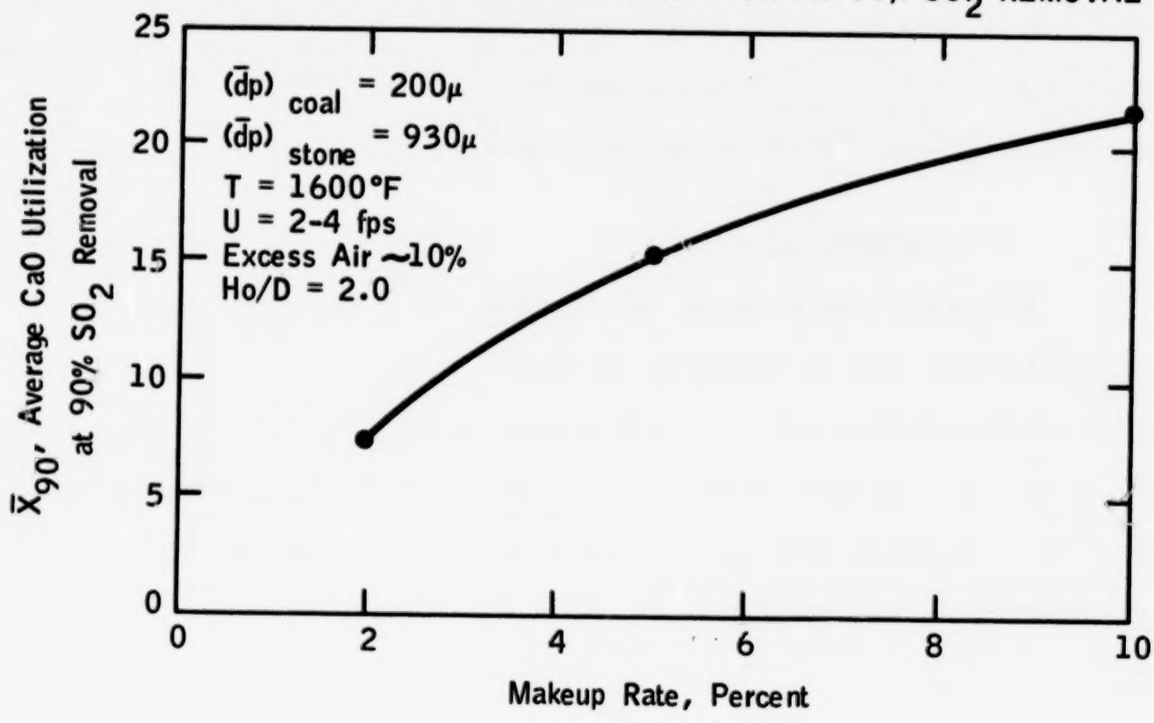

The average CaO utilization in the combustor was used to determine the Ca/S molar ratio required in the feed to the combustor as follows:

$$(Ca/S)_{Total} = \frac{\text{Percent } SO_2 \text{ Removal}}{\text{Average CaO Utilization, Percent}}$$

The total Ca/S feed ratio and fresh feed Ca/S feed ratio required to the combustor are given in Figure 35 . The fresh feed Ca/S ratio was determined as follows:

$$(Ca/S)_{Fresh} = \frac{\alpha}{1 + \alpha} (Ca/S)_{Total}$$

where α is expressed as a fraction.

FIGURE 35

Ca/S RATIOS REQUIRED FOR 90% SO_2 REMOVAL

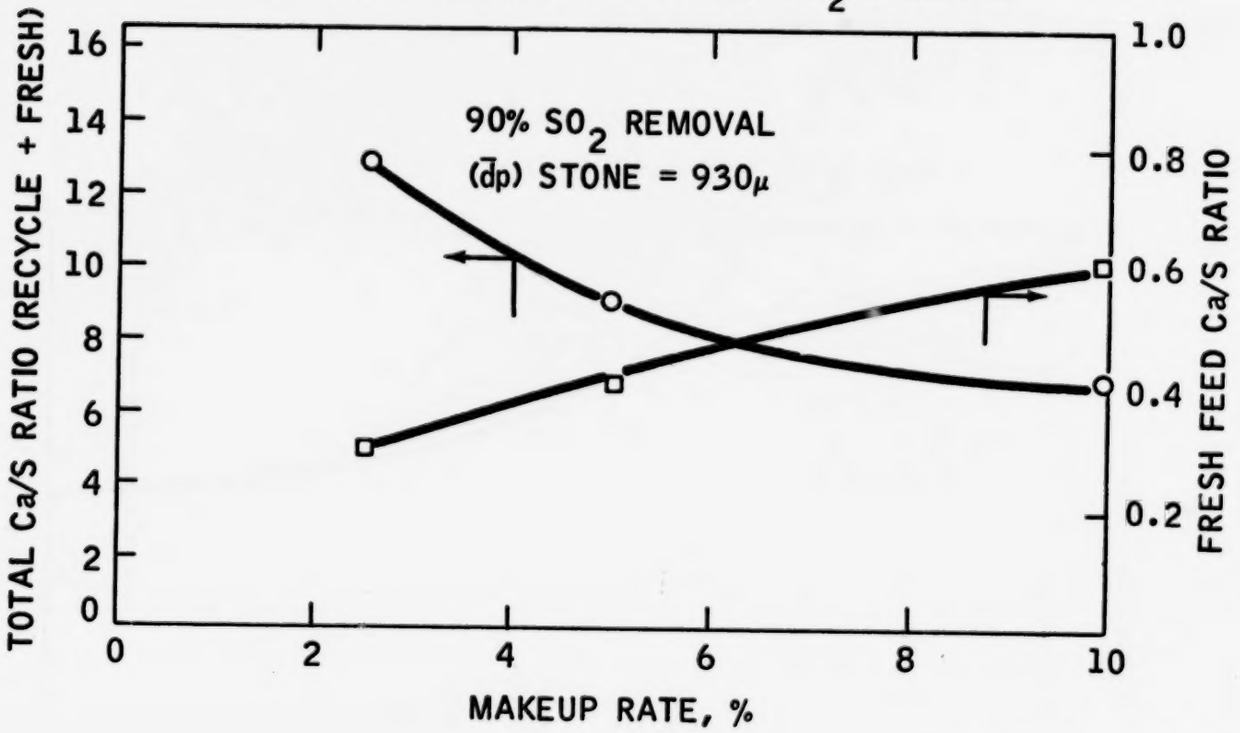

The optimum makeup rate in this system is actually determined by making an economic trade-off between the costs for a given set of fresh and circulating stone feed rates and the power costs for deeper beds. For example, by going to low values of α, the fresh stone feed rate is reduced (lower limestone costs and disposal costs) but the circulating burden is increased (higher investment costs for solid transfer piping and power). Also, low values of α result in deeper beds in the combustor since the equilibrium CaO utilization in the combustor is low. In the limit of no fresh stone makeup an infinite bed height would be required in the combustor.

An estimate of the bed depth required in the combustor as a function of the makeup rate is shown in Figure 36. The calculation procedure used to determine this bed depth from the experimental data taken in our program is illustrated in Appendix 7.

Figure 36

BED HEIGHT REQUIRED FOR 90% SO_2 REMOVAL

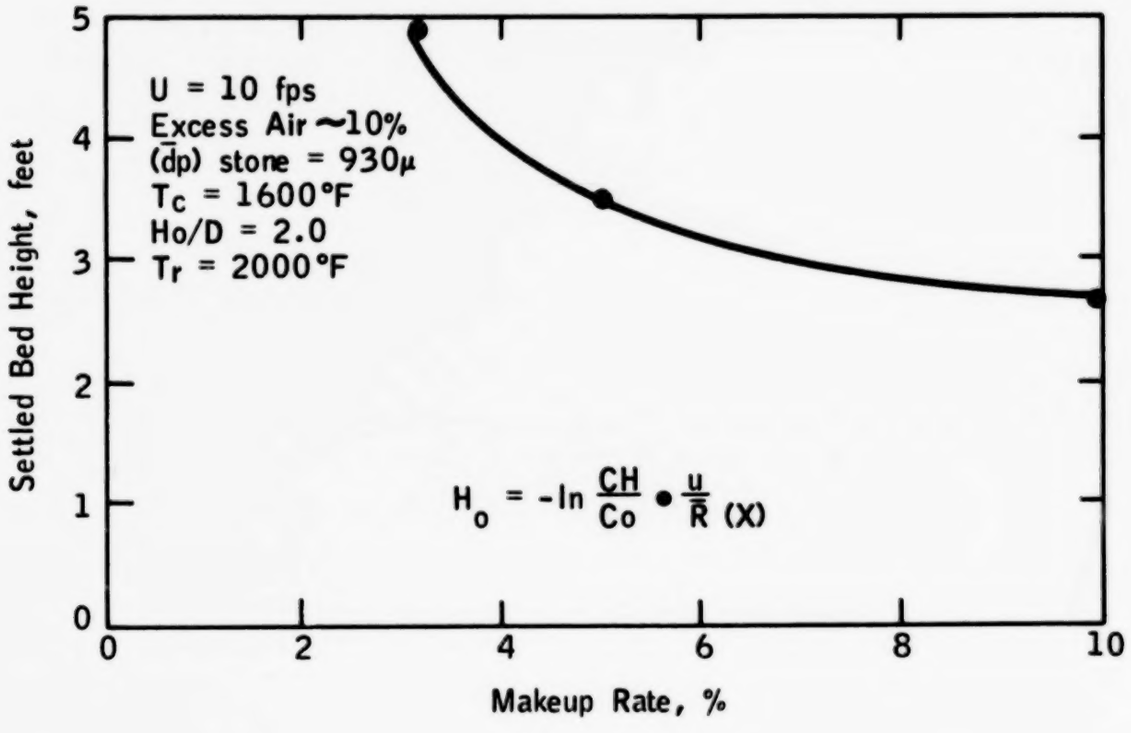

Using Figures 35 and 36, the optimum value of the makeup rate could be determined by making an economic comparison of the costs involved at each makeup rate. In this study, a makeup rate of eight percent was selected since it offered a reasonable compromise between combustor settled bed depth (2.8 feet) and the fresh Ca/S feed ratio (0.55). A calculation to determine the optimal makeup rate was not perfo.med.

There were several key assumptions involved in the calculation procedures to determine limestone feed rates and combustor bed height from the experimental data; these assumptions are as follows:

1. The experimental sorbent capacity data taken in the three inch diameter Esso FBC at an Ho/D of 2.0 (settled bed height of six inches) are representative of stone capacity in a commercial system operating at an Ho/D of one or less.
2. The sorbent capacity data and first order rate constants are independent of superficial gas velocity over the range of 2 to 10 fps.
3. The equilibrium stone capacity in a continuous circulation system could then be calculated by assuming (1) that the batch cyclic capacity data are representative of the capacity that can be attained in a given cycle in a continuous system, and (2) that the continuous system is perfectly mixed.

A few comments are necessary concerning the validity of each of these key assumptions. The experimental stone capacity data were shown in Section 5.7 to be a function of the combustion bed height, or the Ho/D ratio. Data taken at an Ho/D of 2.0 were shown to be in reasonable agreement

with data taken by Argonne at a similar Ho/D ratio in a larger combustor. Also, data taken by Hanway (9) on a large particle fluid bed system indicate that decreasing the Ho/D ratio should increase the overall system performance. The stone capacity data taken in our combustor at an Ho/D of 2.0 are believed to be a realistic estimate of commercial reactor performance when operating with an Ho/D of one or less.

The assumption that the stone capacity data are independent of superficial gas velocity was based on data shown in Section 5.5 for the range of velocities from 2 to 4 fps. However, recent data taken at Argonne National Laboratories (14) indicate that there may be a velocity dependence at higher velocities. We have not attempted to modify our analysis to allow for such a velocity dependence.

- Regenerator Bed Height

The primary reaction occurring in the regenerator was shown in Section 7.3 to attain equilibrium with the gas residence times used. The bed height in the commercial reactor was therefore set by scaling-up from the experimental unit holding gas residence time constant. The (psuedo) gas residence time in the experimental system was as follows:

$$\frac{Ho}{U}, \frac{Ft}{fps} = \frac{0.5}{2} = 0.25 \text{ sec}$$

For a 10 fps superficial gas velocity in the regenerator, the bed height required for a constant gas residence time is therefore:

$$\frac{Ho, Ft}{10 \text{ fps}} = 0.25$$

$$Ho = 2.5 \text{ Ft}$$

This is not necessarily the minimum bed height, since no attempt was made in the experimental program to attain a minimum bed height. However, it should provide a conservative design estimate.

• Material and Energy Balances

A material and an energy balance were made over the regeneration section of a nominal 600 MW fluidized bed boiler system, using the system operating conditions and limestone feed rates previously described. A coal feed rate of 230 tons/hour was set in order to be consistent with design bases proposed by Westinghouse (15). The limestone that was specified was N-1359, which was used throughout our experimental program, and the coal was an Ohio Pittsburgh No. 8 seam coal, specified by Westinghouse (15), with 4.3 percent sulfur. The makeup rate was set at 8 percent, so that the fresh Ca/S ratio was 0.55 and the circulating Ca/S ratio was 6.95. (See Figures 34 and 35). The outlet of the regenerator was assumed to be five mole percent $CaSO_4$. The regeneration reaction (8-1)

$$CaSO_4 + \begin{matrix} CO \\ H_2 \end{matrix} \longrightarrow CaO + SO_2 + \begin{matrix} CO_2 \\ H_2O \end{matrix} \qquad (8\text{-}1)$$

was assumed to proceed to equilibrium and produce an exit gas with 7.5 mole percent SO_2.

The overall material and energy balances are shown in Figure 37. The energy balance was based on using methane as the fuel and producing a reducing gas with 10 volume percent $(CO + H_2)$ and $(CO_2 + H_2O)/(CO + H_2)$ ratio of 2.37. The excess CO over that required for SO_2 production was assumed to be combusted to CO_2. The system was considered to be adiabatic. The excess enthalphy represents the amount of heat that can be lost from the system before becoming thermally deficient. Using coke or coal as a fuel would increase the amount of excess enthalphy. Assuming that the excess CO over that required for SO_2 production appeared in the gaseous products would decrease this excess enthalphy.

Figure 37

MATERIAL BALANCE ON F.B.C. - F.B.R. SYSTEM

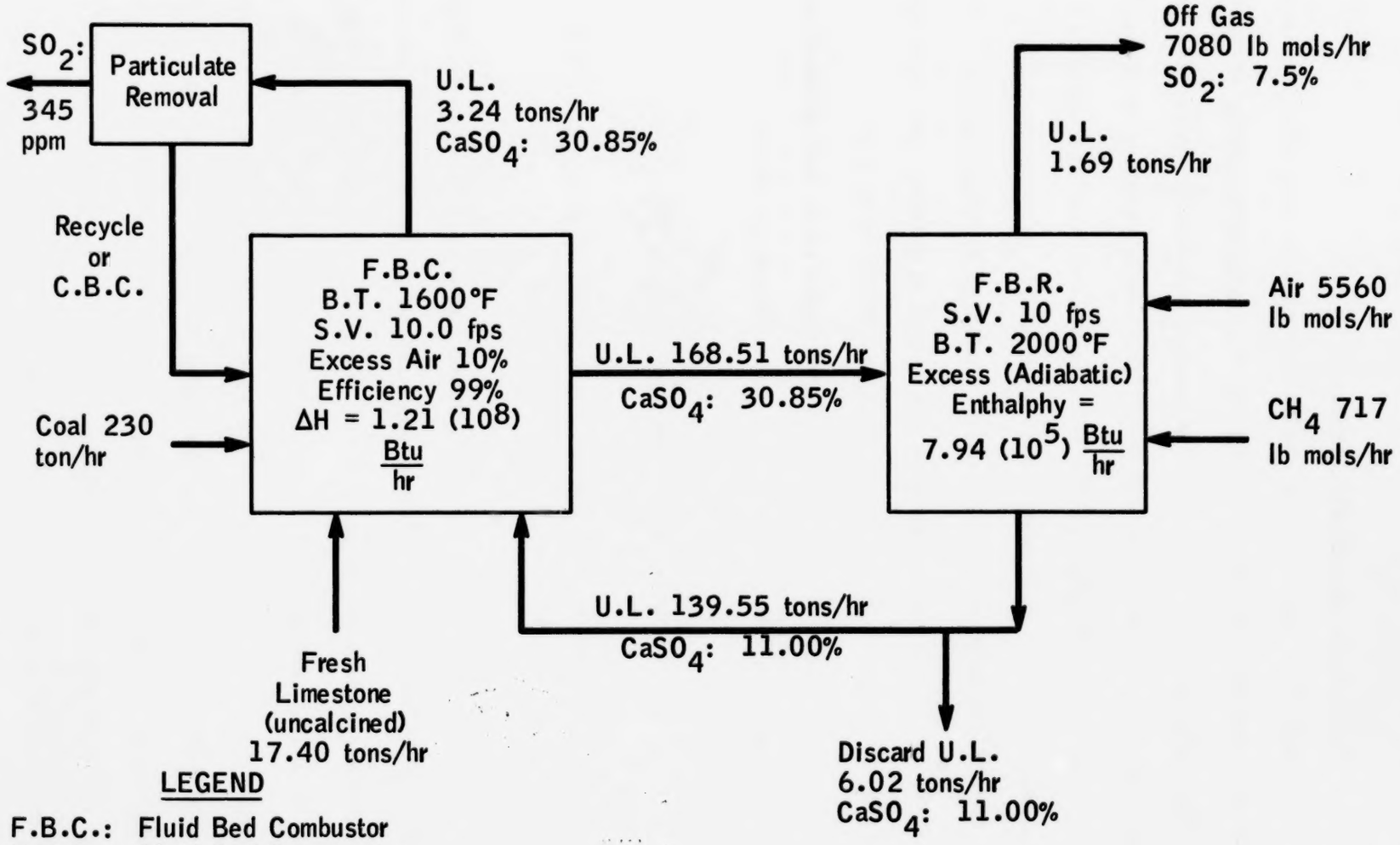
SO_2: 345 ppm
Particulate Removal
U.L. 3.24 tons/hr $CaSO_4$: 30.85%
Off Gas 7080 lb mols/hr SO_2: 7.5%
U.L. 1.69 tons/hr
Recycle or C.B.C.
F.B.C. B.T. 1600°F S.V. 10.0 fps Excess Air 10% Efficiency 99% ΔH = 1.21 (10^8) Btu/hr
U.L. 168.51 tons/hr $CaSO_4$: 30.85%
F.B.R. S.V. 10 fps B.T. 2000°F Excess (Adiabatic) Enthalphy = 7.94 (10^5) Btu/hr
Air 5560 lb mols/hr
CH_4 717 lb mols/hr
Coal 230 ton/hr
U.L. 139.55 tons/hr $CaSO_4$: 11.00%
Fresh Limestone (uncalcined) 17.40 tons/hr
Discard U.L. 6.02 tons/hr $CaSO_4$: 11.00%

LEGEND

F.B.C.: Fluid Bed Combustor
F.B.R.: Fluid Bed Regenerator
S.V.: Superficial Velocity
U.L.: Used Limestone
ΔH.: Exothermic heat available over system without limestone addition

All of the 7.95 (10^5) Btu/hr excess enthalphy in the regenerator would be dissipated as heat loss through the walls. Specifying a nine inch thick refractory lining of super duty firebrick with a mean thermal conductivity of 10 Btu/hr ft^2°F, the heat loss through the walls of the regenerator was calculated to be 1665 Btu/hr ft^2. For an average transfer area, including dome and grid of 3000 ft^2, the total heat loss from the regenerator would be 5.0 (10^6) Btu/hr. This means that approximately 4.2 (10^6) Btu/hr must be supplied to maintain thermal equilibrium in this system. The most obvious method of supplying this energy is by preheating the input air to the regenerator; an air preheat temperature of 180°F is sufficient for this purpose.

- Regenerator Bed Diameter

Setting the superficial gas velocity through the regenerator at 10 fps, based on the outlet gas volume, makes the required inside diameter of the regenerator 21.6 feet.

- Regenerator Off Gas Purification For Acid Plant Use

The regenerator was designed as a refractory lined vessel, with two external refractory lined cyclones. The outlet gas of the regenerator was assumed to be cooled from 2000°F to 800°F in a waste heat boiler. The 800°F flue gas from the waste heat boiler would be used to preheat the inlet air to the regenerator and would then be cooled and cleaned of particulates by passage through a process cooler, a wet scrubber, a mist electrostatic precipitator and a drying tower. The equipment following the air preheater is of the type commonly used in plants producing sulfuric acid from pyrites (16) and is similar to the

Figure 38

GAS PURIFICATION SYSTEM

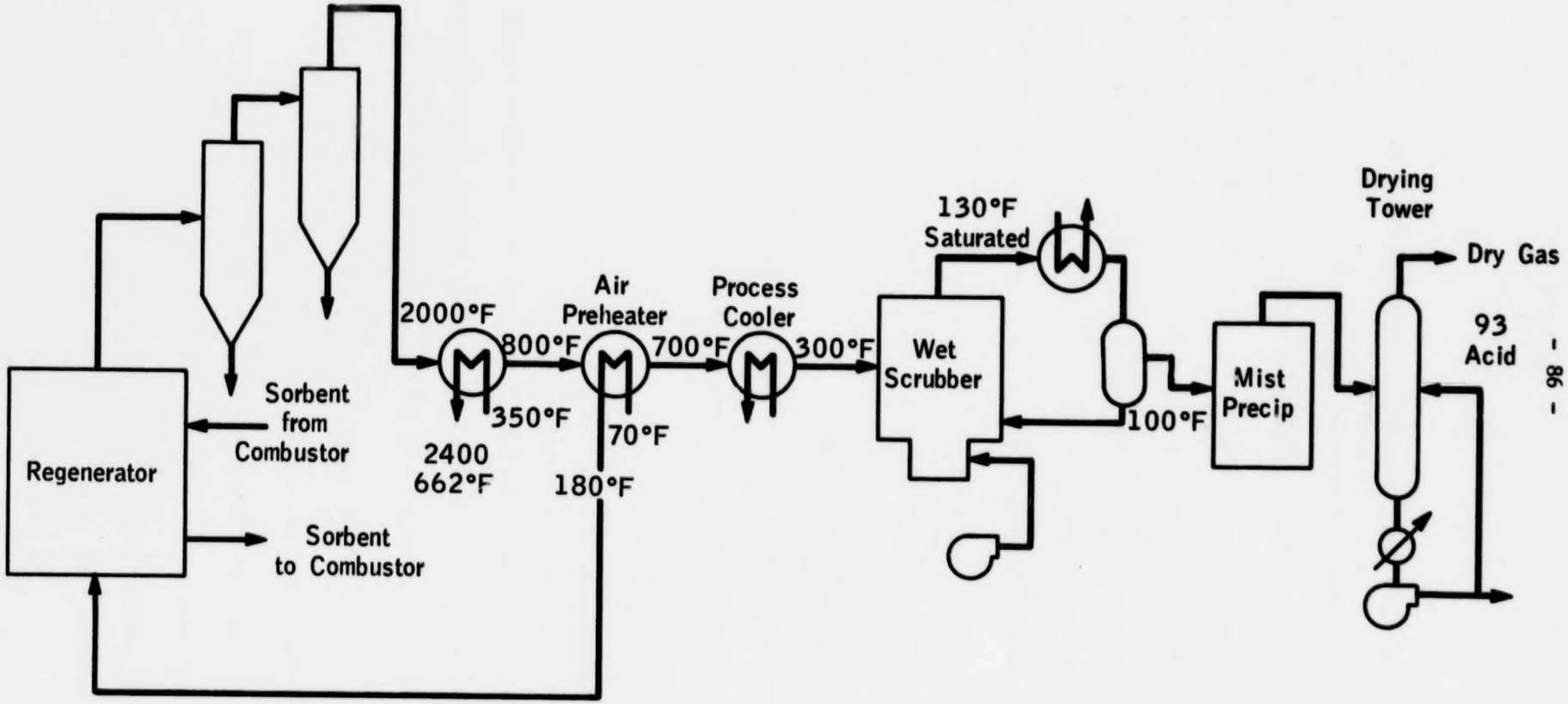

arrangement proposed by Wheelock and Boylen (17) for a plant to produce sulfuric acid from gypsum or anhydride. The exit gas of the drying tower would be sent to the absorption and conversion sections of a conventional sulfuric acid plant. A schematic diagram of the gas purification system is shown in Figure 38.

8.1.2 Single Pass Limestone System

- System Operating Conditions

The operating conditions of the single pass limestone system are the same as those listed for the combustor in Table 10.

- Limestone Feed Rate

The fresh limestone Ca/S feed ratio for 90 percent SO_2 removal was set at four. This is lower than calculated from the experimental data in Section 5.7.3, but it is believed that this limestone rate is about the maximum which should be considered for single pass operation. It was assumed that the required bed depth was the same as the regenerative system, 2.8 feet.

- Material and Energy Balance

A material and energy balance for the limestone section of a 600 MW FBB system using single pass limestone at a Ca/S stoichiometric ratio of 4 is shown in Figure 39. The energy balance is an incremental analysis over a system without limestone feeding and the factors considered are as follows:

- Energy required to calcine $CaCO_3$ to CaO and CO_2
- Energy required to heat inlet stone from 70°F to 1600°F
- Exothermic heat of reaction from $CaSO_4$ formation.

Figure 39

MATERIAL AND ENERGY BALANCE FOR SINGLE PASS
LIMESTONE 600 MW FBB SYSTEM

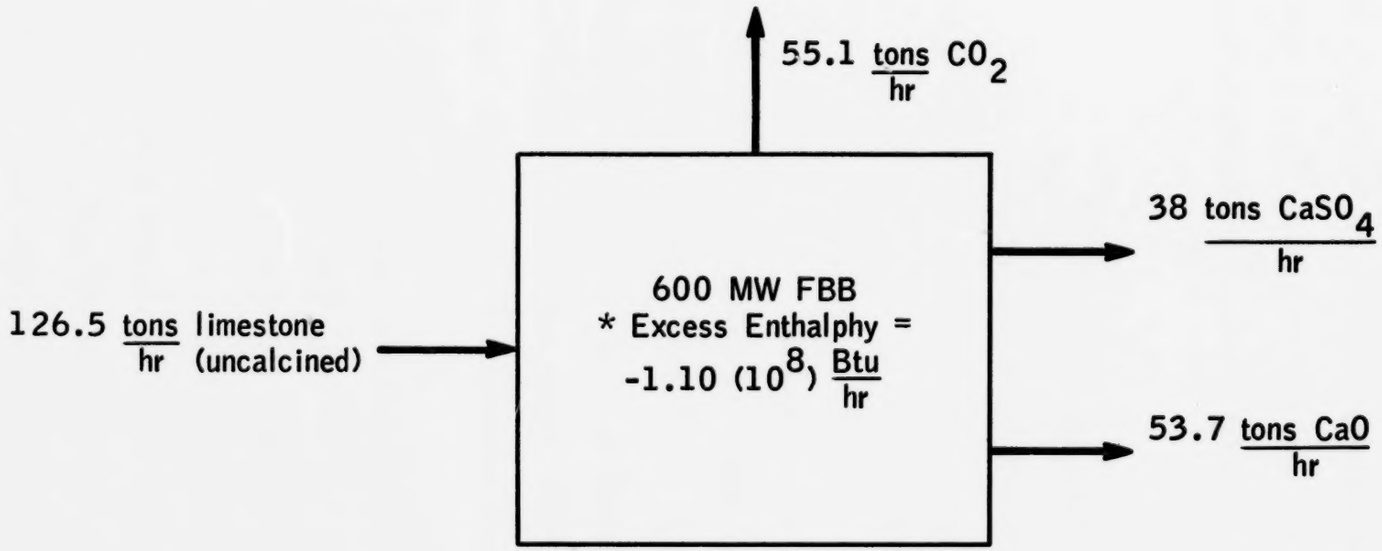

* Endothermic heat required over system without limestone addition.

8.2 Economic Comparison

The incremental investment and operating charges (and credits) for a regenerative 600 MW FBB relative to a single pass (limestone) 600 MW FBB were estimated. The following sections describe the method of estimating the economics of each system and the factors considered in the comparison.

8.2.1 Basis for Cost Estimates

Details of equipment sizing and costing procedures are given in Appendix 8. All equipment was sized for the full-rated capacity power load. Purchased equipment costs were taken from manufacturer's estimates or else based on Esso experience in the area. Total construction costs were obtained from purchased equipment costs by application of factors described by Lang (18) for electrical wiring, piping, buildings, etc. Installation costs were assessed at 43 percent of purchased equipment costs. A contingency fee of 35 percent of direct incremental cost was added to obtain the total incremental cost of the regenerative system. The 35 percent contingency was not applied to the sulfuric acid plant investment since it was believed to be a more reliable estimate. Working capital was estimated for 60 days operating supplies and labor. All investment costs were escalated by eight percent to the end of 1971.

The factors for determining the operating costs, based on the incremental investment required for the regenerative system, are given in Table 11.

TABLE 11

FACTORS FOR ESTIMATING OPERATING COSTS

Item	Factor
Capital Charges	14% Investment
Maintenance	5% Investment
Supplies	15% Maintenance
Power	6 mils/kw hr
Labor	$3/hr
	$12,000/yr/supervisor
Plant Overhead	50% (Maintenance + Supplies + Labor)
Payroll Overhead	20% Labor
Operating Water	7.5¢/M gal
Natural Gas	50 ¢/MM Btu
Acid Plant Operating Costs	Connors Estimate (15)
Working Capital	60 Days Working Supplies + Labor

8.2.2 Important Factors in Comparing Single-Pass & Regenerative Systems

Since an economic comparison was made between two systems, and absolute investment and operating charges were not estimated, the primary objective was to identify the areas in which the two systems differed and to assign appropriate economic credits or debits to these areas. The important areas of difference between a regenerative and single pass FBB system are itemized in Table 12. The credits or debits allowed for each of these items are given in Table 13.

TABLE 12

FACTORS OF IMPORTANCE IN
ECONOMIC COMPARISON OF REGENERATIVE
AND NON-REGENERATIVE FBB SYSTEMS

Credits to Regenerative System	Debits to Regenerative System
• Steam from waste heat boiler off the regenerator	• Investment for regeneration system and acid plant
• Thermal effect due to less limestone calcination and heatup	• Operating cost of reducing fuel
• Investment credit due to less limestone receiving, storing, grinding and disposal equipment	• Acid Plant operating costs
• Operating credit due to purchase of less limestone	
• Sulfuric acid credit	

TABLE 13

CREDITS OR DEBITS ALLOWED
IN ECONOMIC COMPARISONS

Item	Credit or Debit
Steam (Waste Heat Boiler)	$1/Ton (about 50¢/$10^6$ Btus)
Thermal Effect	$6/Ton of 12000 Btu/lb coal required to compensate
Investment Credit for Limestone Handling Equipment	Prorated from TVA estimate (19).
Limestone Costs	$2/Ton
Sulfuric Acid	Variable
Investment for Regenerative System	Details Given in Appendix 1 and 2
Investment for Acid Plant	Taken from Sulfur Institute Figs. (20).
Reducing Fuel for Regenerator	Natural Gas at 50¢/MM Btu

The off gas from the regenerator is assumed to be cooled from 2000°F to 800°F in a waste heat boiler; saturated steam at 2400 psi is generated at a value of $1/ton. There is a thermal credit to the regenerator since a smaller amount of limestone must be calcined and heated to combustor bed temperature.

Less limestone handling equipment is required in the regenerative system and an investment credit is allowed for this; similarly, less limestone must be purchased in the regenerative system. A sulfuric acid credit is also allowed for the regenerative system. Debits against the regenerative system include the additional investment for the regenerator and acid plant, and the additional cost of the reducing fuel.

8.2.3 Operation of Acid Plant by the Power Plant

Two cases were considered in the evaluating the economic attractiveness of using sorbent regeneration in a fluidized bed boiler system. Both economic comparisons were of a regenerative versus a single pass limestone system, as previously described in Section 8.1.1. The basic difference in the two cases was in the mode of operating the by-product sulfuric acid plant. In the first case, it was assumed that the acid plant was constructed and operated by power plant personnel; in the second case, it was assumed that an outside contractor constructed and operated the acid plant and merely paid the power plant a "transfer" price for the produced acid.

The incremental investment required for a regenerative system over a single pass system is given in Table 14 for case 1, in which the acid plant is constructed and operated by the power plant. Details of equipment sizing, specification and costing are given in Appendix 8. Only the incremental costs over the single pass system were estimated and are shown.

TABLE 14

INCREMENTAL INVESTMENT FOR REGENERATIVE FBB SYSTEM
OVER INVESTMENT REQUIRED FOR SINGLE PASS FBB SYSTEM

Item	Cost, M$
Regenerator	
Reactor, Fan, Cyclones, Solid Transfer Piping	797
Limestone Handling Equipment	
Receiving, Storage, Grinding and Disposal (Credit)	(2,619)
Regenerator Waste Heat Boiler and Air Preheater	300
Gas Purification for Acid Plant	1,750
Total Incremental Investment, (Ex. Acid Plant)	228
Engineering Fees, Construction Fees, and Contingency (35%)	80
Sulfuric Acid Plant, Absorption and Conversion	2,160
Total Incremental Investment, Including Acid Plant	2,468
Working Capital (Credit)	(120)
Total Incremental Investment	2,348

The operating charges, based on this incremental investment, are given in Table 15. The investment in Items 1 and 2 refers to the incremental investment, exclusive of the acid plant investment. Operating charges for the acid plant investment are included in Item 10, which also includes a credit for steam produced in the acid plant (16). Labor, exluding the acid plant, was assessed at one full time operator and part time supervision. Operating water and power for the regenerative system were assumed to be incremental costs over the non-regenerative system. This neglects any additional water or power requirements for the additional limestone handling equipment in the non-regenerative system.

TABLE 15

INCREMENTAL OPERATING COSTS FOR A REGENERATIVE FBB SYSTEM AS COMPARED TO A SINGLE PASS SYSTEM

Item		Cost M$ 90% Load Factor	Cost M$ 60% Load Factor
1.	Capital Charges (15% Investment)	28	28
2.	Maintenance (5% Investment)	9	9
3.	Supplies (15% 2)	1	1
4.	Power (6 mils/kw hr)	17	12
5.	Labor	40	40
6.	Plant Overhead	25	25
7.	Payroll Overhead	8	8
8.	Operating Water (1¢/ton)	44	29
9.	Natural Gas (50¢/MM Btu)	976	652
10.	Acid Plant Operating Costs		
	Water + Power ($0.58/ST)	102	68
	Steam Credit ($1.3/ST)	(227)	(152)
	Labor, Supervision, Maintenance ($0.45/ST)	96	96
	Overhead + Capital ($1.40/ST)	298	298
11.	Steam Credit ($1/ton)	(360)	(230)
12.	Limestone Credit ($2/ton)	(1565)	(1018)
13.	Thermal Credit ($6/ton coal equiv)	(417)	(277)
	Incremental Operating Credit - ex. H_2SO_4 Credit	(925)	(411)

The return on the sulfuric acid was not included in the operating credit shown in Table 15 because of its uncertainty. The sensitivity of the operating credit for the regenerative system to the acid return is shown in Figure 40.

Figure 40

EFFECT OF SULFURIC ACID RETURN

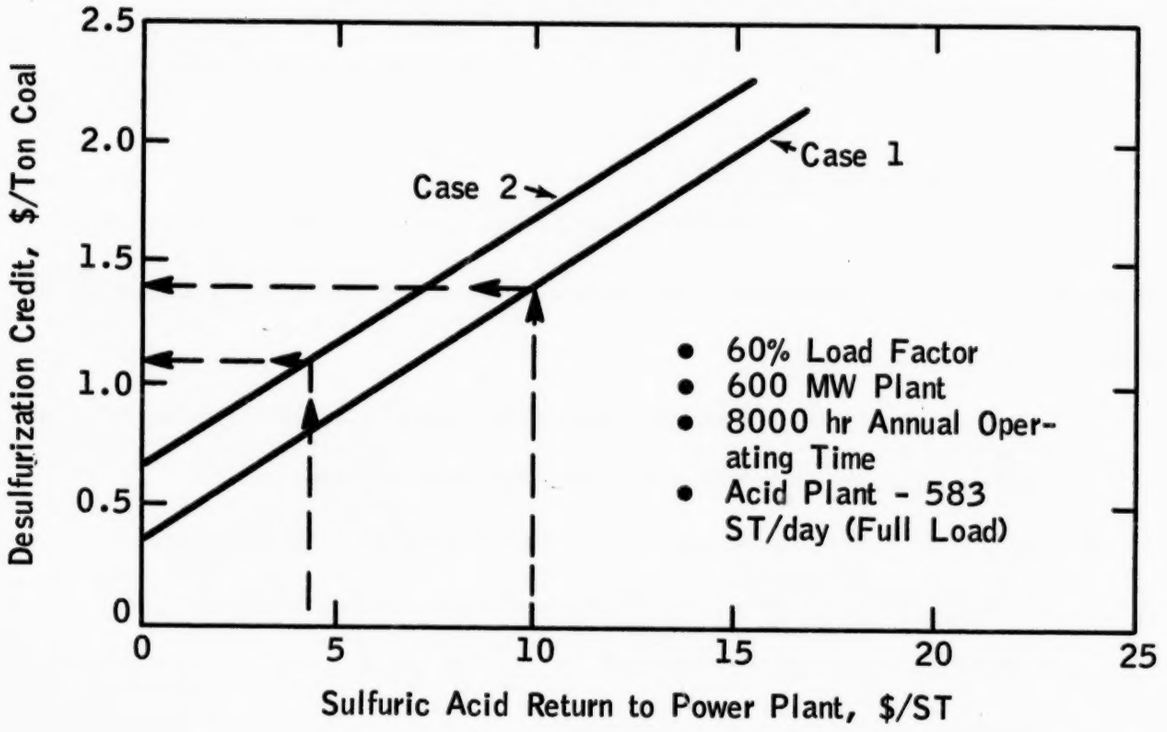

8.2.4 Operation of Acid Plant by Outside Contractor

The incremental investment required to a power plant for a regenerative system as compared to a non-regenerative system is $188,000 if it is assumed that an outside contractor constructs and operates the acid plant (see Table 14). The power plant is required to construct the gas purification system to deliver a clean gas to the acid plant. The total operating credit for the regenerative system can be obtained from Table by eliminating Item 10. The sensitivity of the operating credit for case 2 on the sulfuric acid return is also illustrated in Figure 40.

8.2.5 Sulfuric Acid Return

The return on the sulfuric acid that could be expected for each of the two economic comparisons previously presented would be influenced by the following factors (21).

1. An excess supply of sulfur presently exists in the United States and an excess is projected over the next decade.
2. Only two Frasch producers are also sulfuric acid marketers.
3. A large percentage of the United States sulfur consumption (80-90%) is as sulfuric acid.
4. Sulfuric acid is not stockpiled.
5. Virtually all the sulfuric acid consumed in the United States is produced in the United States.
6. Acid is not generally transported more than 150 miles.
7. The selling price of sulfur and sulfuric acid is variable over the United States because of local supply-demand patterns.

One conclusion that can be drawn from these points is that any abatement derived sulfur or sulfuric acid which enters the market will do so by replacing existing supplies of Frasch sulfur or acid made from Frasch sulfur. There is not enough room in the market for both of these commodities. The second conclusion that can be drawn is that the maximum return to the power plant for the abatement derived acid or sulfur will be set by local prices for the present (pre-abatement) acid or sulfur.

Concerning the question of whether to produce sulfur or sulfuric acid as a by-product, the factors previously mentioned indicate that the choice will depend greatly upon the availability of a nearby market for the produced acid. If the acid cannot be sold locally, transportation costs become prohibitive and the production of sulfur is favored. It appears reasonable to speculate that, depending upon the local market, there will be cases in which it is desirable to produce sulfuric acid from abatement sources and other cases in which it is desirable to produce elemental sulfur.

- Probable Return on Acid - Case 1

An acid return of $5 to $10 per short ton could probably be obtained in the first case considered herein. This return is lower than the anticipated sulfuric acid selling price in 1972 primarily because of marketing costs, which have not been considered in the previous analysis. The investment shown in Table 14 is only for manufacturing the acid; no marketing expenses have been allowed. A possible method of a power plant disposing of abatement derived acid is to contract with an outside company

to market the acid. This arrangement would provide much more stability, from the acid consumers viewpoint, than purchasing the acid directly from the power plant, because the outside marketer would have other acid sources in addition to the power plant. Hence, although the outside marketer would be obtaining full market price for the acid, the return to the power plant would probably be in the $5 to $10/ST range. This return to the power plant is based on the assumption that the market price for sulfuric acid is approximately $15/ST.

- Probable Return on Acid - Case 2

In the second case considered, an outside contractor constructs and operates the acid plant. In this situation, the acid return to the power plant would naturally be lower than in the first case. The reduction in the acid return to the power plant can be calculated as follows:

$$\text{Reduction in Acid Return to Power Plant} = \text{Costs Incurred by Outside Contractor}$$

$$= \text{Manufacturing Costs} + \text{Return on Investment (ROI)}$$

The manufacturing costs are estimated at $1.20/ST acid, including a return on the produced steam (16). The ROI cost is estimated as follows: The base investment for the acid plant of $2.16 MM is increased to $2.59 MM by adding 20 percent for offsites. For a 60% load factor, 8000 hours per year operation, the acid production is 116,800 short tons; the investment is $22.20 per short ton. At a nominal corporate tax rate of 50 percent, and a 10 percent after tax ROI, the increment to the acid price is $4.44/ST acid. Therefore,

$$\text{Total Cost Incurred by Outside Contractor, \$/ST Acid} = 1.20 + 4.44$$

$$\approx \$5.60$$

Hence, the return to the power plant on the produced acid obtained in Case 2 will be decreased by $5.60 from Case 2.

Setting the acid return in Case 1 at $10/ST acid, the corresponding return in Case 2 is $4.40. The credit to the regenerative system for each of these acid returns is illustrated in Figure 40.

NOMENCLATURE

Ca/S	calcium to sulfur molar ratio
C_H	reactor outlet SO_2 concentration
C_o	reactor inlet SO_2 concentration
D	reactor diameter
$(\bar{d}p)$	weight median average particle diameter
E	combustion efficiency, dimensionless
E'	combustion efficiency, percent
fps	feet per second
Ho	settled bed height
hi	heating value of fuel fed to system
ho	heating value of unburned fuel components
In	Inches
Keq	equilibrium constant
L	carbon loss in fly ash as a percent of the carbon fed
M	10^3
MM	10^6
n	number of cycles
ppm	parts per million
R	gas low constant
R(X)	rate constant, function of CaO utilization
ST	short ton
T	bed temperature
T	absolute temperature, °K

NOMENCLATURE (CON'T)

T_c	combustor bed temperature
T_r	regenerator bed temperature
U	superficial gas velocity
X	CaO utilization
$\bar{X}$	average CaO utilization in combustor
X(n)	cyclic CaO utilization required for given SO_2 removal number of cycles
α	$\frac{\text{mols/hr fresh CaO fed to process}}{\text{mols/hr CaO circulated through process}}$
μ	microns (micrometers)
ε	void fraction in a fluidized bed

REFERENCES

(1) May, W. G., "Fluidized Bed Reactor Studies," CEP, Vol. 55, No. 12, (1959).

(2) Williams, D. G. and McLaren, J., "Combustion Efficiency, Sulfur Retention and Heat Transfer in Pilot-Plant Fluidized-Bed Combustors," Journal of the Institute of Fuel, August (1969).

(3) Pope, Evans and Robbins, Study of the Characterization and Control of Air Pollutants from a Fluidized-Bed Combustion Unit, Monthly Reports 1-7 under NAPCA Contract CPA 70-10 (1969).

(4) Skopp, A., et. al., Fluid Bed Studies of the Limestone Based Flue Gas Desulfurization Process, Final Report under NAPCA Contract PH 86-67-130 (1969).

(5) Coutant, R. W., et. al., Investigation of the Reactivity of Limestone and Dolomite for Capturing SO_2 from Flue Gas, Summary Report to NAPCA under Contract No. PH 86-67-115, August (1968).

(6) Skopp, A., et. al., "Fluid Bed Studies of the Limestone Based Flue Gas Desulfurization Process," Quarterly Progress Report No. 5 under NAPCA Contract PH 86-67-130, December (1968).

(7) Borgwardt, R. H., "Kinetics of the Reaction of SO_2 with Calcined Limestone," Environmental Science and Technology, Vol. 4, No. 1 (1970).

(8) Matsen, J. M. and Tarmy, B. L., "Scale-up of Laboratory Fluid-Bed Data: The Significance of Slug Flow," Fundamental Processes in Fluidized Beds, 101, Vol. 66 (1970).

(9) Hanway, J. E., "Industrial Scale-up of Fluidized Bed Systems," Paper Presented at 62 Annual AIChE Meeting, November (1969).

(10) Jonke, A. A., et. al., "Reduction of Atmospheric Pollution by the Application of Fluidized Bed Combustion," Monthly Progress Report No. 20 to NAPCA, May (1970).

(11) Jonke, A. A., "Reduction of Atmospheric Pollution by the Application of Fluidized Bed Combustion," Annual Report to NAPCA, July (1969).

(12) White, S. B., et. al. "Chemical Equilibrium in Complex Mixtures," Rand Corp. Bulletin P-1059.

(13) Curran, G. P., "CO_2 Acceptor Gasification Process," Fuel Gasification, ACS Advances in Chemistry Series 69, Washington, D. C. (1967).

(14) Jonke, A. A., et. al., "Reduction of Atmospheric Pollution by the Application of Fluidized Bed Combustion," NAPCA Monthly Progress Report No. 23, Sept. (1970).

(15) Archer, D. H., et. al., Sixth Monthly Progress Report under NAPCA Contract CPA 70-9, May (1970).

REFERENCES (CON'T)

(16) Connor, J. M., "Economics of Sulfuric Acid Manufacture," CEP, 64 (11): 59-65, (1968).

(17) Wheelock, T. D. and Boylan, D. R., "Sulfuric Acid from Calcium Sulfate," CEP, 64 (11): 87-92 (1968).

(18) Lang, H. J. "Cost Engineering in the Process Industries," C. H. Chilton, Ed., McGraw Hill, New York (1969).

(19) "Sulfur Oxide Removal from Power Plant Stack Gas: Conceptual Design and Cost Study; Sorption by Limestone or Lime; Dry Process," Prepared for NAPCA by TVA. CFSTI: PB-168-972 (1968).

(20) "Guide for Estimating Manufacturing Costs," Prepared by the Sulfur Institute (1968).

(21) Farmer, M. H. "Long Range Sulfur Supply and Demand Model," Monthly Progress Reports 1-4, NAPCA Contract EMSD 71-13 (1970).

APPENDIX 1

CALCINING PROCEDURE

An electrical oven is used to calcine the limestone in this study. The oven is initially brought to 1700°F. Two thousand grams of the limestone are then charged to the oven, resulting in a settled bed of limestone approximately 1-1/2 inches depth. A constant nitrogen bleed of four liters/minute is maintained above the bed. The system is maintained at 1700°F for seven hours, at which time the electrical heat is shut off. The oven is allowed to cool for nine hours before removing the calcined stone at 500°F. The nitrogen sweep gas is maintained during the cooling-down period.

APPENDIX 2

SUMMARY OF OPERATIONS ESSO FBC

Run No.	C1	C2	C3	C4	C6	C7	C8	C10	C12	C13	C14	C15	C16	C17	C18	C19	C21	C22	C23	C24	C25	C26	C27	C28	C29	C30
Run Length, Hrs.	3.8	7.6	5.2	4.3	8.0	3.5	3.5	4.2	4.0	6.0	4.5	5.5	5.0	1.8	5.3	0.8	2.9	5.6	5.4	11.7	4.3	5.0	5.7	5.6	9.3	0.7
Coal	←													Bit. A												→
Coal $\bar{d}p$,	←													200 μ												→
Bed Material	←					BCR-1359 Limestone							1359			Alundum	←	1359		→			BCR-1359			Alundum
Bed material $\bar{d}p$,	←							930 μ								841 μ	←	930 μ		460 μ	←		930 μ		→	841 μ
Settled Bed Height, In.	12	12	6	4	16	6	6	6	6	6	6	12	6	6	6	6	6	6	6	6	6	6	6	6	6	6
Bed Temperature, °F	1630	1600	1600	1600	1600	1700	1500	1800	1600	1600	1600	1600	1600	1600	1700	1600	1600	1600	1600	1600	1600	1600	1800	1700	1800	1600
Gas Velocity, fps	3.0	3.0	3.0	3.0	3.0	3.1	3.0	3.0	4.0	2.0	3.0	3.0	3.0	3.0	2.7	4.0	3.0	3.0	3.0	3.0	3.0	3.0	3.0	2.7	3.0	4.0
Excess Air, %	45.7	8.5	10.7	14.3	10.9	12.3	12.6	2.6	15.2	8.7	11.6	9.8	29.3	4.9	4.2	50.0	19.2	3.0	9.1	8.3	7.4	7.0	15.5	7.5	27.0	15.0
Coal Feed Rate, lbs/hr.	0.70	0.94	0.92	0.80	0.92	0.91	0.94	0.91	1.19	0.63	0.91	0.93	0.79	0.97	0.85	0.87	0.86	0.99	0.93	0.94	0.95	0.95	0.80	0.82	0.75	1.20
Flue Gas Analysis, Mole %, (dry)																										
CO_2,,%	11.6	14.2	14.1	14.7	14.5	15.2	14.7	15.6	14.2	15.8	14.3	14.5	12.9	15.9	15.9	13.5	13.0	14.7	14.4	15.3	15.0	15.5	15.4	14.8	13.8	--
O_2,,%	7.4	4.0	3.9	3.6	4.2	3.6	3.9	2.2	4.8	2.4	4.5	4.2	6.0	2.4	1.8	5.4	5.6	3.3	3.9	2.8	3.2	2.5	3.2	3.4	1.0	--
N_2, %	81.0	81.8	83.0	81.7	81.3	81.2	81.4	82.2	81.0	81.8	81.2	81.3	81.1	81.7	82.3	81.1	81.4	81.3	81.7	81.9	81.3	82.0	81.4	81.8	85.2	--
SO_2,	--	--	--	--	--	--	--	--	--	--	--	--	--	--	--	1670	--	--	--	--	--	--	--	--	--	2150
NO_x, PPM	--	--	--	--	--	--	--	--	1100-600	1225-600	1100-700	1100-700	1100-700	1250-1000	1300-750	500	1300-1050	1250-650	1200-650	900-750	1200-800	1250-820	1500-900	1350-750	1500-850	650
CO	--	--	--	--	--	--	--	--	--	--	400	310	400	1000-400	1200-300	240	400	1200-400	310	1500-400	390	280-1000	140	190	120	--
CaO Utilization at:																										
100% SO_2 Removal	7.7	10.8	17.3	8.5	6.0	10.6	4.2	9.3	8.5	18.2	12.5	9.2	8.9	--	10.5	--	--	14.5	15.0	23.5	11.7	14.5	12.0	13.0	--	--
90% SO_2 Removal	8.5	11.3	18.2	18.4	6.6	12.5	9.0	29.7	16.4	19.2	15.2	11.0	11.7	--	16.7	--	--	20.4	21.0	29.2	16.3	20.6	22.0	18.8	--	--
80% SO_2 Removal	9.0	12.0	19.0	19.5	7.2	14.4	10.5	33.8	20.0	20.2	17.2	11.8	12.4	--	23.8	--	--	23.4	23.3	32.5	19.2	--	--	22.3	--	--
Carbon Lose in Fly ash As a Percent of Carbon Fed	5.4	9.1	5.6	6.4	8.3	5.5	9.4	4.5	9.2	3.9	5.7	8.2	6.0	7.8	6.1	4.5	7.3	7.3	7.1	5.8	7.4	6.8	3.2	5.5	3.1	4.8
Material Balance, Out (100)/In.																										
Carbon	--	99	92.1	100.5	97.3	100.5	100.0	100.0	95.8	100.0	96.2	93.3	96.3	96.8	95.8	102.5	90.3	95.3	97.4	95.7	97.3	100.0	100.0	103.4	98.3	101.5
Oxygen	--	107	96.5	98.0	92.5	95.8	93.3	104.5	96.8	99.0	102.3	96.8	97.7	90.2	87.8	87.8	105.5	88.3	110.0	90.7	96.7	104.3	97.3	90.8	90.8	--
Sulfur			100.5																							

APPENDIX 2 (CON'T)

SUMMARY OF OPERATIONS ESSO FBC(CYCLIC OPERATIONS)

Coal = Bit A
Coal $\bar{d}p$ = 200 u
Bed Material = Limestone BCR-1359
Bed Temperature = 1600°F
Gas Velocity = 3 fps

Run No.	C35	C36	C37	C38	C39	C40	C41	C42	C43	C44	C48	C24	C46	C47
Series Number	1	2	3	4	5	6	7	1	2	3	4	1	2	3
Run Length, Hrs	5.7	6.5	5.5	4.9	5.2	5.0	5.2	8.0	5.0	5.0	4.0	8.0	5.1	5.0
Bed Material $\bar{d}p$	←		930	→				←	460	→		←	460	→
Settled Bed Height, In.	6.0	5.7	5.2	4.8	4.8	4.9	5.2	6.0	5.5	6.4	7.1	6.0	5.5	5.8
Excess Air, %	12.1	6.2	13.0	18.0	18.0	14.6	15.9	13.4	16.5	13.4	18.7	8.3	15.4	13.4
Coal Feed Rate, lbs/hr	0.91	0.96	0.90	0.87	0.86	0.89	0.88	0.90	0.87	0.90	0.86	0.94	0.88	0.90
Flue Gas Analysis, %, (dry)														
CO_2, %	14.7	15.2	15.1	14.5	15.2	15.2	15.2	15.2	14.9	14.9	15.2	15.3	15.0	15.2
O_2, %	3.3	2.6	2.8	2.8	2.7	2.8	2.8	2.8	2.9	2.9	2.8	2.8	2.6	2.7
N_2, %	82.0	82.2	82.1	82.7	82.1	82.0	82.0	82.0	82.2	82.2	82.0	81.9	82.4	82.1
CO, ppm	400	370	400	530	450	530	530	370	370	325	325	310	365	355
NO_x, ppm	1325-800	1300-900	--	1025-850	1000-825	1250-800	1250-900	950-750	1150-755	1225-760	1050-630	875-700	1150-650	975-530
CaO Utilization at:														
100% SO_2 Removal	4.0	12.8	--	2.0	3.0	4.0	4.0	31.5	10.0	8.0	5.0	25.0	8.0	1.0
90% SO_2 Removal	16.4	21.5	--	10.0	13.0	9.2	9.0	36.0	17.0	13.0	7.0	30.0	17.5	8.2
80% SO_2 Removal	19.8	23.5	--	15.2	18.5	14.2	14.0	38.5	21.0	16.2	10.0	33.5	22.0	13.0
Carbon Loss in Flyash as a Percent of Carbon Fed	7.8	7.6	7.5	5.9	5.9	6.0	5.9	11.0	5.2	6.2	6.2	5.8	7.1	7.8
Material Balance, Out (100)/In														
Carbon	100.5	96.3	100.0	110.0	99.2	96.3	96.2	101.0	99.0	90.6	90.8	95.7	99.0	94.8
Oxygen	89.0	89.6	79.0	77.0	81.7	83.5	82.0	82.0	82.0	76.0	82.3	90.7	81.2	82.0

APPENDIX 3

DIFFERENT METHODS OF CALCULATING CaO UTILIZATION IN REASONBALE AGREEMENT

An independent check on the metood of calculating CaO utilization was made bv analytically determining the sulfur content of the discharged bed material of selected runs. The calcium content of the bed was assumed to be the same as at the beginning of the run and all the sulfur was assumed to be present as $CaSO_4$. A comparison between the CaO utilization levels determined by this technique and the CaO utilizations obtained from the chart integration technique is shown in Table 16.

Table 16

Run No.	CaO Utilization by Chart Integration	CaO Utilization by Ca/S Bed Material Ratio
C2	16.6	17.4
C3	20.9	20.3
C7	11.3	15.6

The CaO utilizations as calculated from chart integration and the Ca/S ratio of the bed material are in reasonable agreement for Runs C_2 and C_3 (4 and 3% difference, respectively), but in poorer agreement for Run C7 (27% difference). The Ca/S ratio calculation does not account for fly ash remaining in the bed or for calcium elutriation for the bed and, hence, some discrepancy would be expected.

APPENDIX 4

ESSO KINETIC MODEL DEVELOPMENT

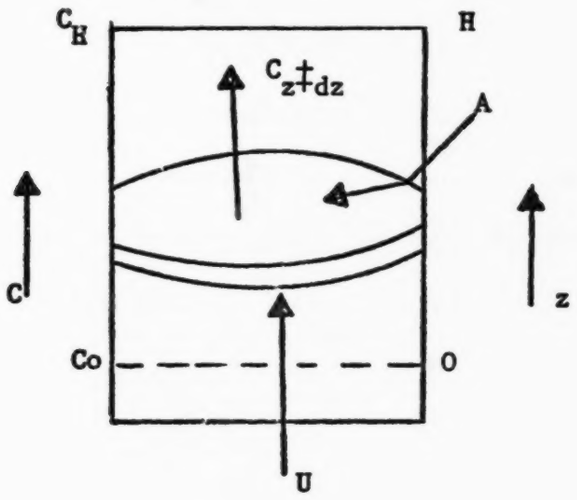

Material Balance:

SO_2 removed from gas = SO_2 absorbed by sorbent

$$-U \cdot A \cdot (C_z - C_{z+dz}) = A \cdot dz \cdot (1-\epsilon) \cdot R(X) \cdot C_z$$

$$= -U \cdot A \cdot dC_z$$

On rearrangement and integration

$$\int_{C_o}^{C_H} U \frac{dC_z}{C_z} = \int_{o}^{H} R(X)\ (1-\epsilon)\, dz$$

$$\ln \frac{C_H}{C_z} = \frac{R(X)\ (1-\epsilon)}{U} \cdot H$$

where H = expanded bed height

assuming: $H = \frac{Ho}{1-}$

yields: $\ln \frac{C_H}{C_o} = -R(X) \cdot \frac{Ho}{U}$

APPENDIX 5

EQUILIBRIUM CALCULATIONS FOR THE REDUCTION OF $CaSO_4$

In order to quantify the effects of temperature and gas composition on the regeneration of sulfated line, equilibrium compositions for both the solid and gas phases were calculated for a series of hypothetical regeneration systems. These calculations were made by a high speed digital IBM 7090 Computer using a program developed by the Rand Corporation. The Rand program calculates the equilibrium composition of a system - subject to material balance restraints - by minimizing the free energy of the system. A partial summary of the results obtained using this program are given in the Table below. It can be seen that temperatures above 1300°K (1880°F) are required for regeneration by CO or H_2 of the sulfate to the oxide. At lower temperatures, the reaction proceeds to the sulfide, while temperatures above 1400°K (2060°F) offer no advantage in terms of equilibrium conversion. It should be noted that complete conversion of $CaSO_4$ to CaS, without SO_2 formation, is predicted for reduction with pure methane at 2240°F.

	Inlet Gas Composition, Mole %					Outlet Gas Composition Mole %				% of Reacted $CaSO_4$ Converted to	
Temp, °F	CO	H_2	CO_2	H_2O	N_2	SO_2	CO_2	H_2O	N_2	CaO	CaS
1880	5	0	10	0	85	0	15	0	85	0	100
1880	0	5	0	10	85	0	0	15	85	0	100
1880	10	0	20	0	70	0	30	0	70	0	100
1880	0	10	0	20	70	0	0	30	70	0	100
1880	15	0	30	0	55	0	45	0	55	0	100
1880	0	15	0	30	55	0	0	45	50	0	100
2060	5	0	10	0	85	4.0	14.4	0	81.6	95	5
2060	0	5	0	10	85	4.0	0	14.4	81.6	95	5
2060	10	0	20	0	70	7.7	27.7	0	64.6	95	5
2060	0	10	0	20	70	7.7	0	27.7	64.6	95	5
2060	15	0	30	0	55	11.1	40	0	48.8	95	5
2240	5	0	10	0	85	3.9	14.4	0	81.7	94	6
2240	0	5	0	10	85	3.9	0	14.4	81.7	94	6
2240	0	10	0	20	70	7.5	0	27.7	64.8	94	6
2240	15	0	30	0	55	10.7	40.2	0	49.1	94	6
2240	10	15	0	30	55	10.8	0	40.2	49.0	94	6
2240	----	100%	CH_4	------		0	33.3	66.7	0	0	100

APPENDIX 6

SULFUR BALANCES OVER REGENERATOR

Sulfur balances over the regenerator were made on all cyclic operations and are shown in Table 17. The following procedure was used to make these balances:

1. The total sulfur contained in the feed to the regenerator was determined by graphically integrating the SO_2 chart from the combustor.
2. The total sulfur out of the regenerator in the off gas was determined by graphically integrating the SO_2 chart on the regenerator outlet.
3. The assumption was made that sorbent regeneration went to completion.

Recognizing that small errors can arise from any one of the above mentioned procedures, it is believed that the accuracy of the sulfur balances shown in Table 17 are adequate.

APPENDIX 6 CON'T

TABLE 17

Treg = 2000°F
$(\bar{d}p)$ stone = 460 μ

Run Number	Number In Series	Sulfur Balance (Out/In) X 100
42	1	90.8
43	2	121.0
44	3	91.3

$(\bar{d}p)$ stone = 930 μ

Run Number	Number In Series	Sulfur Balance (Out/In) X 100
35	1	94.6
37	3	96.8*
38	4	108.5
39	5	101.8
40	6	137.0

* Balance is on analytical results

APPENDIX 7

CALCUALTION PROCEDURE TO DETERMINE COMBUSTOR BED HEIGHT IN A REGENERATIVE SYSTEM

An example of the calculation procedure followed in determining the combustor bed height is given below:

Step 1 - Set makeup rate and desired superficial gas velocity through combustor.

$\alpha = 0.05$

$U = 10$ fps

Step 2 - Determine $\bar{X}$ from Figure 3.

$\bar{X} = 0.097$

Step 3 - From experimentally-determined break through curves shown in Figure 41, calculate a value of k for each cycle, where

$$k = \frac{-\ln \frac{C_H}{C_o}}{\left[\frac{U}{H_o}\right]}$$

Figure 41

EXPERIMENTAL BREAKTHROUGH DATA

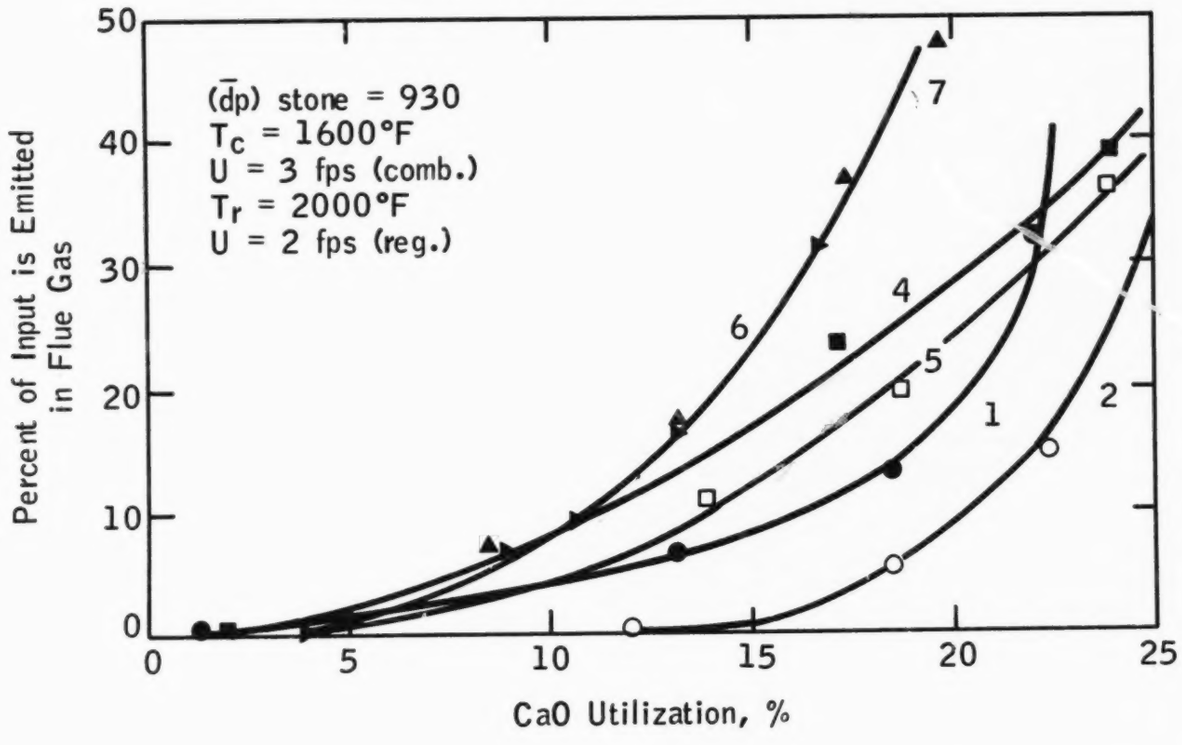

Experimental Conditions

$$U/H_o = 3 \frac{ft}{sec} \times 60 \frac{sec}{min} \times \frac{1}{0.5\ ft} = 180\ min^{-1}$$

Cycle 1

$$k = -\ln \frac{C_H}{C_o} \quad \frac{U}{H_o}$$

$$= \ln (0.025) \cdot (180)$$
$$= 667\ min^{-1}$$

Cycle 2

$$k = -\ln (0.005) \cdot (180)$$
$$= 957\ min^{-1}$$

Continue this calculation procedure for all the cycles.

Step 4 - Plot k vs n on log-log paper. Fit the data with a straight line, obtaining:

$$k = 1030\ n^{-0.527}$$

Step 5 - Determine $\bar{k}$ by a procedure defined by Curran (12).

$$\bar{k} = \int_o^\infty \alpha\, e^{-\alpha n}\, k\,(n)\, dn$$
$$= 400\ min^{-1}$$

Step 6 - Assuming this $\bar{k}$ is independent of velocity, as indicated by the experimental data over the range of 2 to 4 fps, calculate a bed height at the desired conditions as follows:

Let U = 10 fps
90% SO_2 removal

$$H_o = -\ln \frac{C_H}{C_o} \bullet \left(\frac{U}{k}\right)$$

$$= -\ln (0.1) \bullet \left[\frac{10.60}{400}\right]$$

$$= 2.31 \left(\frac{600}{400}\right) = 3.47\ ft.$$

Step 7 - Repeat Steps 1 through 6 to obtain a plot of α versus bed height.

APPENDIX 8

DETAILS OF EQUIPMENT SPECIFICATION AND SIZING

1. Fluidized Bed Regenerator

   A. Process Parameters

Operating Temperature, °F	2000
Operating Pressure, atm	1
Inside Diameter, ft	21.6
Normal Settled Bed Depth, ft	2.5
Total Reactor Height, ft	30
Cyclones	
Primary, number	1
type	External Internally Lined Inlet Area-5.8 ft
Secondary, number	1
type	External Internally Lined Inlet Area-4.3
Grid	
Normal operating temperature, °F	500

   B. Other reactor details

   21.6' inside diameter reactor, refractory lined with 9" thick superduty firebrick. Dome is 13" thick superduty firebrick. Grid is refractory lined SS type 304 plate, 1" thick. Grid is supported by 4 beams, 1-1/2" thick by 18" deep. 3/8" carbon steel shell.

   C. Fan

   Forced draft fan, 36 M CFM, 400 HP motor

2. Waste Heat Boiler

   Produce 2400# saturated steam. Bayonnette tube construction, water on the tube side. Must refractory line entire gas side of tubes. Use maximum bundle diameter of 4'. Use 1-1/2 inch O.D., 1 inch I.D. tubes.

3. Gas Purification System for Acid Plant

   Estimated from Connors for 30°F cooling water approach, 7.5% SO_2

EQUIPMENT PRICING DETAILS

1)	Carbon Steel Shell	$0.50/pound*
2)	Stainless Steel Grid	$0.70/pound*
3)	Waste Heat Boiler	$25/ft^2 transfer area*
4)	Refractory Bricks	a)*$378/thousand bricks for 9 x 4-1/2 x 3 superduty firebrick for walls and grid of regenerator b)*$440/thousand bricks for (equiv) 9 x 4-1/2 x 3 superduty firebricks for dome
5)	Limestone Receiving, Handling Grinding	Estimated from TVA experience
6)	Gas purification system	Estimated from Connors assuming 800°F gas inlet temperature
7)	Solid Transfer Piping	30% of Regenerator Reactor Total Installation Cost

* Purchased Material Cost